VERO CELLS AS A SUBSTRATE FOR HUMAN NOROVIRUS REPLICATION

by

KYLE VAUGHAN TODD

(Under the Direction of Ralph Tripp)

ABSTRACT

Human norovirus (HuNoV) is a principal cause of acute gastroenteritis. Its global prevalence is underscored by ~700 million infections and >200,000 deaths annually. Currently there are no licensed vaccines or therapeutics to lessen HuNoV disease burden. Vaccine options are limited to recombinant approaches because a vaccine-approved cell substrate has not been shown to support HuNoV. Vero cells have been used extensively as a viral vaccine cell substrate because of their deficiency in interferon responsiveness. In these studies, HuNoV replication in Vero cells was examined, host-targeted strategies evaluated, and exosome-mediated HuNoV infection assessed to improve HuNoV replication. These studies provide support for use of Vero cells as a platform-enabling technology for HuNoV vaccine development.

INDEX WORDS: norovirus, human norovirus, cell substrate, Vero cells

VERO CELLS AS A SUBSTRATE FOR HUMAN NOROVIRUS REPLICATION

by

KYLE VAUGHAN TODD

B.S., UNIVERSITY OF MARYLAND, 2013

A Dissertation Submitted to the Graduate Faculty of The University of Georgia in Partial Fulfillment of the Requirements for the Degree

DOCTOR OF PHILOSOPHY

ATHENS, GEORGIA

2020

VERO CELLS AS A SUBSTRATE FOR HUMAN NOROVIRUS REPLICATION

by

KYLE VAUGHAN TODD

Major Professor:	Ralph A. Tripp
Committee:	Donald Harn
	Eric Lafontaine
	Balázs Rada
	Wendy Watford

Electronic Version Approved:

Ron Walcott
Interim Dean of the Graduate School
The University of Georgia
August 2020

DEDICATION

This work is dedicated to my father, Dr. Mark Todd, and my mother, Tamara Todd. I would not be where I am today if not for your unwavering love and support. I love you and will be forever grateful for all that you've done for me throughout my life!

ACKNOWLEDGEMENTS

I would like to thank my advisor, Dr. Ralph Tripp, for his continued support, guidance, and mentorship throughout the entirety of my PhD studies. I'd also like to thank my committee members Drs. Donald Harn, Eric Lafontaine, Balázs Rada, and Wendy Watford for their valuable input and insightful discussions regarding this work.

I would like to acknowledge several Tripp Lab members that have been instrumental both in the completion of this work and my scientific development. Thank you Jackelyn Murray for overseeing lab operations and your assistance with assay development. Thank you Les Jones for your guidance when troubleshooting experiments. Thank you Dr. Abhijeet Bakre for sharing your encyclopedic scientific knowledge over countless discussions regarding my project and otherwise. Thank you Nichole Orr-Burks for being my hood buddy and for always looking out for me. Thank you Harrison Bergeron for making every day in the lab entertaining and fun.

I would like to thank my entire family for their love and support throughout this process most notably my father, Dr. Mark Todd, my mother, Tamara Todd, my brother, Christopher Todd, my sister, Laura Todd, and my sister-in-law Megan Todd. I would also like to thank Drs. Enrico Barrozo and Paeton Wantuch for their lasting friendships since day 1 of this adventure.

I'd like to sincerely thank each and every one of you. Your patience, kindness, thoughtfulness, and effort throughout this journey has been greatly appreciated.

TABLE OF CONTENTS

Page

CHAPTER 1

INTRODUCTION

Human noroviruses (HuNoVs) are a leading cause of foodborne disease and acute gastroenteritis worldwide [1,2]. This association is poised to continue as there are currently no licensed therapeutics or vaccines against HuNoV. Several hurdles have hampered vaccine development of HuNoV countermeasures, most notably the lack of an *in vitro* cell culture system. Recently, strides have been made in studies showing that HuNoVs can be propagated *in vitro* [3,4]. Unfortunately, the methods described are not suitable for most vaccine production. Regulations requiring reproducibility and safety prohibit the use of these uncharacterized cell systems [5]. The most time-efficient and cost-effective solution is to develop a mammalian cell line that has already met the vaccine standards of the pharmaceutical industry. Vero cells are a vaccine-approved African green monkey kidney cell line that support an array of viruses and have been used to generate vaccines against influenza virus, poliovirus, rabies virus, and rotavirus [6]. The *long-term goal* of this research project is to develop a robust vaccine-approved cell line that supports HuNoV replication. The *central hypothesis* of this project is that Vero cells will support HuNoV replication and aid the development of a HuNoV vaccine. The *rationale* is that HuNoV research and translational HuNoV vaccine development will benefit from this cell culture system.

Specific Aim 1: Determine HuNoV replication in Vero cells. The *working hypothesis* is that Vero cells support HuNoV replication.

Specific Aim 2: Determine exosome-driven HuNoV replication in Vero cells. The *working hypothesis* is that HuNoV infects Vero cells through exosomes.

Specific Aim 3: Develop a Vero cell substrate for enhanced HuNoV replication. The *working hypothesis* is that the Vero cell model can be enhanced by media supplementation and host-targeted gene expression disruption.

References

1 Bartsch, S. M., Lopman, B. A., Ozawa, S., Hall, A. J. & Lee, B. Y. Global Economic Burden of Norovirus Gastroenteritis. *PloS one* **11**, e0151219, doi:10.1371/journal.pone.0151219 (2016).

2 Dewey-Mattia, D., Manikonda, K., Hall, A. J., Wise, M. E. & Crowe, S. J. Surveillance for Foodborne Disease Outbreaks - United States, 2009-2015. *Morbidity and mortality weekly report. Surveillance summaries (Washington, D.C. : 2002)* **67**, 1-11, doi:10.15585/mmwr.ss6710a1 (2018).

3 Jones, M. K. *et al.* Enteric bacteria promote human and mouse norovirus infection of B cells. *Science* **346**, 755-759, doi:10.1126/science.1257147 (2014).

4 Ettayebi, K. *et al.* Replication of human noroviruses in stem cell-derived human enteroids. *Science* **353**, 1387-1393, doi:10.1126/science.aaf5211 (2016).

5 WHO. Recommendations for the evaluation of animal cell cultures as substrates for the manufacture of biological medicinal products and for the characterization of cells banks. Report No. 978, 79-187 (Geneva, 2013).

6 Barrett, P. N., Mundt, W., Kistner, O. & Howard, M. K. Vero cell platform in vaccine production: moving towards cell culture-based viral vaccines. *Expert review of vaccines* **8**, 607-618, doi:10.1586/erv.09.19 (2009).

CHAPTER 2

LITERATURE REVIEW[1]

[1] Todd, K. V. & Tripp, R. A. Human Norovirus: Experimental Models of Infection. *Viruses* **11**, doi:10.3390/v11020151 (2019). Reprinted here with permission of publisher.

2.1 Human Norovirus (HuNoV) Introduction

Noroviruses (NoVs) are members of the *Caliciviridae* family [1]. The NoV genus is subdivided into at least ten genogroups containing more than forty genotypes [2,3]. NoV nomenclature constitutes inclusion of the genogroup, represented by a Roman numeral, the genotype, represented by a mathematical numeral, and lastly the strain name, typically the city where it was first isolated (e.g. GII.4 Sydney). Classification of the genogroups and genotypes is based upon the amino acid homology of the major capsid protein-coding region (<2× standard deviation) [3,4]. Generally, genetic diversity of greater than 44.9–61.4% separates the genogroups, while genotypes maintain differences greater than 14.3% but not to exceed 43.8% [4-6]. Genogroups I, II, and, to a lesser extent, IV, VIII, and IX infect humans, while genogroups III (bovine), V (murine), VI (feline/canine), VII (canine), and X (bat) are generally mammalian species-specific; all of which are not believed to be zoonotic [2,3,7-9]. Additionally, only circumstantial evidence of reverse zoonosis exists [10,11]. The genogroups are further stratified into the corresponding number of genotypes: GI (n=9), GII (n=27), GIII (n=3), GIV (n=2), GV (n=2), GVI (n=2), GVII (n=1), GVIII (n=1), GIX (n=1), and GX (n=1) [3].

HuNoVs are non-enveloped, single-stranded, positive-sense, RNA viruses [12-14]. Their 7.5–7.7 kb genomes contain three open reading frames (ORFs) [15]. ORF1 codes for the six nonstructural proteins, in order from N-terminus to C-terminus: p48 (45 kDa), NTPase (40 kDa), p22 (22 kDa), VPg (15 kDa), 3C like protease ($3CL^{pro}$) (20 kDa), and RNA dependent RNA polymerase (RdRp) (55 kDa) [16-18]. Subgenomic RNA, containing ORFs 2 and 3, codes for the major

and minor structural proteins, VP1 (58 kDa) and VP2 (22 kDa) respectively [19]. The polycistronic nature of the subgenomic RNA permits VP2 translation by a ribosome termination-reinitiation mechanism [20]. Short, identical, untranslated regions flank the 5' and 3' ends of the genomic and subgenomic RNAs [21,22]. VPg covalently links to the genomic and subgenomic RNAs at their 5' ends, while the 3' ends are polyadenylated [23-25]. Larger amounts of subgenomic RNA relative to genomic RNA are typically observed in cells because of the substantial demand for structural proteins [24]. The entire HuNoV replication cycle occurs within the cytoplasm and is thought to be membrane-associated (endoplasmic reticulum (ER), endosomes, and Golgi apparatus) [26-28]. Of note, murine NoV (MuNoV) prolongs the G1 phase of the cell cycle to create conditions favorable for virus replication [29]. Lack of permissive cell lines and small animal models has severely hampered HuNoV protein structure and function analyses. To elucidate information about the viral proteins, many studies have been completed in recombinant systems or by analyzing homologous proteins [16].

The six nonstructural proteins of ORF1 are translated as a single 200 kDa polypeptide before co- and post-translational autocatalytic cleavage by the viral protease, $3CL^{pro}$ [17,30]. p48 exists as both a cytosolic protein and as a cleaved variant that is secreted [31]. The secretion of p48 may affect cell tropism *in vivo* [31]. p48 and p22 work in concert to disrupt host cell protein secretion and disassemble the Golgi apparatus [30,32,33]. p48 interrupts vesicle transport along the trans-Golgi network [32]. Likewise, the mimic of an ER export signal motif of p22 prompts secretory pathway antagonism, while a domain outside of this motif

is thought to function in Golgi breakdown [34]. p22 also affects actin mobilization, which may affect tissue repair [35]. The viral NTPase is a nucleoside triphosphatase that traditionally enhances the efficiency of viral genome transcription. The HuNoV NTPase has been shown to bind and hydrolyze nucleoside triphosphates, but conflicting data exist on whether or not the HuNoV NTPase functions as a helicase and RNA chaperone [36,37]. Additionally, the HuNoV NTPase triggers vesicle production, apoptosis [38], and downregulation of MHC class I surface presentation [39]. NTPase interactions with either p48 or p22 enhance the induction of apoptosis [38]. VPg is required for productive infection as it recruits the host eukaryotic translational machinery, eIF4E, to orchestrate the translation of HuNoV proteins [40,41]. G3BP1, a stress granule protein involved in unwinding double-stranded nucleic acids, has also been identified as a necessary host protein required for efficient VPg-mediated HuNoV protein translation [42]. Additionally, VPg assists in transcription through a mechanism known as “protein-priming” [21]. VPg has also been implicated in causing cell cycle arrest at the G1/S phase by decreasing cyclin A production [40]. This mechanism, independent of viral RNA binding, generates conditions favorable for virus replication. $3CL^{pro}$ cleaves the polyprotein temporally depending on the scissile cleavage site: “early” (glutamine-glycine) or “late” (glutamic acid-glycine/alanine) [18,43,44]. Additionally, the $3CL^{pro}$ is functional (possibly more efficient) while still in complex with the RdRp [43]. Using the poly(A) tail as a template, the viral RdRp initiates transcription of the antigenome by uridylylating VPg [21]. The poly(U) sequence serves as a primer for antigenome creation [21]. Subsequent transcription of viral

genomes and subgenomes is carried out *de novo* [21]. HuNoV polymerase mutation rates range from 9.0×10^{-4} to 2.2×10^{-5} substitutions per nucleotide site [45,46]. Additional mutation of HuNoV genomes is carried out by host-encoded adenosine deaminases [45]. VP1 and VP2 serve as the major and minor capsid proteins. 180 copies of VP1 each take the form of one of three capsomeres (A, B, or C), which dimerize (A:B and C:C) to form the 30–40 nm (10 MDa) icosahedral (triangulation number=3) capsid, characterized by 32 cup-shaped indentations [47,48]. The VP1 protein contains two domains: protruding (P) and shell (S) [49]. The P domain is further classified into the P1 (amino acids 226-278 and 406-520) and P2 (amino acids 279-405) subdomains, of which P2 is responsible for virus binding to the host cell [48,50]. VP2 regulates VP1 expression in *cis* [51] and provides interior structural support [52-55]. VP2 is required for feline calicivirus infections [56], possibly because it forms a portal to facilitate genome trafficking out of endosomes and into the cytosol [57]. However, other caliciviruses do not require VP2 [58] and it remains unclear whether or not VP2 is required for HuNoV infections.

2.2 Infection Features

HuNoV causes acute gastroenteritis typified by watery diarrhea and vomiting. HuNoV infections may be transmitted by consumption of contaminated food, water, contact with HuNoV-containing surfaces, or person-to-person transmission through fomites [59-65]. Epidemics arise due to the low infectious dose and short incubation period associated with infection. Experimentally a 50%

infectious dose (ID_{50}) of 18 virions was established for GI.1 Norwalk virus [66], although there were limitations with this study and the ID_{50} is likely closer to 1.32×10^3–2.80×10^3 viral particles [67]. To date, no ID_{50} for humans has been reported for GII.4 HuNoVs. Although a particle to plaque-forming unit (PFU) ratio has not been elucidated for HuNoV, the ratio for MuNoV has been reported at between 100–10,000 genome equivalents (g.e.)/PFU, a value similar to picornaviruses (1,000 g.e./PFU) [67]. Upon ingestion of the virus, a brief incubation period (24–48h) [68-70] is followed by a symptomatic period of 12–60h [69-71]. Antigen detection in the stool occurs as early as 1 day post-infection (dpi), although never before the onset of symptoms [72]. Viral replication is presumed to occur in the duodenum and jejunum of the small intestine based on histopathologies such as intact mucosa with villous blunting, villous shortening, crypt hypertrophy, increased epithelia apoptosis rate, and increased lamina propria cellularity [73-79]. Abnormal mucosal histopathology is visible before clinical symptoms and persists for multiple days after symptoms have resolved [73,77]. Epithelial [80-82] and immune [83,84] cells have been implicated as the potential sites for *in vivo* infection, but the precise cellular tropism for HuNoV remains unclear. M-cells facilitate MuNoV access to immune cells in basal intestinal compartments such as Peyer's patches and the lamina propria [85]. The delivery of HuNoV by multivesicular body-derived exosomes has also been demonstrated [86]. Furthermore, exosome-associated viruses may be more infectious than naked viral particles [86]. Interestingly, one study found that MuNoV could remain infectious in the intestines for 24h without crossing the epithelial barrier or

replicating [87]. HuNoV RNA has been detected in sera [88-91] (<25% of cases) and cerebral spinal fluid [89,91] of symptomatic patients but infection of tissues outside of the intestinal tract has not been proven. The presence of HuNoV RNA in the blood may be associated with higher levels of virus shedding [88,90]. Virus shedding begins at the onset of symptoms and although symptoms are generally short-lived, virus shedding can occur over a month in healthy individuals [67,92-94]. Virus shedding is known to exceed 10^9 particles/gram of stool and 10^6 particles/mL of vomit [95]. Asymptomatic infections are quite prominent [70,96,97] and it remains unclear whether or not asymptomatic individuals shed as much virus as their symptomatic counterparts [98-100]. However, symptomatic individuals generate more robust IgG and IgA antibody responses than asymptomatic individuals [101,102].

When hygienic practices are neglected, high viral titers can persist. Routine drinking water chlorination levels (typically <1.0 part per million (ppm)) may be inadequate for HuNoV inactivation as levels up to 6.25 ppm have failed to stop HuNoV replication [72,103,104]. Chlorine levels of 10 ppm [72,103] or 50 ppm [104] were needed to inactivate HuNoV. The Centers for Disease Control (CDC) and the Environmental Protection Agency state that chlorination levels below 4 ppm are considered safe for consumption. Washing hands with soap and water has been shown to remove HuNoV particles more effectively than alcohol-based hand sanitizers [105]. The simple flushing of a toilet generates aerosols that present another avenue for exposure to HuNoV [95]. How hands are dried after washing also affects the dispersion of HuNoV particles [106]. An increased rate of

HuNoV transfer under wet conditions, as opposed to dry conditions, further highlights the importance of proper handwashing and drying [107]. These compounding factors, and many others, have allowed HuNoVs to become the leading cause of acute gastroenteritis and foodborne illness worldwide [22,108-113].

2.3 Burden

Children, the elderly, and the immunocompromised are predominantly susceptible to severe disease. HuNoVs can infect infants multiple times within their first year of life [100,114,115]. A vaccine would most benefit children, up to age 5 [110], as globally this age group suffers an estimated 70,000 HuNoV-related deaths annually [116]. Given the high infection rates of children, it is not surprising that seropositivity approaches 100% for adults [117,118]. While young adults are typically the least affected by HuNoV, the reemergence of a GII.17 HuNoV in the winter of 2015 was detrimental to this age group [119]. The elderly are at increased risk for HuNoV-associated severe disease, likely because of waning immunity and the need for close quarters assisted living. Long-term care facilities are the most common locale for HuNoV outbreaks (62.5%) [60]. Furthermore, 90% of HuNoV-associated deaths in the United States occur in patients older than 65 years of age [120,121]. Persistently infected immunocompromised individuals maintain a larger pool of viral quasispecies than acutely infected individuals [122]. Emergent pandemic strains were thought to originate from persistently infected immunocompromised individuals [123,124], however recent findings refute this

claim [125] as well as the claim that immunocompromised patients maintain HuNoV populations with higher mutation burdens [126]. Therefore, the reservoir for emerging pandemic strains is still in question.

HuNoVs cause ~700 million infections and ~220,000 deaths annually [116]. This results in an economic burden of ~$64.5 billion, mostly from loss of productivity [116]. In the United States alone, there are 21 million cases annually resulting in 2 million hospital visits and 800 deaths [121,127,128]. HuNoV outbreaks display a winter seasonality with 63–84% of cases occurring between October and April in the United States [121,129,130]. Spontaneous cases arise, but most are associated with outbreaks (basic reproduction rate (R_0)=1.64–2.90) [131-133], especially during cold, dry months. HuNoV outbreaks are discernable from those caused by other gastrointestinal pathogens using the Kaplan criteria (99% specificity and 77% sensitivity) [71,134]. To fulfill these criteria the outbreak should consist of the following clinical and epidemiological characteristics: (1) ≥50% of affected persons should present with vomiting, (2) have a mean (or median) incubation period of 24–48h, (3) have a mean (or median) duration of illness of 12–60h, and (4) stools are negative for bacterial or parasitic pathogens [71,134]. In the United States, HuNoV outbreaks are reported to CaliciNet for epidemiological purposes [135]. CaliciNet data has been published for 2009–2013 [60] and 2009–2016 [130]. 83.7% of outbreaks with a known transmission route were caused by person-to-person transmission, while only 16.1% were food-borne. The outbreaks were mainly concentrated in long-term care facilities (62.5%), restaurants (9.8%), and schools (5.7%). GII HuNoVs caused the majority

of outbreaks (89%), with the remaining 11% caused by GI HuNoVs. 72% of all outbreaks were caused by GII.4 viruses, of which, 94% were the direct result of the circulating pandemic strains, GII.4 New Orleans or GII.4 Sydney.

2.4 GII.4 HuNoVs and Pandemics

A GII.4 HuNoV was the first detected pandemic strain isolated in 1995 (GII.4 US95–96) [2]. Pandemic GII.4 strains then emerged every 2–3 years beginning with GII.4 Farmington Hills (2002), GII.4 Hunter (2004), GII.4 Yerseke, and GII.4 Den Haag (2006), GII.4 New Orleans (2009), and GII.4 Sydney (2012) [2,136]. Since 2001, all GII.4 pandemic strains have encoded an RdRp mutation that increases the incorporation rate of nucleotides, facilitating rapid progeny generation [46]. It is thought that the first four pandemics arose due to antigenic drift through mutations within the P2 domain of the capsid [136]. VP1 nucleotide substitutions occur at a rate of 4.3×10^{-3} substitutions/site/year for GII.4 HuNoVs [5], which is in line with other estimates [119]. Primarily, these mutations map to receptor blockade epitopes [46,137]. As little as a 5% difference in the VP1 amino acid sequence may have drastic effects on the host's ability to protect against infection [138]. The more recent pandemics, New Orleans (2009) and Sydney (2012), may have evolved through both antigenic drift as well as antigenic shift via recombination at the ORF1-ORF2 interface [136]. To monitor the emergence of novel strains, recommendations have been made to report both RdRp (ORF1) and VP1 (ORF2) sequence information to identify novel recombinants [139]. The

current circulating strain is a recombinant of the GII.4 Sydney pandemic strain (GII.P16/GII.4 Sydney 2012) that emerged as early as 2014 [140,141].

GII.4 HuNoVs undergo epochal evolution, by which an emerging strain becomes dominant, effectively replacing the previous circulating strain [142-144]. GI and other GII genotype HuNoVs do not appear to evolve via epochal evolution and have remained relatively static for decades [117,145]. The evolution of GII.4 HuNoVs correlates with increased mutation rate, antigenic space, and herd immunity [137], leading to their dominant prevalence worldwide [146]. GII.4 HuNoVs in particular have evolved novel binding patterns to their cellular attachment factors, histo-blood group antigens (HBGAs).

2.5 Histo-blood Group Antigens

HBGAs constitute a group of O-linked carbohydrate structures that are constructed in a stepwise manner by monosaccharide addition by fucosyltransferases and glycosyltransferases [147]. Nine different HBGAs have been shown to interact with HuNoVs, including the A-, B-, and H-antigens, and Lewis A, B, X, and Y carbohydrates [125,148,149]. Most notable are the interactions between HuNoVs and the ABO blood group members (A-, B-, and H-antigens). Classically, fucosyltransferase 1 (FUT1) catalyzes the transfer of fucose to a quadrasaccharide chain (glucose-galactose-N-acetylglucosamine-galactose) generating the H-antigen that is expressed on red blood cells. The ABO blood gene encodes for the HBG ABO system governing whether glycosyltransferases add either a terminal N-acetylgalactosamine (Type A) or galactose (Type B) to the H-

antigen. No additional ornamentation results in a Type O individual that expresses the H-antigen. Fucosyltransferase 2 (FUT2) enzymatic activity causes the secretion of the H-antigen and its presentation on epithelial cells along mucosal surfaces [24]. Expression of the autosomal dominant *FUT2* gene (*FUT2*$^{+/+}$ or *FUT2*$^{+/-}$) classifies an individual as a secretor or secretor-positive. Individuals that lack a functional *FUT2* or are *FUT2*$^{-/-}$ are termed non-secretors or secretor-negative. Genotypically, the homozygous single nucleotide polymorphisms G428A and A385T most commonly produce a non-functional enzyme. The G428A mutation is observed in 95% of non-secretors of European and African descent, affecting ~20% of these populations [131,150-152], and the A385T mutation is mostly observed in non-secretors of Asian descent [153,154]. Additionally, at least fifteen other rare *FUT2* polymorphisms have been reported [155].

HBGAs became implicated in HuNoV infection upon the determination that non-secretors were immune from infection with the prototype GI.1 Norwalk virus [156,157]. Norwalk virus causes infections in persons with blood type O more readily than other blood types and binds to the H- and A-antigens more efficiently than the B-antigen [156,158]. A different trend was observed for GII.17 HuNoVs in which they preferentially bound the A- and B-antigens, but not the H-antigen [119]. In contrast, a GII.4 HuNoV human challenge study and a GII.6 outbreak report found that no ABO blood group accounted for either increased or decreased susceptibility to infection [146,159]. Additionally, neither secretor status nor ABO blood group has been associated with infectivity of a GI.3 isolate, a GII.2 strain

(Snow Mountain), and two GI.3 strains (Desert Shield and VA115) [102,160-163]. Therefore, HuNoV binding to HBGAs is strain-dependent [164,165].

HBGA binding epitopes are localized to the P2 subdomain of VP1. The docking locations for HBGAs are well-conserved within genogroups but disparate between GI and GII HuNoVs [166]. Binding originates from an anti-parallel β-sheet for GI and the dimeric interface for GII HuNoVs [167]. Interestingly, the dimeric interface of MuNoV also binds bile acids [168]. It is unclear if bile acids affect HBGA binding in GII HuNoV strains [169,170]. HBGA binding to GI uses both the α-fucose and β-galactose of the carbohydrate chain, while GII binding occurs solely via the α-fucose [167]. This may explain the GI HuNoV proclivity for the H-antigen rather than the A- or B-antigens as the interaction with the β-galactose may be sterically hindered by the α-(1,3) addition of either an N-acetylgalactosamine or another galactose respectively [150]. This may partially explain the trend of GII HuNoVs having a broader HBGA binding profile. The same epitopes involved in carbohydrate binding are thought to be immunodominant drivers of antibody neutralization.

Without a direct assay to measure antibody neutralization, an HBGA blocking assay that analyzes antibody disruption of HuNoV binding to carbohydrates has been used [49,171]. These surrogate neutralizing antibody titers are termed HBGA blocking antibody titers. Hemagglutination inhibition assays have also been used to evaluate HBGA blockade [158,172,173]. From these studies six blockade epitopes have been discovered (Epitopes A–F). Epitope A is thought to be immunodominant as blocking this epitope accounts for up to

60% loss of binding to carbohydrates [137,174,175]. Evolutionarily, Epitope A appears to be the major driving factor behind escape from herd immunity of emergent GII.4 HuNoVs [137]. Epitope B is located at the dimeric interface, while Epitope C is adjacent to the HBGA binding pocket [175]. Epitope D alters the HBGA binding of GII.4 strains [144,174], Epitope E is GII.4 Farmington Hills-specific [176], and Epitope F is universally conserved in all GII.4 strains [117]. Recently, GII.4 neutralization epitopes have been mapped [172].

2.6 Vaccines

Several obstacles have prevented the licensing of a HuNoV vaccine, namely lack of a cell culture system, limited small animal models, broad viral genetic diversity, antigen drift, and lack of pre-exposure protection parameters [166,171]. Additionally, the duration and breadth of protection following natural HuNoV infection are unclear [115,131,156,177-180]. Administration of a HuNoV vaccine by 6 months of age has the potential to prevent up to 85% of pediatric HuNoV cases [180,181], thus a HuNoV vaccine could be cost saving [110]. The HuNoV vaccine field has produced several promising candidates that rely on the production of non-replicating, empty, virus-like particles (VLPs). These strategies are categorized as VLPs, P-particles, and P-dimers. The VLPs are produced in insect cells using a baculovirus system that expresses VP1 with or without VP2 [19,53,182,183]. Self-assembling HuNoV VLPs are antigenically and morphologically similar to the native viral capsids [19,147,184]. P-particles are nanoparticles produced in *Escherichia coli* that contain 24 copies of the P domain

[185]. P-dimers are also produced in *E. coli* and only contain two P1 domains linked by a central P2 domain [186].

HuNoV VLPs are antigenically similar to native capsids, safe, and immunogenic when delivered orally [182,184,187], intranasally [127,188], or intramuscularly [108,188,189]. In regards to immunogenicity, VLP immunization induces a robust IgG1 response against VP1 [184]. VLP vaccination also induces the production of serum IgA against VP1 [183-185,189-192]. VLP vaccination generates better memory IgG responses than memory IgA responses [191]. Intramuscular VLP vaccination recapitulates natural infection antibody responses except for the detection of norovirus-specific saliva IgA or fecal IgA beyond 28 days post-vaccination [99,191,193]. Similarly, oral and nasal administration do not reliably induce the production of mucosal IgA [182,187,194,195]. VLP vaccination with a mucosal adjuvant enhances mucosal immunity in large [194,196] and small animal models [186,187,195,197,198]. Although different assays were performed, the intramuscular administration of VLPs showed an increased percentage of memory IgG B cells when compared to oral administration [191]. Interestingly, secretor status does not affect early humoral responses, but a secretor-positive phenotype has been associated with increased persistence of memory antibodies at late time-points (6 months post-VLP vaccination) [117,171]. Currently, the two most promising VLP vaccine candidates are a non-replicating adenovirus-vectored oral GI.1 vaccine [199-201], and an intramuscular bivalent GI.1 and GII.4 vaccine [202], having completed phase I and phase II clinical trials, respectively.

The bivalent vaccine is comprised of a GI.I VLP and a GII.4 VLP that contains consensus sequences from Houston, Yerseke, and Den Haag strains [188,190]. Phase I trials demonstrated that injection of a cocktail containing 50 μg of each VLP adjuvanted by 50 μg of 3-O-desacyl-4'-monophosphoryl lipid A (MPLA) and 500 μg of aluminum hydroxide yielded the highest antibody titers and was selected for further evaluation [190]. Further formulation optimization yielded a final cocktail of 15 μg of GI.1 VLP, 50 μg of GII.4 VLP, and 500 μg of aluminum hydroxide [192]. MPLA did not enhance immune responses to the vaccine or non-vaccine strains in adults (18–85+ years of age) [192,203,204]. A subsequent heterologous (GII.4 Farmington Hill) challenge phase I–II study showed that this vaccine significantly reduced the severity of gastrointestinal disease [108]. No boosting effect has been shown upon the administration of a second dose 28 days after the first dose [108,190,192,204]. Of note, vaccination also elicits increased antibody titers against non-vaccine antigens [203]. Phase II clinical trials are currently underway to evaluate the long-term durability of antibody responses [205].

Several reports have shown that HuNoV P-particles do not trigger T cell production of interferon lambda (IFN-λ) or cross-reactive B and T cell responses [206] and they inefficiently present important surface epitopes [176]. However, P-particle vaccination provides a unique opportunity for vaccination against multiple pathogens. Each of the 24 P domains within the P-particle contains 3 surface-exposed loops each of which can be engineered to present a peptide antigen. This system has been utilized to develop dual-vaccines against influenza virus (HA and

M2e) [207,208] and rotavirus (VP8) [209]. Additionally, edible P-particle vaccines, grown in genetically modified tobacco and potato plants, are safe and immunogenic [210]. Success in developing a HuNoV vaccine is predicated on a strong understanding of HuNoV immune responses.

HBGA blocking antibody titers and HuNoV-specific serum IgA titers are correlates of protection from HuNoV infection [211-213]. HBGA blocking titers >200 have been associated with a reduction in symptoms and HuNoV infection [117,213]. Additionally, HBGA-blocking antibody titers correlate with neutralizing antibody titers [214]. Detection of GII.4-specific IgA has been linked with decreased risk of infection and illness [213]. However, other human infection studies (GI.1) determined that pre-existing IgA levels did not correlate with protection from infection [101,215]. Production of memory IgG correlates with HBGA blockade titers and serum IgA levels but has not been established as a correlate of protection yet [216]. This may be due to more specific targeting of serum IgA antibodies to neutralizing epitopes [189]. None of these represent fully penetrant immunological correlates of protection and therefore are considered correlates of risk [217]. Currently, the field's understanding of the adaptive immune response does not fully explain whether an individual will become infected or not. Nonetheless, MuNoV studies demonstrate that B cells and $CD4^+$ T cells have crucial roles in protection from infection, while $CD8^+$ T cell responses may be ancillary [138,218].

2.7 Innate Immune Responses to Infection

Innate immune responses to MuNoV infection have provided valuable insight into how NoVs replicate and some of the methods used in response to these infections. The predominant contributors in the innate immune response to NoVs are IFNs [219]. Mice lacking IFN-α, IFN-β, and IFN-λ receptors displayed increased MuNoV titers in secondary infection sites such as the brain and lungs [218]. This effect was shown to be dose-dependent because substantial lethality was only observed when larger doses of MuNoV were administered to *IFN-α$^{-/-}$β$^{-/-}$* receptor KO mice [218]. Also, exogenous addition of IFN-λ to *IFN-α$^{-/-}$β$^{-/-}$γ$^{-/-}$* receptor KO mice prevented MuNoV infection and transmission [220]. Alternatively, contrasting results showed that *IFN-α$^{-/-}$β$^{-/-}$* or *IFN-γ$^{-/-}$* receptor KO mice were similarly likely to die from MuNoV infection as wild type controls [221]. However, one study reported that type I IFNs are not required for protection from MuNoV-3 infection [138]. Analysis of chemokine [222,223] and cytokine [223] responses have also been characterized for MuNoV infection *in vitro*. These studies highlighted the complexity of the innate immune response when considering viral strain differences.

Cytokine analysis of human patients experiencing acute HuNoV infections has been examined for GI.1 and GII.2 viruses [98,224]. In these studies, infection with GI.1 Norwalk virus resulted in significantly elevated levels of IFN-γ, interleukin 2 (IL-2), IL-6, IL-8, IL-10, IL-12p70, tumor necrosis factor α (TNF-α), and the chemokine, C-C motif chemokine ligand 2 (CCL2) [98,224]. Serum cytokine levels began to increase at 24 hours post-infection (hpi) and persisted until 48hpi. IL-8

and TNF-α levels remained significant at 72hpi and IL-10 levels persisted to 4dpi, possibly suggesting early B cell maturation [224]. Infected asymptomatic patients maintained significantly lower levels of IFN-γ, IL-1β, IL-1RA, IL-2, IL-4, IL-6, IL-8, IL-10, and TNF-β compared to symptomatic patients [98]. No pre-vaccination serum cytokines were predictive of the duration of HuNoV shedding [98]. However, daily levels of IL-6 were positively associated with HuNoV RNA shedding, while daily levels of IL-12-p40 were negatively associated with HuNoV RNA shedding [98]. Finally, no difference in viral shedding titers was reported between symptomatic and asymptomatic patients suggesting that symptoms may be related to the immune response to HuNoV infection [98]. This is consistent with the roles of CCL2, IL-6, and IL-8 in causing inflammation due to innate immune cell recruitment, and intestinal damage and dysfunction [224]. Experimental infection with a GII.2 HuNoV increased IFN-γ, IL-2, and IL-5 production at 8 or 21dpi [102], while individuals naturally infected with a GII.2 HuNoV, had increased levels of IFN-γ, TNF-α, and IL-10 secretion that persisted to 1 month post-infection [162]. The importance of cytokine responses and innate cell populations for controlling HuNoV disease is unclear.

2.8 Antibody Responses to Infection

Volunteer studies using GI.1 Norwalk virus were invaluable for providing insight into early antibody responses to infection. IgM was detected at 7dpi and peaked by 10–15dpi [101,215,225]. Peak IgM titers dropped by 53% at 28–30dpi [215]. Despite the decrease in virus-specific IgM, its presence has been detected

out to 5 months post-infection [101]. IgG seroconversion occurs by 8–14dpi but was delayed (≥15dpi) in asymptomatic patients [101,102]. IgG titers remained constant following seroconversion [72,215] and primarily belong to the IgG1 subclass [102]. Additionally, seroconversion of IgG in the absence of IgM seroconversion was rare [225]. Serum IgA titers peaked between 10–13dpi and waned by 28–30dpi [102,215]. Symptomatic patients typically mount stronger, longer-lasting IgM, IgG, and IgA responses than their asymptomatic counterparts [101,225]. Some HuNoV antibodies cross-react within genogroups [102,145,156,226-228]. Antibody cross-reactivity has been suggested as a reason why pre-infection serum antibody levels determined by ELISA are not predictive of infection status or antibody responses [102,212,225]. While experimental human infection studies have provided valuable information about virus-host interactions, they do not nullify the necessity for robust HuNoV models.

2.9 Large Animal Models

Efforts to develop large animal models of HuNoV infection began with unsuccessful attempts to infect non-human primates (NHPs), e.g. rhesus monkeys and baboons, with HuNoV [229,230]. It was discovered that chimpanzees produce serum antibodies and shed virus upon oral HuNoV infection but do not develop gastroenteritis [229]. A single passage of HuNoV in chimpanzees did not alter virus shedding, symptom presentation, or antibody production, indicating a lack of adaptation to the chimpanzee host [229]. Intravenous (i.v.) administration of HuNoV resulted in asymptomatic infection and antibody responses that were

dominated by serum IgM and IgG [231]. HuNoV was shed in the feces at similar times following oral or i.v. infection, but the duration of shedding was increased in i.v. infected chimpanzees. Viremia was not detected at any time-points, although viral RNAs were detectable in liver tissue. Interestingly, HuNoV antigens were detected in the duodenum, jejunum, and lamina propria (dendritic cells (DCs)) despite no histological changes to the intestines [231]. Lastly, an ID_{50} of 4.0×10^{7} g.e. was established for i.v. infection of chimpanzees [231]. Regulations and a lack of disease presentation limit the utility of the chimpanzee model for HuNoV studies.

Adult and neonatal pigtail macaques are susceptible to HuNoV infection [232]. The onset of virus shedding and its duration, as well as the presence and duration of diarrhea, are similar between adults and neonates [232]. In one study, an adult pigtail macaque vomited during the study, a symptom not previously observed in any other HuNoV animal model [232]. Evaluation of the pigtail macaque animal model may be useful if these animals consistently display symptomatic diarrhea and vomiting because of HuNoV infection. Experimental oral infection of other NHPs (common marmosets, cotton-top tamarins, and cynomolgus macaques) did not induce the production of HuNoV-specific antibodies or robust virus shedding [233]. However, a single rhesus macaque from this study shed virus for over 2 weeks and maintained robust IgG titers until the end of the experimental time-course [233].

Gnotobiotic (Gn) piglets develop diarrhea, shed virus, and have detectable levels of HuNoV in the intestines upon oral infection [234-240]. Although low, HuNoV-specific serum and mucosal antibodies have been reported in Gn piglets

[240]. Additionally, HuNoV remains infectious after two passages in Gn piglets [234]. Like chimpanzees, the passage of HuNoV in Gn piglets did not improve any infection parameters. An ID_{50} for oral HuNoV infection of Gn piglets has been established at $<2.74\times10^3$ g.e for 4–5-day old piglets and 6.43×10^4 g.e. for 33–34-day old piglets [236]. The Gn piglet model has been used to test adjuvanted HuNoV VLPs [196] and inactivation of HuNoV by high-pressure processing [241]. Work with the Gn piglet model has also been expanded to include *RAG2*$^{-/-}$*IL2RG*$^{-/-}$ double KO piglets that experience prolonged HuNoV antigen retention in the intestines and asymptomatic virus shedding [237]. In contrast, piglet models with natural flora, such as the miniature piglet model, lack substantial disease presentation [242]. Simvastatin, a cholesterol-reducing statin, has been shown to increase HuNoV infectivity and disease in the Gn piglet model [236,243]. These results strengthen a report that statin use is a risk factor for enhanced HuNoV disease in humans [244]. Simvastatin has immunosuppressive properties and has been linked to the downregulation of IFN-α and MHC II expression [236,243]. Oral administration of IFN-α to HuNoV-infected Gn piglets delayed the onset of virus shedding and decreased its duration [243]. The Gn piglet model has also been used to study how human gut microbiota [245] and individual commensal bacteria affect HuNoV replication *in vivo* [246]. Colonization with a healthy human gut microbiota increased titers shed and the duration of shedding but delayed the onset of diarrhea compared to uncolonized Gn piglets [245]. Colonization of the Gn piglet gut with a single bacterial species, the HBGA-expressing *Enterobacter cloacae*, inhibited HuNoV replication and virus shedding, possibly because HuNoV

binds to HBGAs on the bacteria rather than their target eukaryotic cells [246]. This result contrasts with an *in vitro* study that showed *E. cloacae* enhanced HuNoV infection [83]. The effects of gastrointestinal bacteria (both commensal and pathogenic) on enteric viral infections represent important considerations relevant for HuNoV animal model development [247-249]. Furthermore, HuNoV infection of HBGA-typed Gn piglets has been studied [250].

Gn calves develop diarrhea and shed HuNoV for up to 6 days after oral infection [251]. Additionally, HuNoV antigen is readily detectable in enterocytes and the lamina propria of infected calves [251]. Notably, intestinal damage and intestinal/serum IgA and IgG production are observed in this animal model [251]. Collectively, the pigtail macaque, Gn piglet, and Gn calf models represent the most promising large animal models for HuNoV.

2.10 Small Animal Models

Attempts to infect adult and suckling mice, kittens, guinea pigs, or rabbits with HuNoV have been unsuccessful [229,230]. To date, the only mammalian small animal model described is a recombination activation gene (*Rag*$^{-/-}$) and common gamma chain ($\gamma c^{-/-}$) deficient BALB/c mouse [252]. The double KO supported a mixed culture of GII HuNoVs through intraperitoneal (i.p.) but not oral infection. Interestingly, dual administration (oral and i.p.) increased viral loads above those observed after i.p. injection alone [252]. The *Rag*$^{-/-}\gamma c^{-/-}$ BALB/c mouse model has been implemented to demonstrate the antiviral properties of the nucleoside analog, 2'-C-methylcytidine (2CMC), *in vivo* [253]. Commercially

available wild type BALB/c and *Rag*$^{-/-}\gamma c^{-/-}$ C57BL/6J×C57BL/10SgSnAi mice do not support HuNoV replication [252].

Zebrafish larvae have been shown to replicate both GI and GII HuNoVs, with 2CMC treatment substantially decreasing replication [254]. Although HuNoVs can be passaged in this model, limitations exist namely the infection route requires injection of exceptionally high titer viruses into the larval yolk, infections are asymptomatic, and virus shedding has not been successfully detected.

2.11 Reverse Genetic Systems

It has been shown that HuNoV RNA isolated from stool can produce all of the structural and nonstructural proteins upon transfection into either Huh7 or Caco-2 cells [24]. Although virions are produced, the infection does not spread to non-transfected cells indicating blocks at the receptor binding or uncoating stages [24]. Although inefficient, 100–150 positive cells could be detected after transfecting 5.0×10^8 HuNoV RNA molecules into 10^5 cells [24]. This observation initiated the development of HuNoV reverse genetics. The first report of a HuNoV replicon system utilized a recombinant Vaccinia virus strain, modified Vaccinia Ankara, to drive a T7 promoter-controlled plasmid containing a GI.1 Norwalk virus full-length clone in HEK293T cells [25]. This system produced approximately 8.5×10^4 HuNoV particles from 12 T-75 flasks [25]. The first GII HuNoV infectious clone was created shortly after using a similar Vaccinia virus T7 promoter system with the GII.3 U201 strain in HEK293T cells [255]. The particles formed using this system were found to be less dense than naturally isolated HuNoV (1.32 g/cm^3

versus 1.39–1.40 g/cm^3). With both methods, Vaccinia caused HuNoV-independent cytopathic effects at 72hpi, limiting the utility of these systems.

Subsequently, a helper virus-free GI.1 Norwalk virus system was developed [41]. *In vitro* transcription of a plasmid using Vaccinia-T7 produced a recombinant RNA that contained the full-length genome with a neomycin resistance gene inserted into the VP1 gene. The transfection of this recombinant RNA produced the nonstructural proteins and VP2. Disruption of the VP1 gene prevents the use of this system to isolate infectious virus because the major capsid protein is compromised. This system was successfully used to transfect Huh7 and BHK21 cells, but not Vero, 293, 293T, or LLC-PK cells [41]. The transfected cells remained stably transfected after at least 100 passages, with levels of 2.6×10^{11} g.e./1 µg of RNA and 8.0×10^{8} g.e./1 µg of RNA produced in Huh7 and BHK21 cells, respectively. Implementation of this system was used to determine that Norwalk virus was sensitive to 72h treatment with IFN-α (effective dose 50% (ED_{50}) levels of 2 units/mL and 20 units/mL for Huh7 and BHK21 cells, respectively) [41]. Another study using this system demonstrated that Norwalk virus produced in Huh7 cells was also sensitive to IFN-γ, ribavirin, and mycophenolic acid [256]. Nucleoside analog inhibition of viral transcription by 2CMC [122] or 7-deaza-2'-C-methyladenosine [257] treatment decreased Norwalk virus production in this replicon system. Additionally, a GI.1 Norwalk virus replicon-expressing human gastric tumor-1 system was adapted from the Huh7 system to explore the development of resistance to rupintrivir, a viral protease inhibitor [258].

The first true helper virus-free system used the mammalian EF-1α promoter to drive HuNoV RNA production [22]. This system also supported infectious MuNoV production [22]. Originally developed for the GII.3 U201 strain, production of full-length genomes per 10^6 cells were 8.0×10^4, 1.4×10^4, 2.4×10^2, and 1.3×10^1 copies in COS7, 293T, Huh7, and Caco-2 cells, respectively. As evidenced by MuNoV production using this system, HuNoV virion production may be up to 10-fold less than corresponding RNA levels [22]. Differences in virus production levels can be explained by the transformed cell lines (COS7 and HEK293T) expressing the SV40 T antigen, which helps drive the SV40 promoter in the expression system [22]. The utility of this system was enhanced by adding a GFP gene between the NTPase and p22 HuNoV genes, creating a GFP reporter infectious clone [22]. However, insertion of the GFP gene resulted in up to 50-fold fewer HuNoV virions being produced [22]. Despite an inability to detect the capsid proteins by Western blot or immunofluorescence assays, an ORF2 GFP reporter plasmid indicated that the structural proteins were being produced [22]. Unfortunately, attempts to adapt the system to GI.1 NV68, GII.P4-GII.3 chimera TCH04-577, and GII.4 Saga1 viruses resulted in 10- to 1,000-fold less HuNoV production [22]. Although the HuNoV RNA from these recombinant virions is infectious upon transfection, the infectivity of the virions has not been tested [22].

Clinical relevancy of HuNoV reverse genetic systems was an issue until the development of a GII.4 Sydney 2012 infectious clone [259]. Structural proteins were readily detected upon transfection of the plasmid into Caco-2 cells [259]. Insertion of a GFP sequence between the NTPase and p22 viral genes generated

a fluorescent reporter system. However, this negatively affected viral structural protein synthesis, through an unknown mechanism, as previously observed [22,259]. The utility and robustness of this system remain unclear as studies quantifying virus production and demonstrating the passage of the recombinant virions still need to be completed.

The adoption of all current HuNoV reverse genetic systems is impeded by their inefficient virus recovery [260-262]. Further studies are needed to develop a robust HuNoV reverse genetics system to provide a platform for rationally designed live-attenuated HuNoV vaccines. The lack of a HuNoV reverse genetics system consequently puts more pressure on the search to uncover a suitable *in vitro* cell culture system.

2.12 Cell Culture Systems

Attempts to discover a cell line that could support HuNoV culminated in an exhaustive effort in 2004 [263]. A total of 27 cell lines were tested against a panel of 33 HuNoVs spanning GI and GII under multiple experimental conditions. Neither virus replication nor HuNoV-mediated CPE were reported. The first report of *in vitro* HuNoV replication came in 2007 [264]. Infection of fully differentiated 3 dimensional (3D) INT-407 cells with GI and GII HuNoVs produced microvilli shortening and an increase in reverse transcription-polymerase chain reaction (RT-PCR) viral RNA levels at 24hpi. However, this work could not be reproduced [265,266]. For example, one group noted that ~1% of virions were associated with the cells and that the majority of them were not intracellular [265]. Another group

cited the lack of specific carbohydrates as the reason that the 3D INT-407 model did not replicate HuNoVs [266]. The researchers acknowledged the inability of others to reproduce their work while simultaneously reporting GI.1 and GII.4 HuNoV replication in 3D Caco-2 cells [267]. 2–3 $\log_{10}$ increases in viral titers were noted at the 72hpi time-point with undetectable levels of replication occurring within the first 48h [267]. The 3D Caco-2 model had been unsuccessful in previous attempts despite all cellular characteristics hinting at its usefulness for the field [263,265]. A follow-up report demonstrated that a Caco-2 clone (C2BBe1) better supported a GII HuNoV and produced microvilli more representative of the intestinal tract [268]. These models have not been further explored or validated. A spontaneous differentiation 2D Caco-2 model following long-term culture has also yielded inconsistent HuNoV replication [269].

MuNoV infected macrophages and DCs *in vitro* [26], and macrophages, DCs, B cells, and T cells in the gut-associated lymphoid tissue and lamina propria *in vivo* [84,270-272]. B cell-deficient mice also support lower MuNoV titers than wild type mice [138]. Likewise, HuNoV antigen was detected in the lamina propria of experimentally infected chimpanzees and gnotobiotic calves, possibly suggesting infection of immune cells [231,251]. While HuNoV could not be cultured in macrophages or DCs *in vitro [273]*, a GII.4 HuNoV strain could infect a human B cell line (BJAB cells) [83]. BJAB cells have been used to validate the antiviral effects of 2CMC on HuNoV replication *in vitro* [253]. The BJAB system has been incompletely optimized, as reproducibility issues exist [274]. Difficulties with the

robustness of the B cell *in vitro* system may reflect *in vivo* tropism discrepancies [275].

Human intestinal enteroids (HIEs) are currently the most robust HuNoV cell culture system [81]. Intestinal stem cells harvested from routine endoscopies are differentiated *in vitro* into untransformed HIEs that contain enterocytes, enteroendocrine, Paneth, and goblet cells. It is not clear whether HIEs contain tuft cells, a rare intestinal epithelial cell type shown to be a site of MuNoV infection *in vivo* [80]. This cell system allows for both 2D and 3D culture architectures, with 2D monolayers being used for HuNoV propagation. Stem cells harvested from each portion of the small intestine (duodenum, jejunum, and ileum) support the replication of HuNoVs, with jejunal tissues generating the highest viral titers. Cells harvested from secretor-positive individuals readily support the replication of filtered GII.4 HuNoVs. The addition of bile increases GII.4 HuNoV replication and permits GI.1, GII.3, and GII.17 HuNoV replication in HIEs. Bile acids may upregulate endosomal pathways to enhance HuNoV infection in HIEs [276]. However, bile treatment did not support GII.3 HuNoV replication in 293FT, Caco-2, Huh7, or Vero cells [81]. HIEs derived from secretor-negative individuals replicated GII.3, but not GII.4 strains [81]. Further work with HIEs has demonstrated their ability to replicate GII.1, GII.2, and GII.14 HuNoV strains in the presence of bile [104]. IFN pathways are important for HuNoV replication in HIEs as *STAT1*$^{-/-}$ increased HuNoV replication and exogenous addition of IFN-β and IFN-λ decreased virus replication [277]. Additionally, *FUT2*$^{-/-}$ in secretor-positive HIEs demonstrated its necessity for binding and replication of some HuNoV strains

[278]. HIEs have also been used to test antibody neutralization [172], evaluate exosome-mediated HuNoV delivery [86], and HuNoV inactivation by alcohol and chlorine bleach [104].

Unfortunately, neither HIEs nor BJAB cells are suitable for industrial level vaccine production due to the lack of regulatory testing on these cell culture systems [279]. The HIE model also lacks the capacity to establish well-characterized cell banks, limiting their value for vaccine production. This necessitates the exploration of HuNoV infection using a vaccine-approved cell line, such as Vero cells, to progress the HuNoV vaccine development field [280,281]. Vero cells are a kidney cell line isolated from a *Chlorocebus sabaeus* African green monkey [282]. Homozygous deletion of the *IFNα* and *IFNβ* genes renders these cells type-I IFN deficient, allowing them to support a broad spectrum of viruses [282,283]. Previous efforts to grow HuNoVs in Vero cells were not successful [81,263,269]. An attempt at developing a HuNoV replicon in Vero cells was also unsuccessful [41]. Therefore, the development of a vaccine-approved Vero cell model that supports HuNoV replication marks an exciting step forward in the NoV field.

References

1 Maurin, J. B., J. Minutes of the 5th meeting of the ICTV. 5 (Strasbourg, 1981).

2 Vinje, J. Advances in laboratory methods for detection and typing of norovirus. *Journal of clinical microbiology* **53**, 373-381, doi:10.1128/jcm.01535-14 (2015).

3 Chhabra, P. *et al.* Updated classification of norovirus genogroups and genotypes. *The Journal of general virology*, doi:10.1099/jgv.0.001318 (2019).

4 Kroneman, A. *et al.* Proposal for a unified norovirus nomenclature and genotyping. *Archives of virology* **158**, 2059-2068, doi:10.1007/s00705-013-1708-5 (2013).

5 Bok, K. *et al.* Evolutionary dynamics of GII.4 noroviruses over a 34-year period. *Journal of virology* **83**, 11890-11901, doi:10.1128/jvi.00864-09 (2009).

6 Zheng, D. P. *et al.* Norovirus classification and proposed strain nomenclature. *Virology* **346**, 312-323, doi:10.1016/j.virol.2005.11.015 (2006).

7 Taube, S. & Wobus, C. E. A novel reverse genetics system for human norovirus. *Trends in microbiology* **22**, 604-606, doi:10.1016/j.tim.2014.10.001 (2014).

8 Villabruna, N., Koopmans, M. P. G. & de Graaf, M. Animals as Reservoir for Human Norovirus. *Viruses* **11**, doi:10.3390/v11050478 (2019).

9 Chhabra, P. *et al.* Near-Complete Genome Sequences of Several New Norovirus Genogroup II Genotypes. *Genome announcements* **6**, doi:10.1128/genomeA.00007-18 (2018).

10 Wang, Q. H. *et al.* Porcine noroviruses related to human noroviruses. *Emerging infectious diseases* **11**, 1874-1881, doi:10.3201/eid1112.050485 (2005).

11 Charoenkul, K. *et al.* Human Norovirus Infection in Dogs, Thailand. *Emerging infectious diseases* **26**, 350-353, doi:10.3201/eid2602.191151 (2020).

12 Green, K. Y. *Caliciviridae: The Noroviruses*. 6th edn, Vol. 1 582–608 (Wolters Kluwer Health/Lippincott Williams & Wilkins, 2013).

13 Dolin, R. *et al.* Biological properties of Norwalk agent of acute infectious nonbacterial gastroenteritis. *Proceedings of the Society for Experimental Biology and Medicine. Society for Experimental Biology and Medicine (New York, N.Y.)* **140**, 578-583 (1972).

14 Matsui, S. M. *et al.* The isolation and characterization of a Norwalk virus-specific cDNA. *J Clin Invest* **87**, 1456-1461, doi:10.1172/jci115152 (1991).

15 Lambden, P. R., Caul, E. O., Ashley, C. R. & Clarke, I. N. Sequence and genome organization of a human small round-structured (Norwalk-like) virus. *Science* **259**, 516-519 (1993).

16 Hardy, M. E. Norovirus protein structure and function. *FEMS microbiology letters* **253**, 1-8, doi:10.1016/j.femsle.2005.08.031 (2005).

17 Blakeney, S. J., Cahill, A. & Reilly, P. A. Processing of Norwalk virus nonstructural proteins by a 3C-like cysteine proteinase. *Virology* **308**, 216-224 (2003).

18 Sosnovtsev, S. V. *et al.* Cleavage map and proteolytic processing of the murine norovirus nonstructural polyprotein in infected cells. *Journal of virology* **80**, 7816-7831, doi:10.1128/jvi.00532-06 (2006).

19 Jiang, X., Wang, M., Graham, D. Y. & Estes, M. K. Expression, self-assembly, and antigenicity of the Norwalk virus capsid protein. *Journal of virology* **66**, 6527-6532 (1992).

20 Napthine, S. *et al.* Expression of the VP2 protein of murine norovirus by a translation termination-reinitiation strategy. *PloS one* **4**, e8390, doi:10.1371/journal.pone.0008390 (2009).

21 Rohayem, J., Robel, I., Jager, K., Scheffler, U. & Rudolph, W. Protein-primed and de novo initiation of RNA synthesis by norovirus 3Dpol. *Journal of virology* **80**, 7060-7069, doi:10.1128/jvi.02195-05 (2006).

22 Katayama, K. *et al.* Plasmid-based human norovirus reverse genetics system produces reporter-tagged progeny virus containing infectious genomic RNA. *Proceedings of the National Academy of Sciences of the United States of America* **111**, E4043-4052, doi:10.1073/pnas.1415096111 (2014).

23 Qu, L. *et al.* Replication of Human Norovirus RNA in Mammalian Cells Reveals Lack of Interferon Response. *Journal of virology* **90**, 8906-8923, doi:10.1128/jvi.01425-16 (2016).

24 Guix, S. *et al.* Norwalk virus RNA is infectious in mammalian cells. *Journal of virology* **81**, 12238-12248, doi:10.1128/jvi.01489-07 (2007).

25 Asanaka, M. *et al.* Replication and packaging of Norwalk virus RNA in cultured mammalian cells. *Proceedings of the National Academy of Sciences of the United States of America* **102**, 10327-10332, doi:10.1073/pnas.0408529102 (2005).

26 Wobus, C. E. *et al.* Replication of Norovirus in cell culture reveals a tropism for dendritic cells and macrophages. *PLoS biology* **2**, e432, doi:10.1371/journal.pbio.0020432 (2004).

27 O'Donnell, T. B., Hyde, J. L., Mintern, J. D. & Mackenzie, J. M. Mouse Norovirus infection promotes autophagy induction to facilitate replication but prevents final autophagosome maturation. *Virology* **492**, 130-139, doi:10.1016/j.virol.2016.02.018 (2016).

28 Hyde, J. L. *et al.* Mouse norovirus replication is associated with virus-induced vesicle clusters originating from membranes derived from the secretory pathway. *Journal of virology* **83**, 9709-9719, doi:10.1128/jvi.00600-09 (2009).

29 Davies, C., Brown, C. M., Westphal, D., Ward, J. M. & Ward, V. K. Murine norovirus replication induces G0/G1 cell cycle arrest in asynchronously growing cells. *Journal of virology* **89**, 6057-6066, doi:10.1128/jvi.03673-14 (2015).

30 Fernandez-Vega, V. *et al.* Norwalk virus N-terminal nonstructural protein is associated with disassembly of the Golgi complex in transfected cells. *Journal of virology* **78**, 4827-4837 (2004).

31 Lee, S. *et al.* A Secreted Viral Nonstructural Protein Determines Intestinal Norovirus Pathogenesis. *Cell host & microbe* **25**, 845-857.e845, doi:10.1016/j.chom.2019.04.005 (2019).

32 Ettayebi, K. & Hardy, M. E. Norwalk virus nonstructural protein p48 forms a complex with the SNARE regulator VAP-A and prevents cell surface expression of vesicular stomatitis virus G protein. *Journal of virology* **77**, 11790-11797 (2003).

33 Sharp, T. M., Guix, S., Katayama, K., Crawford, S. E. & Estes, M. K. Inhibition of cellular protein secretion by norwalk virus nonstructural protein p22 requires a mimic of an endoplasmic reticulum export signal. *PloS one* **5**, e13130, doi:10.1371/journal.pone.0013130 (2010).

34 Sharp, T. M. *et al.* Secretory pathway antagonism by calicivirus homologues of Norwalk virus nonstructural protein p22 is restricted to noroviruses. *Virology journal* **9**, 181, doi:10.1186/1743-422x-9-181 (2012).

35 Hillenbrand, B. *et al.* Norovirus non-structural protein p20 leads to impaired restitution of epithelial defects by inhibition of actin cytoskeleton remodelling. *Scand J Gastroenterol* **45**, 1307-1319, doi:10.3109/00365521.2010.483013 (2010).

36 Pfister, T. & Wimmer, E. Polypeptide p41 of a Norwalk-like virus is a nucleic acid-independent nucleoside triphosphatase. *Journal of virology* **75**, 1611-1619, doi:10.1128/jvi.75.4.1611-1619.2001 (2001).

37 Li, T. F. *et al.* Human Norovirus NS3 has RNA Helicase and Chaperoning Activities. *Journal of virology*, doi:10.1128/jvi.01606-17 (2017).

38 Yen, J. B. *et al.* Subcellular localization and functional characterization of GII.4 norovirus-encoded NTPase. *Journal of virology*, doi:10.1128/jvi.01824-17 (2017).

39 Fritzlar, S. *et al.* Mouse Norovirus infection reduces the surface expression of MHC class I proteins and inhibits CD8+ T cell recognition and activation. *Journal of virology*, doi:10.1128/jvi.00286-18 (2018).

40 Davies, C. & Ward, V. K. Expression of the NS5 (VPg) Protein of Murine Norovirus Induces a G1/S Phase Arrest. *PloS one* **11**, e0161582, doi:10.1371/journal.pone.0161582 (2016).

41 Chang, K. O., Sosnovtsev, S. V., Belliot, G., King, A. D. & Green, K. Y. Stable expression of a Norwalk virus RNA replicon in a human hepatoma cell line. *Virology* **353**, 463-473, doi:10.1016/j.virol.2006.06.006 (2006).

42 Hosmillo, M. *et al.* Noroviruses subvert the core stress granule component G3BP1 to promote viral VPg-dependent translation. *Elife* **8**, doi:10.7554/eLife.46681 (2019).

43 May, J., Korba, B., Medvedev, A. & Viswanathan, P. Enzyme kinetics of the human norovirus protease control virus polyprotein processing order. *Virology* **444**, 218-224, doi:10.1016/j.virol.2013.06.013 (2013).

44 May, J., Viswanathan, P., Ng, K. K., Medvedev, A. & Korba, B. The p4-p2' amino acids surrounding human norovirus polyprotein cleavage sites define the core sequence regulating self-processing order. *Journal of virology* **88**, 10738-10747, doi:10.1128/jvi.01357-14 (2014).

45 Cuevas, J. M. *et al.* Human norovirus hyper-mutation revealed by ultra-deep sequencing. *Infection, genetics and evolution : journal of molecular epidemiology and evolutionary genetics in infectious diseases* **41**, 233-239, doi:10.1016/j.meegid.2016.04.017 (2016).

46 Bull, R. A., Eden, J. S., Rawlinson, W. D. & White, P. A. Rapid evolution of pandemic noroviruses of the GII.4 lineage. *PLoS pathogens* **6**, e1000831, doi:10.1371/journal.ppat.1000831 (2010).

47 Vinje, J. *et al.* ICTV Virus Taxonomy Profile: Caliciviridae. *The Journal of general virology*, doi:10.1099/jgv.0.001332 (2019).

48 Prasad, B. V. *et al.* X-ray crystallographic structure of the Norwalk virus capsid. *Science* **286**, 287-290 (1999).

49 Lucero, Y., Vidal, R. & O'Ryan, G. M. Norovirus vaccines under development. *Vaccine*, doi:10.1016/j.vaccine.2017.06.043 (2017).

50 Cao, S. *et al.* Structural basis for the recognition of blood group trisaccharides by norovirus. *Journal of virology* **81**, 5949-5957, doi:10.1128/jvi.00219-07 (2007).

51 Bertolotti-Ciarlet, A., Crawford, S. E., Hutson, A. M. & Estes, M. K. The 3' end of Norwalk virus mRNA contains determinants that regulate the expression and stability of the viral capsid protein VP1: a novel function for the VP2 protein. *Journal of virology* **77**, 11603-11615 (2003).

52 Vongpunsawad, S., Venkataram Prasad, B. V. & Estes, M. K. Norwalk Virus Minor Capsid Protein VP2 Associates within the VP1 Shell Domain. *Journal of virology* **87**, 4818-4825, doi:10.1128/jvi.03508-12 (2013).

53 Lin, Y., Fengling, L., Lianzhu, W., Yuxiu, Z. & Yanhua, J. Function of VP2 protein in the stability of the secondary structure of virus-like particles of genogroup II norovirus at different pH levels: function of VP2 protein in the stability of NoV VLPs. *Journal of microbiology (Seoul, Korea)* **52**, 970-975, doi:10.1007/s12275-014-4323-6 (2014).

54 Shoemaker, G. K. *et al.* Norwalk virus assembly and stability monitored by mass spectrometry. *Molecular & cellular proteomics : MCP* **9**, 1742-1751, doi:10.1074/mcp.M900620-MCP200 (2010).

55 Kapikian, A. Z. *et al.* Visualization by immune electron microscopy of a 27-nm particle associated with acute infectious nonbacterial gastroenteritis. *Journal of virology* **10**, 1075-1081 (1972).

56 Sosnovtsev, S. V., Belliot, G., Chang, K. O., Onwudiwe, O. & Green, K. Y. Feline calicivirus VP2 is essential for the production of infectious virions. *Journal of virology* **79**, 4012-4024, doi:10.1128/jvi.79.7.4012-4024.2005 (2005).

57 Conley, M. J. *et al.* Calicivirus VP2 forms a portal-like assembly following receptor engagement. *Nature* **565**, 377-381, doi:10.1038/s41586-018-0852-1 (2019).

58 Liu, G. *et al.* A DNA-launched reverse genetics system for rabbit hemorrhagic disease virus reveals that the VP2 protein is not essential for virus infectivity. *The Journal of general virology* **89**, 3080-3085, doi:10.1099/vir.0.2008/003525-0 (2008).

59 Bonifait, L. *et al.* Detection and quantification of airborne norovirus during outbreaks in healthcare facilities. *Clinical infectious diseases : an official publication of the Infectious Diseases Society of America* **61**, 299-304, doi:10.1093/cid/civ321 (2015).

60 Vega, E. *et al.* Genotypic and epidemiologic trends of norovirus outbreaks in the United States, 2009 to 2013. *Journal of clinical microbiology* **52**, 147-155, doi:10.1128/jcm.02680-13 (2014).

61 Kroneman, A. *et al.* Analysis of integrated virological and epidemiological reports of norovirus outbreaks collected within the Foodborne Viruses in Europe network from 1 July 2001 to 30 June 2006. *Journal of clinical microbiology* **46**, 2959-2965, doi:10.1128/jcm.00499-08 (2008).

62 Matthews, J. E. *et al.* The epidemiology of published norovirus outbreaks: a review of risk factors associated with attack rate and genogroup. *Epidemiology and infection* **140**, 1161-1172, doi:10.1017/s0950268812000234 (2012).

63 Fankhauser, R. L., Noel, J. S., Monroe, S. S., Ando, T. & Glass, R. I. Molecular epidemiology of "Norwalk-like viruses" in outbreaks of gastroenteritis in the United States. *The Journal of infectious diseases* **178**, 1571-1578 (1998).

64 Verhoef, L. *et al.* Use of norovirus genotype profiles to differentiate origins of foodborne outbreaks. *Emerging infectious diseases* **16**, 617-624, doi:10.3201/eid1604.090723 (2010).

65 Verhoef, L. *et al.* Norovirus genotype profiles associated with foodborne transmission, 1999-2012. *Emerging infectious diseases* **21**, 592-599, doi:10.3201/eid2104.141073 (2015).

66 Teunis, P. F. *et al.* Norwalk virus: how infectious is it? *Journal of medical virology* **80**, 1468-1476, doi:10.1002/jmv.21237 (2008).

67 Atmar, R. L. *et al.* Determination of the 50% human infectious dose for Norwalk virus. *The Journal of infectious diseases* **209**, 1016-1022, doi:10.1093/infdis/jit620 (2014).

68 Lee, R. M. *et al.* Incubation periods of viral gastroenteritis: a systematic review. *BMC infectious diseases* **13**, 446, doi:10.1186/1471-2334-13-446 (2013).

69 Devasia, T., Lopman, B., Leon, J. & Handel, A. Association of host, agent and environment characteristics and the duration of incubation and symptomatic periods of norovirus gastroenteritis. *Epidemiology and infection* **143**, 2308-2314, doi:10.1017/s0950268814003288 (2015).

70 Graham, D. Y. *et al.* Norwalk virus infection of volunteers: new insights based on improved assays. *The Journal of infectious diseases* **170**, 34-43, doi:10.1093/infdis/170.1.34 (1994).

71 Kaplan, J. E., Feldman, R., Campbell, D. S., Lookabaugh, C. & Gary, G. W. The frequency of a Norwalk-like pattern of illness in outbreaks of acute gastroenteritis. *American journal of public health* **72**, 1329-1332 (1982).

72 Gary, G. W. *et al.* Norwalk virus antigen and antibody response in an adult volunteer study. *Journal of clinical microbiology* **25**, 2001-2003 (1987).

73 Schreiber, D. S., Blacklow, N. R. & Trier, J. S. The mucosal lesion of the proximal small intestine in acute infectious nonbacterial gastroenteritis. *The New England journal of medicine* **288**, 1318-1323, doi:10.1056/nejm197306212882503 (1973).

74 Dolin, R., Levy, A. G., Wyatt, R. G., Thornhill, T. S. & Gardner, J. D. Viral gastroenteritis induced by the Hawaii agent. Jejunal histopathology and serologic response. *The American journal of medicine* **59**, 761-768 (1975).

75 Agus, S. G., Dolin, R., Wyatt, R. G., Tousimis, A. J. & Northrup, R. S. Acute infectious nonbacterial gastroenteritis: intestinal histopathology. Histologic and enzymatic alterations during illness produced by the Norwalk agent in man. *Annals of internal medicine* **79**, 18-25 (1973).

76 Karandikar, U. C. *et al.* Detection of human norovirus in intestinal biopsies from immunocompromised transplant patients. *The Journal of general virology* **97**, 2291-2300, doi:10.1099/jgv.0.000545 (2016).

77 Schreiber, D. S., Blacklow, N. R. & Trier, J. S. The small intestinal lesion induced by Hawaii agent acute infectious nonbacterial gastroenteritis. *The Journal of infectious diseases* **129**, 705-708, doi:10.1093/infdis/129.6.705 (1974).

78 Levy, A. G. *et al.* Jejunal adenylate cyclase activity in human subjects during viral gastroenteritis. *Gastroenterology* **70**, 321-325 (1976).

79 Troeger, H. *et al.* Structural and functional changes of the duodenum in human norovirus infection. *Gut* **58**, 1070-1077, doi:10.1136/gut.2008.160150 (2009).

80 Wilen, C. B. *et al.* Tropism for tuft cells determines immune promotion of norovirus pathogenesis. *Science* **360**, 204-208, doi:10.1126/science.aar3799 (2018).

81 Ettayebi, K. *et al.* Replication of human noroviruses in stem cell-derived human enteroids. *Science* **353**, 1387-1393, doi:10.1126/science.aaf5211 (2016).

82 Green, K. Y. *et al.* Human norovirus targets enteroendocrine epithelial cells in the small intestine. *Nature communications* **11**, 2759, doi:10.1038/s41467-020-16491-3 (2020).

83 Jones, M. K. *et al.* Enteric bacteria promote human and mouse norovirus infection of B cells. *Science* **346**, 755-759, doi:10.1126/science.1257147 (2014).

84 Grau, K. R. *et al.* The major targets of acute norovirus infection are immune cells in the gut-associated lymphoid tissue. *Nature microbiology* **2**, 1586-1591, doi:10.1038/s41564-017-0057-7 (2017).

85 Gonzalez-Hernandez, M. B. *et al.* Efficient norovirus and reovirus replication in the mouse intestine requires microfold (M) cells. *Journal of virology* **88**, 6934-6943, doi:10.1128/jvi.00204-14 (2014).

86 Santiana, M. *et al.* Vesicle-Cloaked Virus Clusters Are Optimal Units for Inter-organismal Viral Transmission. *Cell host & microbe* **24**, 208-220.e208, doi:10.1016/j.chom.2018.07.006 (2018).

87 Kolawole, A. O. *et al.* Oral Norovirus Infection Is Blocked in Mice Lacking Peyer's Patches and Mature M Cells. *Journal of virology* **90**, 1499-1506, doi:10.1128/jvi.02872-15 (2015).

88 Reymao, T. K. A. *et al.* Norovirus RNA in serum associated with increased fecal viral load in children: Detection, quantification and molecular analysis. *PloS one* **13**, e0199763, doi:10.1371/journal.pone.0199763 (2018).

89 Frange, P. *et al.* Prevalence and clinical impact of norovirus fecal shedding in children with inherited immune deficiencies. *The Journal of infectious diseases* **206**, 1269-1274, doi:10.1093/infdis/jis498 (2012).

90 Takanashi, S. *et al.* Detection, genetic characterization, and quantification of norovirus RNA from sera of children with gastroenteritis. *Journal of clinical virology : the official publication of the Pan American Society for Clinical Virology* **44**, 161-163, doi:10.1016/j.jcv.2008.11.011 (2009).

91 Ito, S. *et al.* Norovirus-associated encephalopathy. *The Pediatric infectious disease journal* **25**, 651-652, doi:10.1097/01.inf.0000225789.92512.6d (2006).

92 Atmar, R. L. *et al.* Norwalk virus shedding after experimental human infection. *Emerging infectious diseases* **14**, 1553-1557, doi:10.3201/eid1410.080117 (2008).

93 Roth, A. N. & Karst, S. M. Norovirus mechanisms of immune antagonism. *Current opinion in virology* **16**, 24-30, doi:10.1016/j.coviro.2015.11.005 (2016).

94 Gustavsson, L., Skovbjerg, S., Lindh, M., Westin, J. & Andersson, L. M. Low serum levels of CCL5 are associated with longer duration of viral shedding in norovirus infection. *Journal of clinical virology : the official publication of the Pan American Society for Clinical Virology* **69**, 133-137, doi:10.1016/j.jcv.2015.06.088 (2015).

95 Johnson, D. L., Mead, K. R., Lynch, R. A. & Hirst, D. V. Lifting the lid on toilet plume aerosol: a literature review with suggestions for future research. *American journal of infection control* **41**, 254-258, doi:10.1016/j.ajic.2012.04.330 (2013).

96 Gallimore, C. I., Cubitt, D., du Plessis, N. & Gray, J. J. Asymptomatic and symptomatic excretion of noroviruses during a hospital outbreak of gastroenteritis. *Journal of clinical microbiology* **42**, 2271-2274 (2004).

97 Miura, F., Matsuyama, R. & Nishiura, H. Estimating the Asymptomatic Ratio of Norovirus Infection During Foodborne Outbreaks With Laboratory Testing in Japan. *Journal of epidemiology*, doi:10.2188/jea.JE20170040 (2018).

98 Newman, K. L. *et al.* Norovirus in symptomatic and asymptomatic individuals: cytokines and viral shedding. *Clinical and experimental immunology* **184**, 347-357, doi:10.1111/cei.12772 (2016).

99 Ramani, S. *et al.* Mucosal and Cellular Immune Responses to Norwalk Virus. *The Journal of infectious diseases* **212**, 397-405, doi:10.1093/infdis/jiv053 (2015).

100 Hassan, F. *et al.* Viral Etiology of Acute Gastroenteritis in <2-Year-Old US Children in the Post-Rotavirus Vaccine Era. *Journal of the Pediatric Infectious Diseases Society*, doi:10.1093/jpids/piy077 (2018).

101 Gray, J. J. *et al.* Detection of immunoglobulin M (IgM), IgA, and IgG Norwalk virus-specific antibodies by indirect enzyme-linked immunosorbent assay with baculovirus-expressed Norwalk virus capsid antigen in adult volunteers challenged with Norwalk virus. *Journal of clinical microbiology* **32**, 3059-3063 (1994).

102 Lindesmith, L. *et al.* Cellular and humoral immunity following Snow Mountain virus challenge. *Journal of virology* **79**, 2900-2909, doi:10.1128/jvi.79.5.2900-2909.2005 (2005).

103 Keswick, B. H. *et al.* Inactivation of Norwalk virus in drinking water by chlorine. *Applied and environmental microbiology* **50**, 261-264 (1985).

104 Costantini, V. *et al.* Human Norovirus Replication in Human Intestinal Enteroids as Model to Evaluate Virus Inactivation. *Emerging infectious diseases* **24**, 1453-1464, doi:10.3201/eid2408.180126 (2018).

105 Tuladhar, E. *et al.* Reducing viral contamination from finger pads: handwashing is more effective than alcohol-based hand disinfectants. *The Journal of hospital infection* **90**, 226-234, doi:10.1016/j.jhin.2015.02.019 (2015).

106 Kimmitt, P. T. & Redway, K. F. Evaluation of the potential for virus dispersal during hand drying: a comparison of three methods. *Journal of applied microbiology* **120**, 478-486, doi:10.1111/jam.13014 (2016).

107 Sharps, C. P., Kotwal, G. & Cannon, J. L. Human norovirus transfer to stainless steel and small fruits during handling. *J Food Prot* **75**, 1437-1446, doi:10.4315/0362-028x.jfp-12-052 (2012).

108 Bernstein, D. I. *et al.* Norovirus vaccine against experimental human GII.4 virus illness: a challenge study in healthy adults. *The Journal of infectious diseases* **211**, 870-878, doi:10.1093/infdis/jiu497 (2015).

109 Batz, M. B., Hoffmann, S. & Morris, J. G., Jr. Ranking the disease burden of 14 pathogens in food sources in the United States using attribution data from outbreak investigations and expert elicitation. *J Food Prot* **75**, 1278-1291, doi:10.4315/0362-028x.jfp-11-418 (2012).

110 Bartsch, S. M., Lopman, B. A., Hall, A. J., Parashar, U. D. & Lee, B. Y. The potential economic value of a human norovirus vaccine for the United States. *Vaccine* **30**, 7097-7104, doi:10.1016/j.vaccine.2012.09.040 (2012).

111 Scallan, E. *et al.* Foodborne illness acquired in the United States--major pathogens. *Emerging infectious diseases* **17**, 7-15, doi:10.3201/eid1701.P11101 (2011).

112 Payne, D. C. *et al.* Norovirus and medically attended gastroenteritis in U.S. children. *The New England journal of medicine* **368**, 1121-1130, doi:10.1056/NEJMsa1206589 (2013).

113 Halasa, N. *et al.* The Changing Landscape of Pediatric Viral Enteropathogens in the Post-Rotavirus Vaccine Era. *Clinical infectious diseases : an official publication of the Infectious Diseases Society of America*, doi:10.1093/cid/ciaa100 (2020).

114 Blazevic, V. *et al.* Development and maturation of norovirus antibodies in childhood. *Microbes and infection* **18**, 263-269, doi:10.1016/j.micinf.2015.12.004 (2016).

115 Blazevic, V. *et al.* Multiple consecutive norovirus infections in the first 2 years of life. *European journal of pediatrics* **174**, 1679-1683, doi:10.1007/s00431-015-2591-8 (2015).

116 Bartsch, S. M., Lopman, B. A., Ozawa, S., Hall, A. J. & Lee, B. Y. Global Economic Burden of Norovirus Gastroenteritis. *PloS one* **11**, e0151219, doi:10.1371/journal.pone.0151219 (2016).

117 Lindesmith, L. C. *et al.* Broad blockade antibody responses in human volunteers after immunization with a multivalent norovirus VLP candidate vaccine: immunological analyses from a phase I clinical trial. *PLoS medicine* **12**, e1001807, doi:10.1371/journal.pmed.1001807 (2015).

118 Kirby, A. E. *et al.* Norovirus Seroprevalence among Adults in the United States: Analysis of NHANES Serum Specimens from 1999-2000 and 2003-2004. *Viruses* **12**, doi:10.3390/v12020179 (2020).

119 Chan, M. C. *et al.* Rapid emergence and predominance of a broadly recognizing and fast-evolving norovirus GII.17 variant in late 2014. *Nature communications* **6**, 10061, doi:10.1038/ncomms10061 (2015).

120 Cardemil, C. V., Parashar, U. D. & Hall, A. J. Norovirus Infection in Older Adults: Epidemiology, Risk Factors, and Opportunities for Prevention and Control. *Infectious disease clinics of North America*, doi:10.1016/j.idc.2017.07.012 (2017).

121 Hall, A. J. *et al.* Norovirus disease in the United States. *Emerging infectious diseases* **19**, 1198-1205, doi:10.3201/eid1908.130465 (2013).

122 Rocha-Pereira, J. *et al.* The viral polymerase inhibitor 2'-C-methylcytidine inhibits Norwalk virus replication and protects against norovirus-induced diarrhea and mortality in a mouse model. *Journal of virology* **87**, 11798-11805, doi:10.1128/jvi.02064-13 (2013).

123 de Graaf, M., van Beek, J. & Koopmans, M. P. Human norovirus transmission and evolution in a changing world. *Nature reviews. Microbiology* **14**, 421-433, doi:10.1038/nrmicro.2016.48 (2016).

124 Karst, S. M. & Baric, R. S. What is the reservoir of emergent human norovirus strains? *Journal of virology* **89**, 5756-5759, doi:10.1128/jvi.03063-14 (2015).

125 Doerflinger, S. Y. *et al.* Human Norovirus Evolution in a Chronically Infected Host. *mSphere* **2**, doi:10.1128/mSphere.00352-16 (2017).

126 Vega, E. *et al.* RNA populations in immunocompromised patients as reservoirs for novel norovirus variants. *Journal of virology* **88**, 14184-14196, doi:10.1128/jvi.02494-14 (2014).

127 Atmar, R. L. *et al.* Norovirus vaccine against experimental human Norwalk Virus illness. *The New England journal of medicine* **365**, 2178-2187, doi:10.1056/NEJMoa1101245 (2011).

128 Burke, R. M. *et al.* The Burden of Norovirus in the United States, as Estimated Based on Administrative Data: Updates for Medically Attended Illness and Mortality, 2001 - 2015. *Clinical infectious diseases : an official*

publication of the Infectious Diseases Society of America, doi:10.1093/cid/ciaa438 (2020).

129 Osuka, H., Hall, A. J., Wikswo, M. E., Baker, J. M. & Lopman, B. A. Temporal Relationship Between Healthcare-Associated and Nonhealthcare-Associated Norovirus Outbreaks and Google Trends Data in the United States. *Infection control and hospital epidemiology* **39**, 355-358, doi:10.1017/ice.2017.322 (2018).

130 Burke, R. M. *et al.* The Norovirus Epidemiologic Triad: Predictors of Severe Outcomes in US Norovirus Outbreaks, 2009-2016. *The Journal of infectious diseases*, doi:10.1093/infdis/jiy569 (2018).

131 Simmons, K., Gambhir, M., Leon, J. & Lopman, B. Duration of immunity to norovirus gastroenteritis. *Emerging infectious diseases* **19**, 1260-1267, doi:10.3201/eid1908.130472 (2013).

132 Solano, R. *et al.* Person-to-person transmission of norovirus resulting in an outbreak of acute gastroenteritis at a summer camp. *Eur J Gastroenterol Hepatol* **26**, 1160-1166, doi:10.1097/meg.0000000000000179 (2014).

133 O'Dea, E. B., Pepin, K. M., Lopman, B. A. & Wilke, C. O. Fitting outbreak models to data from many small norovirus outbreaks. *Epidemics* **6**, 18-29, doi:10.1016/j.epidem.2013.12.002 (2014).

134 Turcios, R. M., Widdowson, M. A., Sulka, A. C., Mead, P. S. & Glass, R. I. Reevaluation of epidemiological criteria for identifying outbreaks of acute gastroenteritis due to norovirus: United States, 1998-2000. *Clinical*

infectious diseases : an official publication of the Infectious Diseases Society of America **42**, 964-969, doi:10.1086/500940 (2006).

135 Vega, E. *et al.* Novel surveillance network for norovirus gastroenteritis outbreaks, United States. *Emerging infectious diseases* **17**, 1389-1395, doi:10.3201/eid1708.101837 (2011).

136 White, P. A. Evolution of norovirus. *Clinical microbiology and infection : the official publication of the European Society of Clinical Microbiology and Infectious Diseases* **20**, 741-745, doi:10.1111/1469-0691.12746 (2014).

137 Debbink, K. *et al.* Emergence of new pandemic GII.4 Sydney norovirus strain correlates with escape from herd immunity. *The Journal of infectious diseases* **208**, 1877-1887, doi:10.1093/infdis/jit370 (2013).

138 Zhu, S. *et al.* Identification of immune and viral correlates of norovirus protective immunity through comparative study of intra-cluster norovirus strains. *PLoS pathogens* **9**, e1003592, doi:10.1371/journal.ppat.1003592 (2013).

139 Tohma, K., Lepore, C. J., Ford-Siltz, L. A. & Parra, G. I. Phylogenetic Analyses Suggest that Factors Other Than the Capsid Protein Play a Role in the Epidemic Potential of GII.2 Norovirus. *mSphere* **2**, doi:10.1128/mSphereDirect.00187-17 (2017).

140 Lun, J. H. *et al.* Recombinant GII.P16/GII.4 Sydney 2012 Was the Dominant Norovirus Identified in Australia and New Zealand in 2017. *Viruses* **10**, doi:10.3390/v10100548 (2018).

141 Ruis, C. *et al.* The emerging GII.P16-GII.4 Sydney 2012 norovirus lineage is circulating worldwide, arose by late-2014 and contains polymerase changes that may increase virus transmission. *PloS one* **12**, e0179572, doi:10.1371/journal.pone.0179572 (2017).

142 Zhang, J. *et al.* Genotype distribution of norovirus around the emergence of Sydney_2012 and the antigenic drift of contemporary GII.4 epidemic strains. *Journal of clinical virology : the official publication of the Pan American Society for Clinical Virology* **72**, 95-101, doi:10.1016/j.jcv.2015.09.009 (2015).

143 Siebenga, J. J. *et al.* Epochal evolution of GGII.4 norovirus capsid proteins from 1995 to 2006. *Journal of virology* **81**, 9932-9941, doi:10.1128/jvi.00674-07 (2007).

144 Lindesmith, L. C. *et al.* Mechanisms of GII.4 norovirus persistence in human populations. *PLoS medicine* **5**, e31, doi:10.1371/journal.pmed.0050031 (2008).

145 Parra, G. I. *et al.* Static and Evolving Norovirus Genotypes: Implications for Epidemiology and Immunity. *PLoS pathogens* **13**, e1006136, doi:10.1371/journal.ppat.1006136 (2017).

146 Frenck, R. *et al.* Predicting susceptibility to norovirus GII.4 by use of a challenge model involving humans. *The Journal of infectious diseases* **206**, 1386-1393, doi:10.1093/infdis/jis514 (2012).

147 Tan, M. *et al.* Mutations within the P2 domain of norovirus capsid affect binding to human histo-blood group antigens: evidence for a binding pocket. *Journal of virology* **77**, 12562-12571 (2003).

148 Koromyslova, A. D., Leuthold, M. M., Bowler, M. W. & Hansman, G. S. The sweet quartet: Binding of fucose to the norovirus capsid. *Virology* **483**, 203-208, doi:10.1016/j.virol.2015.04.006 (2015).

149 Carmona-Vicente, N., Allen, D. J., Rodriguez-Diaz, J., Iturriza-Gomara, M. & Buesa, J. Antibodies against Lewis antigens inhibit the binding of human norovirus GII.4 virus-like particles to saliva but not to intestinal Caco-2 cells. *Virology journal* **13**, 82, doi:10.1186/s12985-016-0538-y (2016).

150 Marionneau, S. *et al.* Norwalk virus binds to histo-blood group antigens present on gastroduodenal epithelial cells of secretor individuals. *Gastroenterology* **122**, 1967-1977 (2002).

151 Thorven, M. *et al.* A homozygous nonsense mutation (428G-->A) in the human secretor (FUT2) gene provides resistance to symptomatic norovirus (GGII) infections. *Journal of virology* **79**, 15351-15355, doi:10.1128/jvi.79.24.15351-15355.2005 (2005).

152 Wacklin, P. *et al.* Faecal microbiota composition in adults is associated with the FUT2 gene determining the secretor status. *PloS one* **9**, e94863, doi:10.1371/journal.pone.0094863 (2014).

153 Currier, R. L. *et al.* Innate Susceptibility to Norovirus Infections Influenced by FUT2 Genotype in a United States Pediatric Population. *Clinical*

infectious diseases : an official publication of the Infectious Diseases Society of America **60**, 1631-1638, doi:10.1093/cid/civ165 (2015).

154 Hutson, A. M., Airaud, F., LePendu, J., Estes, M. K. & Atmar, R. L. Norwalk virus infection associates with secretor status genotyped from sera. *Journal of medical virology* **77**, 116-120, doi:10.1002/jmv.20423 (2005).

155 Ferrer-Admetlla, A. *et al.* A natural history of FUT2 polymorphism in humans. *Molecular biology and evolution* **26**, 1993-2003, doi:10.1093/molbev/msp108 (2009).

156 Lindesmith, L. *et al.* Human susceptibility and resistance to Norwalk virus infection. *Nature medicine* **9**, 548-553, doi:10.1038/nm860 (2003).

157 Hutson, A. M., Atmar, R. L., Graham, D. Y. & Estes, M. K. Norwalk virus infection and disease is associated with ABO histo-blood group type. *The Journal of infectious diseases* **185**, 1335-1337, doi:10.1086/339883 (2002).

158 Hutson, A. M., Atmar, R. L., Marcus, D. M. & Estes, M. K. Norwalk virus-like particle hemagglutination by binding to h histo-blood group antigens. *Journal of virology* **77**, 405-415 (2003).

159 Sharma, S. *et al.* Secretor Status is Associated with Susceptibility to Disease in a Large GII.6 Norovirus Foodborne Outbreak. *Food and environmental virology*, doi:10.1007/s12560-019-09410-3 (2019).

160 Huang, P. *et al.* Norovirus and histo-blood group antigens: demonstration of a wide spectrum of strain specificities and classification of two major

binding groups among multiple binding patterns. *Journal of virology* **79**, 6714-6722, doi:10.1128/jvi.79.11.6714-6722.2005 (2005).

161 Nordgren, J., Sharma, S., Kambhampati, A., Lopman, B. & Svensson, L. Innate Resistance and Susceptibility to Norovirus Infection. *PLoS pathogens* **12**, e1005385, doi:10.1371/journal.ppat.1005385 (2016).

162 Lindesmith, L. C. *et al.* Virus-Host Interactions Between Nonsecretors and Human Norovirus. *Cell Mol Gastroenterol Hepatol*, doi:10.1016/j.jcmgh.2020.03.006 (2020).

163 Nordgren, J., Kindberg, E., Lindgren, P. E., Matussek, A. & Svensson, L. Norovirus gastroenteritis outbreak with a secretor-independent susceptibility pattern, Sweden. *Emerging infectious diseases* **16**, 81-87, doi:10.3201/eid1601.090633 (2010).

164 Liao, Y., Xue, L., Gao, J., Wu, A. & Kou, X. ABO blood group-associated susceptibility to norovirus infection: A systematic review and meta-analysis. *Infection, genetics and evolution : journal of molecular epidemiology and evolutionary genetics in infectious diseases*, 104245, doi:10.1016/j.meegid.2020.104245 (2020).

165 Halperin, T. *et al.* No association between histo-blood group antigens and susceptibility to clinical infections with genogroup II norovirus. *The Journal of infectious diseases* **197**, 63-65, doi:10.1086/524145 (2008).

166 Debbink, K., Lindesmith, L. C. & Baric, R. S. The state of norovirus vaccines. *Clinical infectious diseases : an official publication of the*

Infectious Diseases Society of America **58**, 1746-1752, doi:10.1093/cid/ciu120 (2014).

167 Choi, J. M., Hutson, A. M., Estes, M. K. & Prasad, B. V. Atomic resolution structural characterization of recognition of histo-blood group antigens by Norwalk virus. *Proceedings of the National Academy of Sciences of the United States of America* **105**, 9175-9180, doi:10.1073/pnas.0803275105 (2008).

168 Nelson, C. A. *et al.* Structural basis for murine norovirus engagement of bile acids and the CD300lf receptor. *Proceedings of the National Academy of Sciences of the United States of America*, doi:10.1073/pnas.1805797115 (2018).

169 Kilic, T., Koromyslova, A. & Hansman, G. S. Structural Basis for Human Norovirus Capsid Binding to Bile Acids. *Journal of virology* **93**, doi:10.1128/jvi.01581-18 (2019).

170 Creutznacher, R. *et al.* Chemical-Shift Perturbations Reflect Bile Acid Binding to Norovirus Coat Protein: Recognition Comes in Different Flavors. *Chembiochem* **21**, 1007-1021, doi:10.1002/cbic.201900572 (2020).

171 Lindesmith, L. C. *et al.* Impact of Pre-exposure History and Host Genetics on Antibody Avidity Following Norovirus Vaccination. *The Journal of infectious diseases* **215**, 984-991, doi:10.1093/infdis/jix045 (2017).

172 Alvarado, G. *et al.* Human Monoclonal Antibodies That Neutralize Pandemic GII.4 Noroviruses. *Gastroenterology*, doi:10.1053/j.gastro.2018.08.039 (2018).

173 Czako, R. *et al.* Serum hemagglutination inhibition activity correlates with protection from gastroenteritis in persons infected with Norwalk virus. *Clinical and vaccine immunology : CVI* **19**, 284-287, doi:10.1128/cvi.05592-11 (2012).

174 Debbink, K., Donaldson, E. F., Lindesmith, L. C. & Baric, R. S. Genetic mapping of a highly variable norovirus GII.4 blockade epitope: potential role in escape from human herd immunity. *Journal of virology* **86**, 1214-1226, doi:10.1128/jvi.06189-11 (2012).

175 Lindesmith, L. C. *et al.* Immunogenetic mechanisms driving norovirus GII.4 antigenic variation. *PLoS pathogens* **8**, e1002705, doi:10.1371/journal.ppat.1002705 (2012).

176 Lindesmith, L. C. *et al.* Monoclonal antibody-based antigenic mapping of norovirus GII.4-2002. *Journal of virology* **86**, 873-883, doi:10.1128/jvi.06200-11 (2012).

177 Parrino, T. A., Schreiber, D. S., Trier, J. S., Kapikian, A. Z. & Blacklow, N. R. Clinical immunity in acute gastroenteritis caused by Norwalk agent. *The New England journal of medicine* **297**, 86-89, doi:10.1056/nejm197707142970204 (1977).

178 Johnson, P. C., Mathewson, J. J., DuPont, H. L. & Greenberg, H. B. Multiple-challenge study of host susceptibility to Norwalk gastroenteritis in US adults. *The Journal of infectious diseases* **161**, 18-21 (1990).

179 LoBue, A. D. *et al.* Multivalent norovirus vaccines induce strong mucosal and systemic blocking antibodies against multiple strains. *Vaccine* **24**, 5220-5234, doi:10.1016/j.vaccine.2006.03.080 (2006).

180 Lopman, B. A. *et al.* Norovirus Infection and Disease in an Ecuadorian Birth Cohort: Association of Certain Norovirus Genotypes With Host FUT2 Secretor Status. *The Journal of infectious diseases* **211**, 1813-1821, doi:10.1093/infdis/jiu672 (2015).

181 Shioda, K., Kambhampati, A., Hall, A. J. & Lopman, B. A. Global age distribution of pediatric norovirus cases. *Vaccine* **33**, 4065-4068, doi:10.1016/j.vaccine.2015.05.051 (2015).

182 Tacket, C. O., Sztein, M. B., Losonsky, G. A., Wasserman, S. S. & Estes, M. K. Humoral, mucosal, and cellular immune responses to oral Norwalk virus-like particles in volunteers. *Clinical immunology (Orlando, Fla.)* **108**, 241-247 (2003).

183 El-Kamary, S. S. *et al.* Adjuvanted intranasal Norwalk virus-like particle vaccine elicits antibodies and antibody-secreting cells that express homing receptors for mucosal and peripheral lymphoid tissues. *The Journal of infectious diseases* **202**, 1649-1658, doi:10.1086/657087 (2010).

184 Ball, J. M. *et al.* Recombinant Norwalk virus-like particles given orally to volunteers: phase I study. *Gastroenterology* **117**, 40-48 (1999).

185 Baehner, F., Bogaerts, H. & Goodwin, R. Vaccines against norovirus: state of the art trials in children and adults. *Clinical microbiology and infection : the official publication of the European Society of Clinical Microbiology and Infectious Diseases* **22 Suppl 5**, S136-s139, doi:10.1016/j.cmi.2015.12.023 (2016).

186 Verma, V. *et al.* Norovirus (NoV) specific protective immune responses induced by recombinant P dimer vaccine are enhanced by the mucosal adjuvant FlaB. *Journal of translational medicine* **14**, 135, doi:10.1186/s12967-016-0899-4 (2016).

187 Ball, J. M., Hardy, M. E., Atmar, R. L., Conner, M. E. & Estes, M. K. Oral immunization with recombinant Norwalk virus-like particles induces a systemic and mucosal immune response in mice. *Journal of virology* **72**, 1345-1353 (1998).

188 Parra, G. I. *et al.* Immunogenicity and specificity of norovirus Consensus GII.4 virus-like particles in monovalent and bivalent vaccine formulations. *Vaccine* **30**, 3580-3586, doi:10.1016/j.vaccine.2012.03.050 (2012).

189 Onodera, T. *et al.* Immune-Focusing Properties of Virus-like Particles Improve Protective IgA Responses. *Journal of immunology (Baltimore, Md. : 1950)* **203**, 3282-3292, doi:10.4049/jimmunol.1900481 (2019).

190 Treanor, J. J. *et al.* A novel intramuscular bivalent norovirus virus-like particle vaccine candidate--reactogenicity, safety, and immunogenicity in a phase 1 trial in healthy adults. *The Journal of infectious diseases* **210**, 1763-1771, doi:10.1093/infdis/jiu337 (2014).

191 Ramani, S. *et al.* B-Cell Responses to Intramuscular Administration of a Bivalent Virus-Like Particle Human Norovirus Vaccine. *Clinical and vaccine immunology : CVI* **24**, doi:10.1128/cvi.00571-16 (2017).

192 Leroux-Roels, G. *et al.* Safety and Immunogenicity of Different Formulations of Norovirus Vaccine Candidate in Healthy Adults: A Randomized, Controlled, Double-Blind Clinical Trial. *The Journal of infectious diseases* **217**, 597-607, doi:10.1093/infdis/jix572 (2018).

193 Atmar, R. L. *et al.* An exploratory study of the salivary IgA responses to one dose of a Norovirus VLP candidate vaccine in healthy adults. *The Journal of infectious diseases*, doi:10.1093/infdis/jiy529 (2018).

194 Han, M. G., Cheetham, S., Azevedo, M., Thomas, C. & Saif, L. J. Immune responses to bovine norovirus-like particles with various adjuvants and analysis of protection in gnotobiotic calves. *Vaccine* **24**, 317-326, doi:10.1016/j.vaccine.2005.07.071 (2006).

195 Heinimaki, S., Malm, M., Vesikari, T. & Blazevic, V. Parenterally Administered Norovirus GII.4 Virus-Like Particle Vaccine Formulated with Aluminum Hydroxide or Monophosphoryl Lipid A Adjuvants Induces Systemic but Not Mucosal Immune Responses in Mice. *Journal of immunology research* **2018**, 3487095, doi:10.1155/2018/3487095 (2018).

196 Souza, M., Costantini, V., Azevedo, M. S. & Saif, L. J. A human norovirus-like particle vaccine adjuvanted with ISCOM or mLT induces cytokine and antibody responses and protection to the homologous GII.4 human

norovirus in a gnotobiotic pig disease model. *Vaccine* **25**, 8448-8459, doi:10.1016/j.vaccine.2007.09.040 (2007).

197 Hwang, H. S. *et al.* More robust gut immune responses induced by combining intranasal and sublingual routes for prime-boost immunization. *Human vaccines & immunotherapeutics*, 1-9, doi:10.1080/21645515.2018.1472185 (2018).

198 Guerrero, R. A. *et al.* Recombinant Norwalk virus-like particles administered intranasally to mice induce systemic and mucosal (fecal and vaginal) immune responses. *Journal of virology* **75**, 9713-9722, doi:10.1128/jvi.75.20.9713-9722.2001 (2001).

199 Singh, K. H. a. S. 2 (Vaxart, 2017).

200 Sterling, L. *Phase 1 Placebo-controlled, Randomized Trial of an Adenoviral-vector Based Norovirus Vaccine*, <https://clinicaltrials.gov/ct2/show/NCT02868073> (2016).

201 Kim, L. *et al.* Safety and immunogenicity of an oral tablet norovirus vaccine, a phase I randomized, placebo-controlled trial. *JCI insight* **3**, doi:10.1172/jci.insight.121077 (2018).

202 Limited, T. P. C. (Osaka, Japan, 2016).

203 Haynes, J. *et al.* In Depth Breadth Analyses of Human Blockade Responses to Norovirus and Response to Vaccination. *Viruses* **11**, doi:10.3390/v11050392 (2019).

204 Treanor, J. *et al.* A phase 2 study of the bivalent VLP norovirus vaccine candidate in older adults; impact of MPL adjuvant or a second dose. *Vaccine*, doi:10.1016/j.vaccine.2020.06.011 (2020).

205 *Long-Term Immunogenicity of the Norovirus GI.1/GII.4 Bivalent Virus-like Particle (VLP) Vaccine (NoV Vaccine) in Adults*, <https://ClinicalTrials.gov/show/NCT03039790> (2017).

206 Tamminen, K. *et al.* A comparison of immunogenicity of norovirus GII-4 virus-like particles and P-particles. *Immunology* **135**, 89-99, doi:10.1111/j.1365-2567.2011.03516.x (2012).

207 Xia, M. *et al.* A candidate dual vaccine against influenza and noroviruses. *Vaccine* **29**, 7670-7677, doi:10.1016/j.vaccine.2011.07.139 (2011).

208 Elaish, M. *et al.* Protective immunity against influenza virus challenge by norovirus P particle-M2e and HA2-AtCYN vaccines in chickens. *Vaccine*, doi:10.1016/j.vaccine.2019.08.082 (2019).

209 Tan, M. *et al.* Norovirus P particle, a novel platform for vaccine development and antibody production. *Journal of virology* **85**, 753-764, doi:10.1128/jvi.01835-10 (2011).

210 Mason, H. S. *et al.* Expression of Norwalk virus capsid protein in transgenic tobacco and potato and its oral immunogenicity in mice. *Proceedings of the National Academy of Sciences of the United States of America* **93**, 5335-5340 (1996).

211 Knoll, B. M., Lindesmith, L. C., Yount, B. L., Baric, R. S. & Marty, F. M. Resolution of diarrhea in an immunocompromised patient with chronic

norovirus gastroenteritis correlates with constitution of specific antibody blockade titer. *Infection* **44**, 551-554, doi:10.1007/s15010-016-0875-1 (2016).

212 Reeck, A. *et al.* Serological correlate of protection against norovirus-induced gastroenteritis. *The Journal of infectious diseases* **202**, 1212-1218, doi:10.1086/656364 (2010).

213 Atmar, R. L. *et al.* Serological Correlates of Protection against a GII.4 Norovirus. *Clinical and vaccine immunology : CVI* **22**, 923-929, doi:10.1128/cvi.00196-15 (2015).

214 Atmar, R. L. *et al.* Comparison of Microneutralization and Histo-blood Group Antigen-Blocking Assays for Functional Norovirus Antibody Detection. *The Journal of infectious diseases*, doi:10.1093/infdis/jiz526 (2019).

215 Erdman, D. D., Gary, G. W. & Anderson, L. J. Serum immunoglobulin A response to Norwalk virus infection. *Journal of clinical microbiology* **27**, 1417-1418 (1989).

216 Ramani, S., Estes, M. K. & Atmar, R. L. Correlates of Protection against Norovirus Infection and Disease-Where Are We Now, Where Do We Go? *PLoS pathogens* **12**, e1005334, doi:10.1371/journal.ppat.1005334 (2016).

217 Qin, L., Gilbert, P. B., Corey, L., McElrath, M. J. & Self, S. G. A framework for assessing immunological correlates of protection in vaccine trials. *The Journal of infectious diseases* **196**, 1304-1312, doi:10.1086/522428 (2007).

218 Thackray, L. B. *et al.* Critical role for interferon regulatory factor 3 (IRF-3) and IRF-7 in type I interferon-mediated control of murine norovirus replication. *Journal of virology* **86**, 13515-13523, doi:10.1128/jvi.01824-12 (2012).

219 Dang, W. *et al.* IRF-1, RIG-I and MDA5 display potent antiviral activities against norovirus coordinately induced by different types of interferons. *Antiviral research* **155**, 48-59, doi:10.1016/j.antiviral.2018.05.004 (2018).

220 Rocha-Pereira, J. *et al.* Interferon lambda (IFN-lambda) efficiently blocks norovirus transmission in a mouse model. *Antiviral research* **149**, 7-15, doi:10.1016/j.antiviral.2017.10.017 (2017).

221 Karst, S. M., Wobus, C. E., Lay, M., Davidson, J. & Virgin, H. W. t. STAT1-dependent innate immunity to a Norwalk-like virus. *Science* **299**, 1575-1578, doi:10.1126/science.1077905 (2003).

222 Waugh, E., Chen, A., Baird, M. A., Brown, C. M. & Ward, V. K. Characterization of the chemokine response of RAW264.7 cells to infection by murine norovirus. *Virus research* **181**, 27-34, doi:10.1016/j.virusres.2013.12.025 (2014).

223 Enosi Tuipulotu, D., Netzler, N. E., Lun, J. H., Mackenzie, J. M. & White, P. A. RNA Sequencing of Murine Norovirus-Infected Cells Reveals Transcriptional Alteration of Genes Important to Viral Recognition and Antigen Presentation. *Frontiers in immunology* **8**, 959, doi:10.3389/fimmu.2017.00959 (2017).

224 Newman, K. L. *et al.* Human norovirus infection and the acute serum cytokine response. *Clinical and experimental immunology* **182**, 195-203, doi:10.1111/cei.12681 (2015).

225 Cukor, G., Nowak, N. A. & Blacklow, N. R. Immunoglobulin M responses to the Norwalk virus of gastroenteritis. *Infection and immunity* **37**, 463-468 (1982).

226 Hale, A. D. *et al.* Identification of an epitope common to genogroup 1 "norwalk-like viruses". *Journal of clinical microbiology* **38**, 1656-1660 (2000).

227 Kitamoto, N. *et al.* Cross-reactivity among several recombinant calicivirus virus-like particles (VLPs) with monoclonal antibodies obtained from mice immunized orally with one type of VLP. *Journal of clinical microbiology* **40**, 2459-2465, doi:10.1128/jcm.40.7.2459-2465.2002 (2002).

228 Parker, T. D., Kitamoto, N., Tanaka, T., Hutson, A. M. & Estes, M. K. Identification of Genogroup I and Genogroup II broadly reactive epitopes on the norovirus capsid. *Journal of virology* **79**, 7402-7409, doi:10.1128/jvi.79.12.7402-7409.2005 (2005).

229 Wyatt, R. G. *et al.* Experimental infection of chimpanzees with the Norwalk agent of epidemic viral gastroenteritis. *Journal of medical virology* **2**, 89-96 (1978).

230 Wyatt, R. G. & Zapikian, A. Z. Viral agents associated with acute gastroenteritis in humans. *Am J Clin Nutr* **30**, 1857-1870, doi:10.1093/ajcn/30.11.1857 (1977).

231 Bok, K. *et al.* Chimpanzees as an animal model for human norovirus infection and vaccine development. *Proceedings of the National Academy of Sciences of the United States of America* **108**, 325-330, doi:10.1073/pnas.1014577107 (2011).

232 Subekti, D. S. *et al.* Experimental infection of Macaca nemestrina with a Toronto Norwalk-like virus of epidemic viral gastroenteritis. *Journal of medical virology* **66**, 400-406 (2002).

233 Rockx, B. H., Bogers, W. M., Heeney, J. L., van Amerongen, G. & Koopmans, M. P. Experimental norovirus infections in non-human primates. *Journal of medical virology* **75**, 313-320, doi:10.1002/jmv.20273 (2005).

234 Cheetham, S. *et al.* Pathogenesis of a genogroup II human norovirus in gnotobiotic pigs. *Journal of virology* **80**, 10372-10381, doi:10.1128/jvi.00809-06 (2006).

235 Takanashi, S. *et al.* Characterization of emerging GII.g/GII.12 noroviruses from a gastroenteritis outbreak in the United States in 2010. *Journal of clinical microbiology* **49**, 3234-3244, doi:10.1128/jcm.00305-11 (2011).

236 Bui, T. *et al.* Median infectious dose of human norovirus GII.4 in gnotobiotic pigs is decreased by simvastatin treatment and increased by age. *The Journal of general virology* **94**, 2005-2016, doi:10.1099/vir.0.054080-0 (2013).

237 Lei, S. *et al.* Increased and prolonged human norovirus infection in RAG2/IL2RG deficient gnotobiotic pigs with severe combined

immunodeficiency. *Scientific reports* **6**, 25222, doi:10.1038/srep25222 (2016).

238 Park, B. J. *et al.* Pathogenesis of human norovirus genogroup II genotype 4 in post-weaning gnotobiotic pigs. *Journal of microbiology and biotechnology*, doi:10.4014/jmb.1810.09061 (2018).

239 Kocher, J. *et al.* Intranasal P particle vaccine provided partial cross-variant protection against human GII.4 norovirus diarrhea in gnotobiotic pigs. *Journal of virology* **88**, 9728-9743, doi:10.1128/jvi.01249-14 (2014).

240 Souza, M., Cheetham, S. M., Azevedo, M. S., Costantini, V. & Saif, L. J. Cytokine and antibody responses in gnotobiotic pigs after infection with human norovirus genogroup II.4 (HS66 strain). *Journal of virology* **81**, 9183-9192, doi:10.1128/jvi.00558-07 (2007).

241 Lou, F. *et al.* A Gnotobiotic Pig Model for Determining Human Norovirus Inactivation by High-Pressure Processing. *Applied and environmental microbiology* **81**, 6679-6687, doi:10.1128/aem.01566-15 (2015).

242 Seo, D. J. *et al.* Experimental miniature piglet model for the infection of human norovirus GII. *Journal of medical virology*, doi:10.1002/jmv.24991 (2017).

243 Jung, K. *et al.* The effects of simvastatin or interferon-alpha on infectivity of human norovirus using a gnotobiotic pig model for the study of antivirals. *PloS one* **7**, e41619, doi:10.1371/journal.pone.0041619 (2012).

244 Rondy, M. *et al.* Norovirus disease associated with excess mortality and use of statins: a retrospective cohort study of an outbreak following a

pilgrimage to Lourdes. *Epidemiology and infection* **139**, 453-463, doi:10.1017/s0950268810000993 (2011).

245 Lei, S. *et al.* Enhanced GII.4 human norovirus infection in gnotobiotic pigs transplanted with a human gut microbiota. *The Journal of general virology*, doi:10.1099/jgv.0.001336 (2019).

246 Lei, S. *et al.* Enterobacter cloacae inhibits human norovirus infectivity in gnotobiotic pigs. *Scientific reports* **6**, 25017, doi:10.1038/srep25017 (2016).

247 Pfeiffer, J. K. & Virgin, H. W. Viral immunity. Transkingdom control of viral infection and immunity in the mammalian intestine. *Science* **351**, doi:10.1126/science.aad5872 (2016).

248 Erickson, A. K. *et al.* Bacteria Facilitate Enteric Virus Co-infection of Mammalian Cells and Promote Genetic Recombination. *Cell host & microbe* **23**, 77-88.e75, doi:10.1016/j.chom.2017.11.007 (2018).

249 Almand, E. A., Moore, M. D., Outlaw, J. & Jaykus, L. A. Human norovirus binding to select bacteria representative of the human gut microbiota. *PloS one* **12**, e0173124, doi:10.1371/journal.pone.0173124 (2017).

250 Cheetham, S. *et al.* Binding patterns of human norovirus-like particles to buccal and intestinal tissues of gnotobiotic pigs in relation to A/H histo-blood group antigen expression. *Journal of virology* **81**, 3535-3544, doi:10.1128/jvi.01306-06 (2007).

251 Souza, M., Azevedo, M. S., Jung, K., Cheetham, S. & Saif, L. J. Pathogenesis and immune responses in gnotobiotic calves after infection

with the genogroup II.4-HS66 strain of human norovirus. *Journal of virology* **82**, 1777-1786, doi:10.1128/jvi.01347-07 (2008).

252 Taube, S. *et al.* A mouse model for human norovirus. *mBio* **4**, doi:10.1128/mBio.00450-13 (2013).

253 Kolawole, A. O., Rocha-Pereira, J., Elftman, M. D., Neyts, J. & Wobus, C. E. Inhibition of human norovirus by a viral polymerase inhibitor in the B cell culture system and in the mouse model. *Antiviral research* **132**, 46-49, doi:10.1016/j.antiviral.2016.05.011 (2016).

254 Van Dycke, J. *et al.* A robust human norovirus replication model in zebrafish larvae. *PLoS pathogens* **15**, e1008009, doi:10.1371/journal.ppat.1008009 (2019).

255 Katayama, K., Hansman, G. S., Oka, T., Ogawa, S. & Takeda, N. Investigation of norovirus replication in a human cell line. *Archives of virology* **151**, 1291-1308, doi:10.1007/s00705-005-0720-9 (2006).

256 Chang, K. O. & George, D. W. Interferons and ribavirin effectively inhibit Norwalk virus replication in replicon-bearing cells. *Journal of virology* **81**, 12111-12118, doi:10.1128/jvi.00560-07 (2007).

257 Van Dycke, J. *et al.* A Single Nucleoside Viral Polymerase Inhibitor Against Norovirus, Rotavirus, and Sapovirus-Induced Diarrhea. *The Journal of infectious diseases* **218**, 1753-1758, doi:10.1093/infdis/jiy398 (2018).

258 Kitano, M., Hosmillo, M., Emmott, E., Lu, J. & Goodfellow, I. Selection and Characterization of Rupintrivir-Resistant Norwalk Virus Replicon Cells in

vitro. *Antimicrobial agents and chemotherapy*, doi:10.1128/aac.00201-18 (2018).

259 Oliveira, L. M. *et al.* Development of an infectious clone and replicon system of norovirus GII.4. *J Virol Methods* **258**, 49-53, doi:10.1016/j.jviromet.2018.05.011 (2018).

260 Chaudhry, Y., Skinner, M. A. & Goodfellow, I. G. Recovery of genetically defined murine norovirus in tissue culture by using a fowlpox virus expressing T7 RNA polymerase. *The Journal of general virology* **88**, 2091-2100, doi:10.1099/vir.0.82940-0 (2007).

261 Ward, V. K. *et al.* Recovery of infectious murine norovirus using pol II-driven expression of full-length cDNA. *Proceedings of the National Academy of Sciences of the United States of America* **104**, 11050-11055, doi:10.1073/pnas.0700336104 (2007).

262 Yunus, M. A., Chung, L. M., Chaudhry, Y., Bailey, D. & Goodfellow, I. Development of an optimized RNA-based murine norovirus reverse genetics system. *J Virol Methods* **169**, 112-118, doi:10.1016/j.jviromet.2010.07.006 (2010).

263 Duizer, E. *et al.* Laboratory efforts to cultivate noroviruses. *The Journal of general virology* **85**, 79-87, doi:10.1099/vir.0.19478-0 (2004).

264 Straub, T. M. *et al.* In vitro cell culture infectivity assay for human noroviruses. *Emerging infectious diseases* **13**, 396-403, doi:10.3201/eid1303.060549 (2007).

265 Takanashi, S. *et al.* Failure of propagation of human norovirus in intestinal epithelial cells with microvilli grown in three-dimensional cultures. *Archives of virology* **159**, 257-266, doi:10.1007/s00705-013-1806-4 (2014).

266 Herbst-Kralovetz, M. M. *et al.* Lack of norovirus replication and histo-blood group antigen expression in 3-dimensional intestinal epithelial cells. *Emerging infectious diseases* **19**, 431-438, doi:10.3201/eid1903.121029 (2013).

267 Straub, T. M. *et al.* Human norovirus infection of caco-2 cells grown as a three-dimensional tissue structure. *Journal of water and health* **9**, 225-240 (2011).

268 Straub, T. M. *et al.* Defining cell culture conditions to improve human norovirus infectivity assays. *Water science and technology : a journal of the International Association on Water Pollution Research* **67**, 863-868, doi:10.2166/wst.2012.636 (2013).

269 Oka, T. *et al.* Attempts to grow human noroviruses, a sapovirus, and a bovine norovirus in vitro. *PloS one* **13**, e0178157, doi:10.1371/journal.pone.0178157 (2018).

270 Grau, K. R. *et al.* The intestinal regionalization of acute norovirus infection is regulated by the microbiota via bile acid-mediated priming of type III interferon. *Nature microbiology* **5**, 84-92, doi:10.1038/s41564-019-0602-7 (2020).

271 Basic, M. *et al.* Norovirus triggered microbiota-driven mucosal inflammation in interleukin 10-deficient mice. *Inflammatory bowel diseases* **20**, 431-443, doi:10.1097/01.MIB.0000441346.86827.ed (2014).

272 Mumphrey, S. M. *et al.* Murine norovirus 1 infection is associated with histopathological changes in immunocompetent hosts, but clinical disease is prevented by STAT1-dependent interferon responses. *Journal of virology* **81**, 3251-3263, doi:10.1128/jvi.02096-06 (2007).

273 Lay, M. K. *et al.* Norwalk virus does not replicate in human macrophages or dendritic cells derived from the peripheral blood of susceptible humans. *Virology* **406**, 1-11, doi:10.1016/j.virol.2010.07.001 (2010).

274 Jones, M. K. *et al.* Human norovirus culture in B cells. *Nature protocols* **10**, 1939-1947, doi:10.1038/nprot.2015.121 (2015).

275 Brown, J. R., Gilmour, K. & Breuer, J. Norovirus Infections Occur in B-Cell-Deficient Patients. *Clinical infectious diseases : an official publication of the Infectious Diseases Society of America* **62**, 1136-1138, doi:10.1093/cid/ciw060 (2016).

276 Murakami, K. *et al.* Bile acids and ceramide overcome the entry restriction for GII.3 human norovirus replication in human intestinal enteroids. *Proceedings of the National Academy of Sciences of the United States of America* **117**, 1700-1710, doi:10.1073/pnas.1910138117 (2020).

277 Hosmillo, M. *et al.* Norovirus Replication in Human Intestinal Epithelial Cells Is Restricted by the Interferon-Induced JAK/STAT Signaling Pathway

and RNA Polymerase II-Mediated Transcriptional Responses. *mBio* **11**, doi:10.1128/mBio.00215-20 (2020).

278 Haga, K. *et al.* Genetic Manipulation of Human Intestinal Enteroids Demonstrates the Necessity of a Functional Fucosyltransferase 2 Gene for Secretor-Dependent Human Norovirus Infection. *mBio* **11**, doi:10.1128/mBio.00251-20 (2020).

279 WHO. Recommendations for the evaluation of animal cell cultures as substrates for the manufacture of biological medicinal products and for the characterization of cells banks. Report No. 978, 79-187 (Geneva, 2013).

280 Sheets, R. History and Characterization of the Vero Cell Line. (2000).

281 IPOL - Polio Vaccine Inactivated (Monkey Kidney Cell). <https://www.fda.gov/biologicsbloodvaccines/vaccines/approvedproducts/ucm180053.htm>.

282 Osada, N. *et al.* The genome landscape of the african green monkey kidney-derived vero cell line. *DNA research : an international journal for rapid publication of reports on genes and genomes* **21**, 673-683, doi:10.1093/dnares/dsu029 (2014).

283 Desmyter, J., Melnick, J. L. & Rawls, W. E. Defectiveness of interferon production and of rubella virus interference in a line of African green monkey kidney cells (Vero). *Journal of virology* **2**, 955-961 (1968).

CHAPTER 3

HUMAN NOROVIRUS REPLICATION IN VERO CELLS[2]

[2] Todd, K. V. & Tripp, R. A. Vero Cells as a Mammalian Cell Substrate for Human Norovirus. *Viruses* **12**, doi:10.3390/v12040439 (2020). Reprinted here with permission of publisher.

Abstract

Human norovirus (HuNoV) is a principal cause of acute gastroenteritis worldwide, particularly in developing countries. Its global prevalence is underscored by more serious morbidity and some mortality in the young (<5 years) and the elderly. To date, there are no licensed vaccines or approved therapeutics for HuNoV, mostly because there are limited cell culture systems and small animal models available. Recently described cell culture systems are not ideal substrates for HuNoV vaccine development because they are not clonal or only support a single strain. In this study, we show Vero cell-based replication of two pandemic GII.4 HuNoV strains and one GII.3 strain. These data provide support for Vero cells as a cell culture model for HuNoV.

Introduction

HuNoV is a member of the *Caliciviridae* family [1] and is a non-enveloped, positive-sense, single-stranded RNA virus [2]. HuNoVs have 7.5–7.7 kb genomes that contain three open reading frames (ORFs) [3]. ORF1 codes for the six nonstructural proteins, in order from N-terminus to C-terminus: p48, NTPase, p22, VPg, 3C like protease ($3CL^{pro}$), and RNA-dependent RNA polymerase (RdRp) [4,5]. Subgenomic RNA, containing ORFs 2 and 3, codes for the major and minor structural proteins, VP1 and VP2 [6]. Noroviruses (NoVs) are subdivided into ten genogroups (GI-GX) based upon sequence homology of VP1 [7]. GI, GII, and to a lesser extent, GIV, GVIII, and GIX viruses infect humans. These genogroups are stratified into genotypes: GI (n=9), GII (n=27), GIV (n=2), GVIII (n=1), and GIX

(n=1) [7]. The GII.4 HuNoV strains account for ~70% of HuNoV infections [8]. GII.4 HuNoVs have caused pandemics and are now the major circulating strains [9-11]. Currently, a recombinant GII.4 Sydney pandemic strain (GII.P16-GII.4 Sydney) causes the majority of infections making it the most suitable strain for vaccine development [12,13].

HuNoVs are transmitted by the fecal-oral route causing acute, self-limiting infections typified by vomiting and diarrhea [14-17]. Considerable quantities of virus are shed in the feces for several weeks even after symptoms have resolved [18-21]. The stability of the viral capsid and a low infectious dose facilitate person-to-person transmission. HuNoVs cause ~700 million infections and ~219,000 deaths annually [22-24]. HuNoV infections can be debilitating particularly in developing countries where the young (<5 years), the elderly, and the immunocompromised are most susceptible.

Currently, there are no licensed vaccines or approved therapeutics for HuNoV. This is related to the lack of a characterized and reproducible mammalian cell substrate, a lack of a small animal model that emulates infection and disease, and the absence of methods to properly assess vaccine efficacy or protection [25-27]. The most progressed HuNoV vaccine candidates are subunit vaccines generated from virus-like particles (VLPs) [28-32]. Although VLP vaccines appear promising, a well-characterized mammalian cell culture substrate is required for the development of inactivated or live-attenuated HuNoV vaccines [33]. Histo-blood group antigens (HBGAs), which are terminal carbohydrates of lipid- or protein-linked glycan chains, are attachment factors for HuNoV [34]. However, it

has been shown that HBGA expression does not make a cell permissive for HuNoV infection [35]. CD300ld/CD300lf have been identified as murine NoV receptors and are the only functional receptors known for NoVs [36,37]. Recently, HuNoVs have been propagated in human intestinal enteroids (HIEs) and a human Burkitt lymphoma B cell (BJAB) cell line [38,39]. These findings are encouraging, but as HIEs are not a stable or clonal cell line, and have a limited lifespan, HIEs are unqualified for vaccine production. Also, the BJAB cell line has been reported to support only a single strain of HuNoV, require HBGA cell culture supplementation, and has reproducibility issues [39,40] making these cells inadequate for vaccine production. In contrast, Vero cells are a continuous mammalian cell line derived from an African green monkey cell line deficient for interferon-α (IFN-α) and IFN-β due to a fortuitous genetic deletion [41,42]. This feature has made Vero cells a leading cell line to use for poliovirus, rabies virus, influenza virus, and rotavirus vaccine propagation [43]. However, past attempts to propagate HuNoVs in Vero cells have been ineffective [38,44,45], possibly because the earlier studies used inadequate virus incubation times. In contrast, this study shows that Vero cells can function as a mammalian cell substrate for HuNoV. Specifically, this study shows that HuNoV modestly replicates in Vero cells as determined by indirect ELISA and quantitative reverse-transcriptase PCR (qRT-PCR) endpoint assays. We examined HuNoV genome replication of two pandemic GII.4 strains and one GII.3 strain by qRT-PCR and using indirect ELISA, flow cytometry, and immunofluorescence show that both structural and nonstructural HuNoV protein levels are increased. Additionally, we show that Vero cells were

permissive for both filtered and unfiltered clinical stool samples at a wide MOI range. These findings provide support for the use of Vero cells as a cell culture model for HuNoV replication.

Materials and Methods

Cells

Vero cells (African green monkey kidney) were obtained from the American Type Culture Collection (ATCC; CCL81.4; lot #738812; Manassas, VA, USA) and cultured at low passage at 37ºC/5% CO_2 in Dulbecco's Modified Eagle's Media (DMEM; GIBCO, Gaithersburg, MD, USA) with or without 5% heat-inactivated fetal bovine serum (FBS; HyClone, Logan, UT, USA). Caco-2 cells (HTB-37; ATCC) were cultured using DMEM supplemented with 20% FBS. The creation of a master cell line bank ensured that cells with low passage numbers were used for all experiments.

Viruses

Stool samples containing GII.3, GII.4 Sydney, or GII.4 Yerseke HuNoVs, or HuNoV-negative samples were obtained from Murdoch Children's Research Institute (MCRI; Melbourne Victoria, AUS) or the Viral Gastroenteritis Branch in the Division of Viral Diseases (DVD) at the Centers for Disease Control and Prevention (CDC, Atlanta, GA, USA) and stored at −80ºC upon receipt. Stool samples were confirmed to only have GII HuNoV using a TaqMan Array that evaluated 53 enteropathogen species and subspecies [46,47] and sequenced followed by

BLAST analysis. The stool samples were thawed on ice before making 10% (*w*/*v*) dilutions in sterile phosphate-buffered saline (PBS; HyClone). All samples were centrifuged 2× at 1500× *g* for 10 min at 4ºC then 5000× *g* for 10 min at 4ºC. Stool dilutions were passed through 100 µm and 40 µm cell strainers and filtered samples were passed through 0.45 µm or 0.20 µm filters (GE Healthcare, Chicago, IL, USA) before aliquots were made and stored at −80ºC until use.

HuNoV Genome Equivalents (g.e.) Quantification by qRT-PCR

Processed stool samples were treated with RNAzol (Molecular Research Center Inc., Cincinnati, OH, USA) according to the manufacturer's instructions to generate total RNA to be used for amplification and detection by qRT-PCR. Integrated DNA Technologies (IDT; Coralville, IA, USA) synthesized GII NoV-specific DNA primers and probes to be used with an AgPath-ID One-Step RT-PCR kit (Thermo Fisher Scientific, Waltham, MA, USA). The primers: NK2P2F (+) 5′–ATGTTCAGATGGATGAGATTCTC and NKP2R (−) 5′–TCGACGCCATCTTCATTCAC were used to amplify a segment of the HuNoV RdRp at a final reaction concentration of [300 nM] [48]. Probe-based amplification was detected by RING2-TP 5′–FAM–TGGGAGGGCGATCGCAATCT–BHQ at a final reaction concentration of [120 nM] [48]. 4.25 µL of each RNA sample were used in final reaction volumes of 12.5 µL. Reverse transcription and PCR amplification were carried out using an Mx3005P qPCR System (Agilent, Santa Clara, CA, USA) under the following cycling conditions: 45ºC for 10 min, 95ºC for 10 min, followed by 40 cycles of 95ºC for 15s, 50ºC for 30s, and 60ºC for 30s. The

resulting RdRp qRT-PCR levels are considered genome equivalents (g.e.) because the amplified site occurs once in each full-length genome. The g.e. RNA levels for the experimental time-points were divided by the mean g.e. RNA levels from the input time-point (i.e., 0h) to calculate fold-increases, normalizing the fold-change of input time-points to 1.

qRT-PCR Standard Curve and Controls

A HuNoV dsDNA standard was generated by synthesizing a 100 bp sequence that encompassed the primer and amplification sites (IDT). For each qRT-PCR run, standards containing 10^1, 10^2, 10^3, 10^4, 10^5, 10^6, and 10^7 copies/well of the amplified sequence were performed in triplicate. For experimental infection qRT-PCRs, 100 ng of Vero cell RNA was added to each standard. Additionally, no template controls (Vero cell RNA only), and no RT/polymerase controls were run in triplicate for each experiment. Wells containing unknown quantities of HuNoV were plotted against the standard curve to determine their g.e. MOI was calculated as the ratio of input g.e. to the number of cells.

HuNoV qRT-PCR

Vero cells were mock-infected or infected (MOI=1.0) with HuNoV in serum-free DMEM (SF-DMEM) before incubation at 37ºC/5% CO_2 for either 1h or 6h. The virus was removed from all wells except virus input controls and the cells were washed 2× with PBS. RNAzol was used to extract RNA from the cellular fractions

as described above. The intracellular levels of HuNoV were determined by dividing the cellular fraction g.e. by the total virus input controls across triplicate experimental and control wells.

H-Antigen ELISA

Vero cells or Caco-2 cells were grown in DMEM + 5% or DMEM + 20% FBS, respectively. Caco-2 cells were differentiated for 21 days before performing the ELISA. The media was decanted and cold 4% paraformaldehyde was added to each well and incubated for 30 min at room temperature (RT). After fixing, the cells were washed 1× with PBS and non-specific binding was blocked by the addition of PBS + 5% BSA for 1h at RT. Following incubation, a 1:1000 dilution of a mouse IgM anti-blood group H-antigen antibody (Santa Cruz Biotech, Santa Cruz, CA, USA) in PBS + 5% BSA was added to the cells overnight at 4ºC. The solution was decanted and the cells were washed 3× with KPL wash buffer (Seracare, Milford, MA, USA). A 1:2000 dilution of HRP-conjugated goat anti-mouse IgM antibody (Thermo Fisher Scientific) in PBS + 5% BSA was added to the cells for 1h at RT. The solution was decanted and washed 3× with KPL wash buffer then a 1-step TMB ELISA Substrate Solution (Thermo Fisher Scientific) was used for colorimetric visualization, before determining the optical densities (OD) at 450 nm on an Epoch Microplate Spectrophotometer (Biotek, Winooski, VT, USA).

CD300ld/CD300lf ELISA and Immunofluorescence Assay (IFA)

The H-antigen ELISA protocol was used with the following modifications: (1) a 1:100 dilution of a polyclonal rabbit anti-CD300lf antibody (Lifespan Biosciences, Seattle, WA, USA) was used as the primary antibody, and (2) a 1:1000 dilution of either a goat anti-rabbit IgG antibody conjugated to HRP (Thermo Fisher Scientific) or a goat anti-rabbit IgG (H + L) antibody conjugated to Alexa Fluor 488 (Thermo Fisher Scientific) was used as the secondary antibody. The primary antibody reacts with the ectodomains of both CD300ld and CD300lf because their amino acid sequences are highly conserved [37], meaning the ELISA and IFA likely detect both proteins.

HuNoV Infection

Cell-free supernatants from stool samples, either filtered or unfiltered, were used for infections. A virus master mixture was generated by normalizing the volume of filtered or unfiltered HuNoV for each infection condition using SF-DMEM. The media from Vero cells was decanted and infections were performed with MOI=1.0 HuNoV g.e. unless otherwise indicated. The plated cells were gently rocked before incubation at 37ºC/5% CO_2. At each experimental time-point, the HuNoV g.e. were evaluated as described above. Although included for every experiment, uninfected controls were not graphed to improve the clarity of the graphed data, and because no changes were observed in these samples. For HuNoV passage experiments, Vero cells were infected at MOI=1.0 with native

stool, freeze-thawed 2× at the indicated time-point, then freeze-thawed supernatants were transferred to fresh Vero cells for 72h.

HuNoV Inactivation

UV irradiation (Spectronics, Westbury, NY, USA) of HuNoV was performed for 1h at RT. Controls included foil-covered HuNoV to prevent inactivation, which were placed near the UV lamp for 1h at RT.

HuNoV Replication ELISA

HuNoV-infected Vero cells were freeze-thawed 2× then the supernatants were transferred to high binding ELISA plates (Corning, Corning, NY, USA) and incubated at 4ºC overnight. The plates were washed 3× with PBS before blocking 2× with SuperBlock (Thermo Fisher Scientific) for 15 min at RT. Following the incubation, a 1:1000 dilution of either a polyclonal rabbit IgG anti-VP1 antibody (Abcam, Cambridge, UK) or a polyclonal rabbit IgG anti-p48 antibody (gift from Christiane Wobus) in SuperBlock was added to the wells for 1h at 37ºC. After removal of the solution, the wells were washed 3× with KPL wash buffer and a 1:1000 dilution of HRP-conjugated goat anti-rabbit IgG antibody (Thermo Fisher Scientific) in SuperBlock was added to the wells and incubated at 37ºC for 1h. The solution was decanted and the cells were washed 3× with KPL wash buffer and a TMB ELISA Substrate Solution (Thermo Fisher Scientific) was added for colorimetric visualization. OD_{450} was read using an Epoch Microplate Spectrophotometer (Biotek).

Flow Cytometry and IFA

10^5 Vero cells were infected or mock-infected in a 24-well plate for 72h, the media decanted, and the cells washed 1× with PBS before 0.05% trypsin addition for 10 min at 37ºC /5% CO_2. DMEM + 5% FBS was added to the cells, which were gently pelleted at 200× *g* for 5 min. Supernatants were decanted and the cells suspended in Cytofix (Thermo Fisher Scientific) for 10 min at 4ºC. Cells were again pelleted at 200× *g* for 5 min and washed with PBS + 5% BSA. After washing, the cells were pelleted and resuspended in −20ºC methanol and incubated at 4ºC for 30 min. Following permeabilization, the cells were washed with PBS + 5% BSA and blocked with PBS + 5% BSA for 20 min at 4ºC. Monoclonal mouse IgG anti-VP1 (Abcam) and polyclonal rabbit IgG anti-p48 (gift from Christiane Wobus) antibodies were diluted 1:500 in PBS + 5% BSA and incubated at RT for 30 min. The primary antibodies were removed and the cells were washed 3× then resuspended in a 1:500 dilution of polyclonal PE-conjugated goat anti-mouse IgG (BD Biosciences, Franklin Lakes, NJ, USA) and Alexa Fluor 488-conjugated goat anti-rabbit IgG (Thermo Fisher Scientific) in PBS + 5% BSA for 30 min at RT. The cells were washed 3× in PBS + 5% and resuspended in PBS + 5% BSA and analyzed on an LSR II flow cytometer (BD). Data analysis was performed using FlowJo with ≥10,000 gated cells/condition. For IFA, the flow cytometry protocol was used with the following modifications: (1) cells were not trypsinized, (2) cells were fixed/permeabilized with acetone:methanol (60:40), (3) nuclei were counterstained with 4′,6-diamidino-2-phenylindole (DAPI) [1 μg/mL] (Thermo Fisher Scientific) for 15 min at RT following the secondary antibody incubation, and

(4) fluorescence images were acquired at 40× magnification using an EVOS FL imaging system (Thermo Fisher Scientific).

Statistical Analyses

Unpaired two-tailed t-tests and one-way ANOVA with Dunnett's post hoc tests were performed with 95% confidence intervals using GraphPad Prism. *p*-values < 0.05 were considered significant: * $p < 0.05$, ** $p < 0.01$, *** $p < 0.001$, and **** $p < 0.0001$. Unless otherwise indicated, $n = 3$ wells/condition/experiment from $n \geq 3$ independent experiments were performed. Error bars represent + standard error of the mean (SEM).

Results

While others were unsuccessful in propagating HuNoV in Vero cells [38,44,45], we show that low-passed Vero cells can be used as a cell substrate for HuNoV. We previously used low-passaged Vero cells in the development of vaccine substrates for several viruses [49,50]. To begin to evaluate HuNoV infection, we showed that HuNoV RNAs are present within Vero cells following a 1h or 6h incubation by qRT-PCR (Figure 3.1). HuNoVs use HBGAs, such as the H-antigen, as attachment factors [51-53], however, they are not a requirement for HuNoV infection [54-58]. We examined the level of H-antigen expression on Vero cells or Caco-2 cells and showed that Vero cells do not express the H-antigen by ELISA (Figure 3.2). Also, we showed that Vero cells express the murine NoV receptor, CD300ld/CD300lf [36,37,59] (Figures 3.3 and 3.4). We attempted to

inhibit HuNoV entry into Vero cells using antibody blockade of CD300ld/CD300lf, and by saturating of potential CD300ld/CD300lf binding sites using a CD300ld/CD300lf ectodomain peptide, but both treatments were unsuccessful. These findings are consistent with the report that CD300ld/CD300lf are not receptors for HuNoV [60].

Following the investigation of HuNoV binding, replication in Vero cells was determined and quantified by examining HuNoV genomes from infected Vero cells by qRT-PCR (Figures 3.5–3.8). In these studies, GII.4 Sydney genome replication peaked between 48-72hpi (Figure 3.5) and was ablated by UV irradiation as expected (Figure 3.6). The fold-decrease following UV-inactivated HuNoV incubation for 72h likely corresponds to the degradation of non-replicative HuNoV RNA by Vero cells (Figure 3.6). To determine if the findings for GII.4 Sydney were strain-specific, Vero cells were examined for their ability to propagate GII.3 and GII.4 Yerseke HuNoV strains (Figures 3.7 and 3.8). Of note, replication for these three HuNoV strains produced no detectable cytopathic effects at any MOI or time-points tested. To support replication, HuNoV protein expression was examined for GII.4 Sydney (Figure 3.9) and GII.3 (Figure 3.10) HuNoVs using rabbit anti-VP1 antibody indirect ELISAs. Statistically significant ($p < 0.0001$) dose-dependent detection of VP1 was observed at an input time-point (Figure 3.9). Furthermore, the ELISA showed increases in HuNoV capsid and p48, a nonstructural protein (Figures 3.9–3.11). ELISAs were evaluated instead of western blots because they are quantitative and allow for the detection of low protein levels. We also examined the expression of VP1 and p48 in HuNoV-infected Vero cells by flow cytometry

(Figure 3.12) and showed both proteins were expressed in a low percentage of cells, a result similar to the findings observed by immunofluorescence assay (Figure 3.13).

Despite evidence of a full replication cycle, prolonged incubation of HuNoV with Vero cells impedes their ability to replicate after passaging (Figure 3.14). A decreased replication potential is observed after a 12h incubation and incubation for 24h prevents HuNoV replication on fresh Vero cells (Figure 3.14). This may indicate that following virus uncoating, a new infection cycle is not initiated but this has not been experimentally confirmed. This study also examined the tempo and peak of HuNoV replication from filtered or unfiltered stool samples. There were no substantial differences detected suggesting that bacteria or other filterable agents from stool samples did not facilitate HuNoV replication (Figure 3.15), contrary to culturing HuNoVs in BJAB cells [39]. Additionally, HuNoV replication in Vero cells was similar for a wide MOI range (1.0–100) (Figure 3.16).

Discussion

We re-examined HuNoV replication in Vero cells to clarify whether Vero cells could be used in HuNoV vaccine development. A comparable attempt at using Vero cells did not increase the g.e. of HuNoV following infection likely because later time-points (4–9 dpi) were evaluated [45], which likely missed the peak HuNoV replication (Figure 3.5). We found that for all HuNoV strains tested, virus attachment to Vero cells was low ranging from 2-4%, a finding consistent with a previous report [61]. Cell-surface expression of CD300ld/CD300lf on Vero cells

was unexpected because it had only been previously observed on immune cells [37,62], and more recently on tuft cells, an uncommon gastrointestinal epithelial cell type [63]. We attempted to inhibit HuNoV entry into Vero cells using antibody blockade, and by saturation of potential CD300ld/CD300lf binding sites using a CD300ld/CD300lf ectodomain peptide, but both attempts were unsuccessful. We showed that the tempo of HuNoV replication in Vero cells was similar to HIEs [38], BJAB cells [39], gnotobiotic pigs [64], and gnotobiotic calves [65]. Efforts to detect HuNoV replication in Caco-2 cells, HEp-2 cells, HepG2 cells, INT-407 cells, RAW264.7 cells, and RAW264.7+ Caco-2 co-cultured cells using comparable methodologies were unsuccessful. We found HuNoV replication in Vero cells to be reduced when compared to BJAB cells (up to 25-fold), or HIE cells (up to 1,000-fold) possibly because HuNoV replication in Vero cells may be limited to a single replication cycle. Notably, a single replication cycle is common among HuNoV replicon models [27].

HBGA-expressing bacteria have been implicated in regulating HuNoV infections [39,66-68]; however, in our studies, filtration of stool samples did not markedly affect HuNoV replication in Vero cells which was similar to findings for HuNoV replication in HIEs [38]. These data imply that, unlike BJAB cells, Vero cells do not appear to require exogenous HBGAs to aid HuNoV replication.

In summary, infection of Vero cells can occur and these data provide preliminary support for the use of Vero cells as a cell culture model. Although replication of HuNoVs in Vero cells is low, infection rates and viral replication are poised to increase dramatically with the impending discovery of the HuNoV

receptor. Ectopic expression of the HuNoV receptor in a Vero cell line would provide greatly enhanced HuNoV replication in this model, providing a robust system that is more applicable for industrial HuNoV vaccine production.

References

1 Maurin, J. B., J. Minutes of the 5th meeting of the ICTV. 5 (Strasbourg, 1981).

2 Dolin, R. *et al.* Biological properties of Norwalk agent of acute infectious nonbacterial gastroenteritis. *Proceedings of the Society for Experimental Biology and Medicine. Society for Experimental Biology and Medicine (New York, N.Y.)* **140**, 578-583 (1972).

3 Lambden, P. R., Caul, E. O., Ashley, C. R. & Clarke, I. N. Sequence and genome organization of a human small round-structured (Norwalk-like) virus. *Science* **259**, 516-519 (1993).

4 Hardy, M. E. Norovirus protein structure and function. *FEMS microbiology letters* **253**, 1-8, doi:10.1016/j.femsle.2005.08.031 (2005).

5 Blakeney, S. J., Cahill, A. & Reilly, P. A. Processing of Norwalk virus nonstructural proteins by a 3C-like cysteine proteinase. *Virology* **308**, 216-224 (2003).

6 Jiang, X., Wang, M., Graham, D. Y. & Estes, M. K. Expression, self-assembly, and antigenicity of the Norwalk virus capsid protein. *Journal of virology* **66**, 6527-6532 (1992).

7 Chhabra, P. *et al.* Updated classification of norovirus genogroups and genotypes. *The Journal of general virology*, doi:10.1099/jgv.0.001318 (2019).

8 Vega, E. *et al.* Genotypic and epidemiologic trends of norovirus outbreaks in the United States, 2009 to 2013. *Journal of clinical microbiology* **52**, 147-155, doi:10.1128/jcm.02680-13 (2014).

9 Vinje, J. Advances in laboratory methods for detection and typing of norovirus. *Journal of clinical microbiology* **53**, 373-381, doi:10.1128/jcm.01535-14 (2015).

10 White, P. A. Evolution of norovirus. *Clinical microbiology and infection : the official publication of the European Society of Clinical Microbiology and Infectious Diseases* **20**, 741-745, doi:10.1111/1469-0691.12746 (2014).

11 Zhang, J. *et al.* Genotype distribution of norovirus around the emergence of Sydney_2012 and the antigenic drift of contemporary GII.4 epidemic strains. *Journal of clinical virology : the official publication of the Pan American Society for Clinical Virology* **72**, 95-101, doi:10.1016/j.jcv.2015.09.009 (2015).

12 Ruis, C. *et al.* The emerging GII.P16-GII.4 Sydney 2012 norovirus lineage is circulating worldwide, arose by late-2014 and contains polymerase changes that may increase virus transmission. *PloS one* **12**, e0179572, doi:10.1371/journal.pone.0179572 (2017).

13 Lun, J. H. *et al.* Recombinant GII.P16/GII.4 Sydney 2012 Was the Dominant Norovirus Identified in Australia and New Zealand in 2017. *Viruses* **10**, doi:10.3390/v10100548 (2018).

14 Lee, R. M. *et al.* Incubation periods of viral gastroenteritis: a systematic review. *BMC infectious diseases* **13**, 446, doi:10.1186/1471-2334-13-446 (2013).

15 Devasia, T., Lopman, B., Leon, J. & Handel, A. Association of host, agent and environment characteristics and the duration of incubation and symptomatic periods of norovirus gastroenteritis. *Epidemiology and infection* **143**, 2308-2314, doi:10.1017/s0950268814003288 (2015).

16 Kaplan, J. E., Feldman, R., Campbell, D. S., Lookabaugh, C. & Gary, G. W. The frequency of a Norwalk-like pattern of illness in outbreaks of acute gastroenteritis. *American journal of public health* **72**, 1329-1332 (1982).

17 Turcios, R. M., Widdowson, M. A., Sulka, A. C., Mead, P. S. & Glass, R. I. Reevaluation of epidemiological criteria for identifying outbreaks of acute gastroenteritis due to norovirus: United States, 1998-2000. *Clinical infectious diseases : an official publication of the Infectious Diseases Society of America* **42**, 964-969, doi:10.1086/500940 (2006).

18 Atmar, R. L. *et al.* Determination of the 50% human infectious dose for Norwalk virus. *The Journal of infectious diseases* **209**, 1016-1022, doi:10.1093/infdis/jit620 (2014).

19 Atmar, R. L. *et al.* Norwalk virus shedding after experimental human infection. *Emerging infectious diseases* **14**, 1553-1557, doi:10.3201/eid1410.080117 (2008).

20 Roth, A. N. & Karst, S. M. Norovirus mechanisms of immune antagonism. *Current opinion in virology* **16**, 24-30, doi:10.1016/j.coviro.2015.11.005 (2016).

21 Gustavsson, L., Skovbjerg, S., Lindh, M., Westin, J. & Andersson, L. M. Low serum levels of CCL5 are associated with longer duration of viral shedding in norovirus infection. *Journal of clinical virology : the official publication of the Pan American Society for Clinical Virology* **69**, 133-137, doi:10.1016/j.jcv.2015.06.088 (2015).

22 Batz, M. B., Hoffmann, S. & Morris, J. G., Jr. Ranking the disease burden of 14 pathogens in food sources in the United States using attribution data from outbreak investigations and expert elicitation. *J Food Prot* **75**, 1278-1291, doi:10.4315/0362-028x.jfp-11-418 (2012).

23 Scallan, E. *et al.* Foodborne illness acquired in the United States--major pathogens. *Emerging infectious diseases* **17**, 7-15, doi:10.3201/eid1701.P11101 (2011).

24 Bartsch, S. M., Lopman, B. A., Ozawa, S., Hall, A. J. & Lee, B. Y. Global Economic Burden of Norovirus Gastroenteritis. *PloS one* **11**, e0151219, doi:10.1371/journal.pone.0151219 (2016).

25 Debbink, K., Lindesmith, L. C. & Baric, R. S. The state of norovirus vaccines. *Clinical infectious diseases : an official publication of the*

Infectious Diseases Society of America **58**, 1746-1752, doi:10.1093/cid/ciu120 (2014).

26 Lindesmith, L. C. *et al.* Impact of Pre-exposure History and Host Genetics on Antibody Avidity Following Norovirus Vaccination. *The Journal of infectious diseases* **215**, 984-991, doi:10.1093/infdis/jix045 (2017).

27 Todd, K. V. & Tripp, R. A. Human Norovirus: Experimental Models of Infection. *Viruses* **11**, doi:10.3390/v11020151 (2019).

28 Atmar, R. L. *et al.* Norovirus vaccine against experimental human Norwalk Virus illness. *The New England journal of medicine* **365**, 2178-2187, doi:10.1056/NEJMoa1101245 (2011).

29 Zhu, S. *et al.* Identification of immune and viral correlates of norovirus protective immunity through comparative study of intra-cluster norovirus strains. *PLoS pathogens* **9**, e1003592, doi:10.1371/journal.ppat.1003592 (2013).

30 Tacket, C. O., Sztein, M. B., Losonsky, G. A., Wasserman, S. S. & Estes, M. K. Humoral, mucosal, and cellular immune responses to oral Norwalk virus-like particles in volunteers. *Clinical immunology (Orlando, Fla.)* **108**, 241-247 (2003).

31 Ball, J. M. *et al.* Recombinant Norwalk virus-like particles given orally to volunteers: phase I study. *Gastroenterology* **117**, 40-48 (1999).

32 Parra, G. I. *et al.* Immunogenicity and specificity of norovirus Consensus GII.4 virus-like particles in monovalent and bivalent vaccine formulations. *Vaccine* **30**, 3580-3586, doi:10.1016/j.vaccine.2012.03.050 (2012).

33 WHO. Recommendations for the evaluation of animal cell cultures as substrates for the manufacture of biological medicinal products and for the characterization of cells banks. Report No. 978, 79-187 (Geneva, 2013).

34 Graziano, V. R., Wei, J. & Wilen, C. B. Norovirus Attachment and Entry. *Viruses* **11**, doi:10.3390/v11060495 (2019).

35 Guix, S. *et al.* Norwalk virus RNA is infectious in mammalian cells. *Journal of virology* **81**, 12238-12248, doi:10.1128/jvi.01489-07 (2007).

36 Orchard, R. C. *et al.* Discovery of a proteinaceous cellular receptor for a norovirus. *Science* **353**, 933-936, doi:10.1126/science.aaf1220 (2016).

37 Haga, K. *et al.* Functional receptor molecules CD300lf and CD300ld within the CD300 family enable murine noroviruses to infect cells. *Proceedings of the National Academy of Sciences of the United States of America* **113**, E6248-e6255, doi:10.1073/pnas.1605575113 (2016).

38 Ettayebi, K. *et al.* Replication of human noroviruses in stem cell-derived human enteroids. *Science* **353**, 1387-1393, doi:10.1126/science.aaf5211 (2016).

39 Jones, M. K. *et al.* Enteric bacteria promote human and mouse norovirus infection of B cells. *Science (New York, N.Y.)* **346**, 755-759, doi:10.1126/science.1257147 (2014).

40 Jones, M. K. *et al.* Human norovirus culture in B cells. *Nature protocols* **10**, 1939-1947, doi:10.1038/nprot.2015.121 (2015).

41 Osada, N. *et al.* The genome landscape of the african green monkey kidney-derived vero cell line. *DNA research : an international journal for*

rapid publication of reports on genes and genomes **21**, 673-683, doi:10.1093/dnares/dsu029 (2014).

42 Desmyter, J., Melnick, J. L. & Rawls, W. E. Defectiveness of interferon production and of rubella virus interference in a line of African green monkey kidney cells (Vero). *Journal of virology* **2**, 955-961 (1968).

43 Barrett, P. N., Mundt, W., Kistner, O. & Howard, M. K. Vero cell platform in vaccine production: moving towards cell culture-based viral vaccines. *Expert review of vaccines* **8**, 607-618, doi:10.1586/erv.09.19 (2009).

44 Duizer, E. *et al.* Laboratory efforts to cultivate noroviruses. *The Journal of general virology* **85**, 79-87, doi:10.1099/vir.0.19478-0 (2004).

45 Oka, T. *et al.* Attempts to grow human noroviruses, a sapovirus, and a bovine norovirus in vitro. *PloS one* **13**, e0178157, doi:10.1371/journal.pone.0178157 (2018).

46 Liu, J. *et al.* A laboratory-developed TaqMan Array Card for simultaneous detection of 19 enteropathogens. *Journal of clinical microbiology* **51**, 472-480, doi:10.1128/jcm.02658-12 (2013).

47 Liu, J. *et al.* Development and assessment of molecular diagnostic tests for 15 enteropathogens causing childhood diarrhoea: a multicentre study. *The Lancet. Infectious diseases* **14**, 716-724, doi:10.1016/s1473-3099(14)70808-4 (2014).

48 Park, Y., Cho, Y. H. & Ko, G. A duplex real-time RT-PCR assay for the simultaneous genogroup-specific detection of noroviruses in both clinical

and environmental specimens. *Virus genes* **43**, 192-200, doi:10.1007/s11262-011-0626-4 (2011).

49 Murray, J. *et al.* A universal mammalian vaccine cell line substrate. *PloS one* **12**, e0188333, doi:10.1371/journal.pone.0188333 (2017).

50 van der Sanden, S. M. *et al.* Engineering Enhanced Vaccine Cell Lines To Eradicate Vaccine-Preventable Diseases: the Polio End Game. *Journal of virology* **90**, 1694-1704, doi:10.1128/jvi.01464-15 (2016).

51 Doerflinger, S. Y. *et al.* Human Norovirus Evolution in a Chronically Infected Host. *mSphere* **2**, doi:10.1128/mSphere.00352-16 (2017).

52 Koromyslova, A. D., Leuthold, M. M., Bowler, M. W. & Hansman, G. S. The sweet quartet: Binding of fucose to the norovirus capsid. *Virology* **483**, 203-208, doi:10.1016/j.virol.2015.04.006 (2015).

53 Carmona-Vicente, N., Allen, D. J., Rodriguez-Diaz, J., Iturriza-Gomara, M. & Buesa, J. Antibodies against Lewis antigens inhibit the binding of human norovirus GII.4 virus-like particles to saliva but not to intestinal Caco-2 cells. *Virology journal* **13**, 82, doi:10.1186/s12985-016-0538-y (2016).

54 Lindesmith, L. *et al.* Cellular and humoral immunity following Snow Mountain virus challenge. *Journal of virology* **79**, 2900-2909, doi:10.1128/jvi.79.5.2900-2909.2005 (2005).

55 Rockx, B. H., Vennema, H., Hoebe, C. J., Duizer, E. & Koopmans, M. P. Association of histo-blood group antigens and susceptibility to norovirus infections. *The Journal of infectious diseases* **191**, 749-754, doi:10.1086/427779 (2005).

56 Lopman, B. A. *et al.* Norovirus Infection and Disease in an Ecuadorian Birth Cohort: Association of Certain Norovirus Genotypes With Host FUT2 Secretor Status. *The Journal of infectious diseases* **211**, 1813-1821, doi:10.1093/infdis/jiu672 (2015).

57 Nordgren, J., Kindberg, E., Lindgren, P. E., Matussek, A. & Svensson, L. Norovirus gastroenteritis outbreak with a secretor-independent susceptibility pattern, Sweden. *Emerging infectious diseases* **16**, 81-87, doi:10.3201/eid1601.090633 (2010).

58 Halperin, T. *et al.* No association between histo-blood group antigens and susceptibility to clinical infections with genogroup II norovirus. *The Journal of infectious diseases* **197**, 63-65, doi:10.1086/524145 (2008).

59 Hutson, A. M., Atmar, R. L., Graham, D. Y. & Estes, M. K. Norwalk virus infection and disease is associated with ABO histo-blood group type. *The Journal of infectious diseases* **185**, 1335-1337, doi:10.1086/339883 (2002).

60 Graziano, V. R. *et al.* CD300lf is the primary physiologic receptor of murine norovirus but not human norovirus. *PLoS pathogens* **16**, e1008242, doi:10.1371/journal.ppat.1008242 (2020).

61 White, L. J. *et al.* Attachment and entry of recombinant Norwalk virus capsids to cultured human and animal cell lines. *Journal of virology* **70**, 6589-6597 (1996).

62 Grau, K. R. *et al.* The major targets of acute norovirus infection are immune cells in the gut-associated lymphoid tissue. *Nature microbiology* **2**, 1586-1591, doi:10.1038/s41564-017-0057-7 (2017).

63 Wilen, C. B. *et al.* Tropism for tuft cells determines immune promotion of norovirus pathogenesis. *Science* **360**, 204-208, doi:10.1126/science.aar3799 (2018).

64 Takanashi, S. *et al.* Characterization of emerging GII.g/GII.12 noroviruses from a gastroenteritis outbreak in the United States in 2010. *Journal of clinical microbiology* **49**, 3234-3244, doi:10.1128/jcm.00305-11 (2011).

65 Souza, M., Azevedo, M. S., Jung, K., Cheetham, S. & Saif, L. J. Pathogenesis and immune responses in gnotobiotic calves after infection with the genogroup II.4-HS66 strain of human norovirus. *Journal of virology* **82**, 1777-1786, doi:10.1128/jvi.01347-07 (2008).

66 Miura, T. *et al.* Histo-blood group antigen-like substances of human enteric bacteria as specific adsorbents for human noroviruses. *Journal of virology* **87**, 9441-9451, doi:10.1128/jvi.01060-13 (2013).

67 Furuya, K., Nakajima, H., Sasaki, Y. & Urita, Y. An examination of co-infection in acute gastroenteritis and histo-blood group antigens leading to viral infection susceptibility. *Biomedical reports* **4**, 331-334, doi:10.3892/br.2016.585 (2016).

68 Li, D., Breiman, A., le Pendu, J. & Uyttendaele, M. Binding to histo-blood group antigen-expressing bacteria protects human norovirus from acute heat stress. *Front Microbiol* **6**, 659, doi:10.3389/fmicb.2015.00659 (2015).

Figures

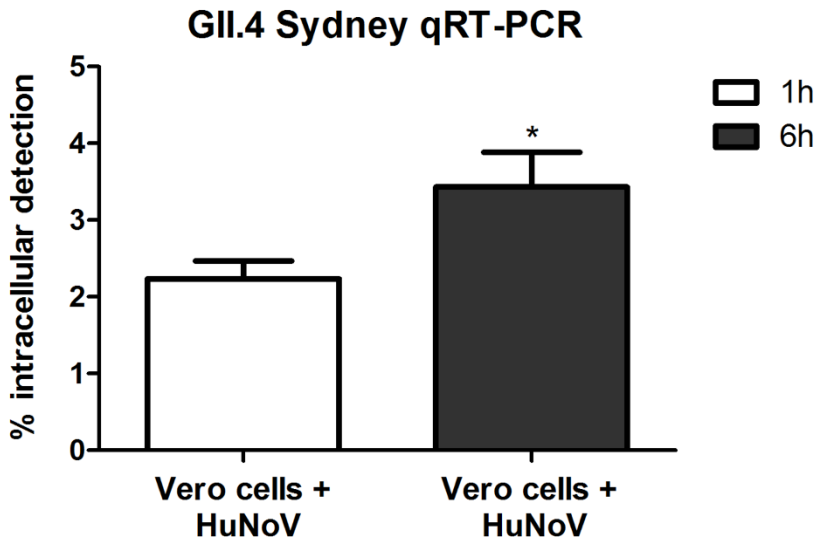

Figure 3.1: GII.4 HuNoV detection by qRT-PCR. qRT-PCR analysis of RNA extracted from HuNoV-infected Vero cells. Data represent n=3 + SEM. * $p < 0.05$.

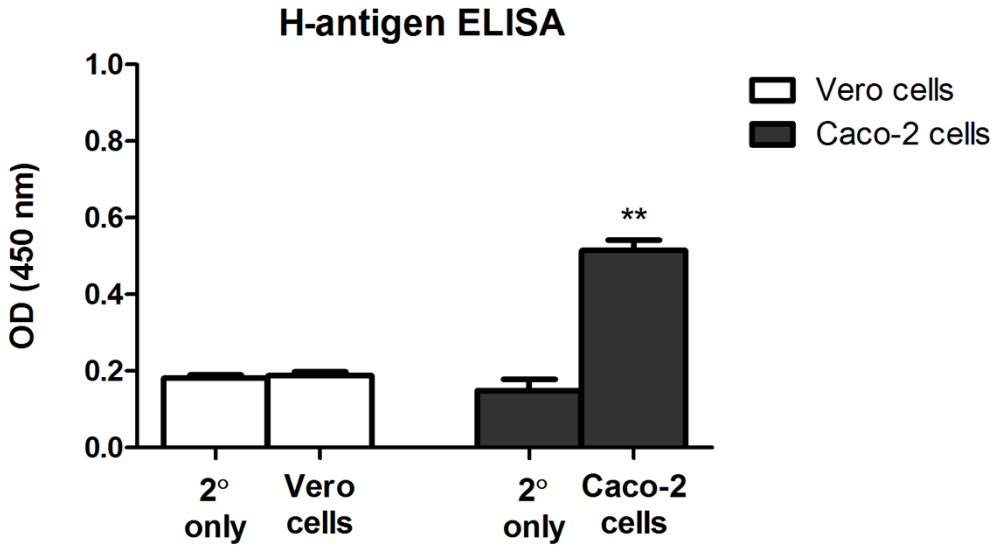

Figure 3.2: Vero cells do not express the H-antigen. An indirect ELISA was used to detect the H-antigen on the cell surface of Vero and Caco-2 cells. Data represent n=4 (Vero cells H-antigen ELISAs) or n=1 (Caco-2 cell H-antigen ELISA) + SEM. ** $p < 0.01$.

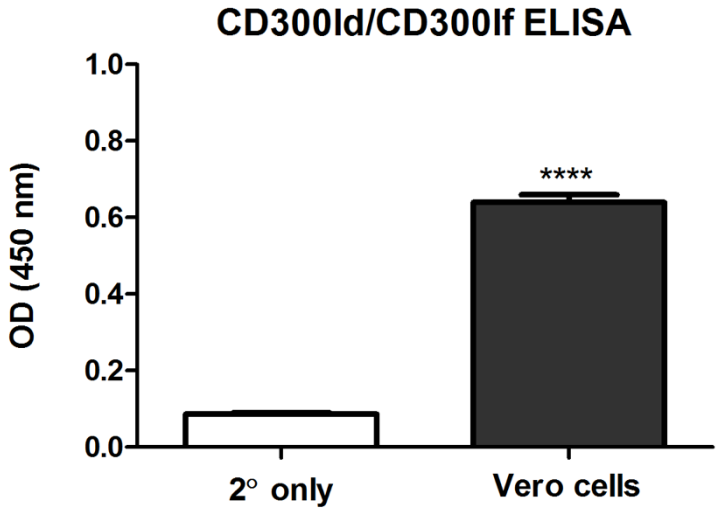

Figure 3.3: Vero cells express CD300ld/CD300lf. Anti-CD300lf (ectodomain) indirect ELISA of Vero cells. Data represent n=3 + SEM. **** $p < 0.0001$.

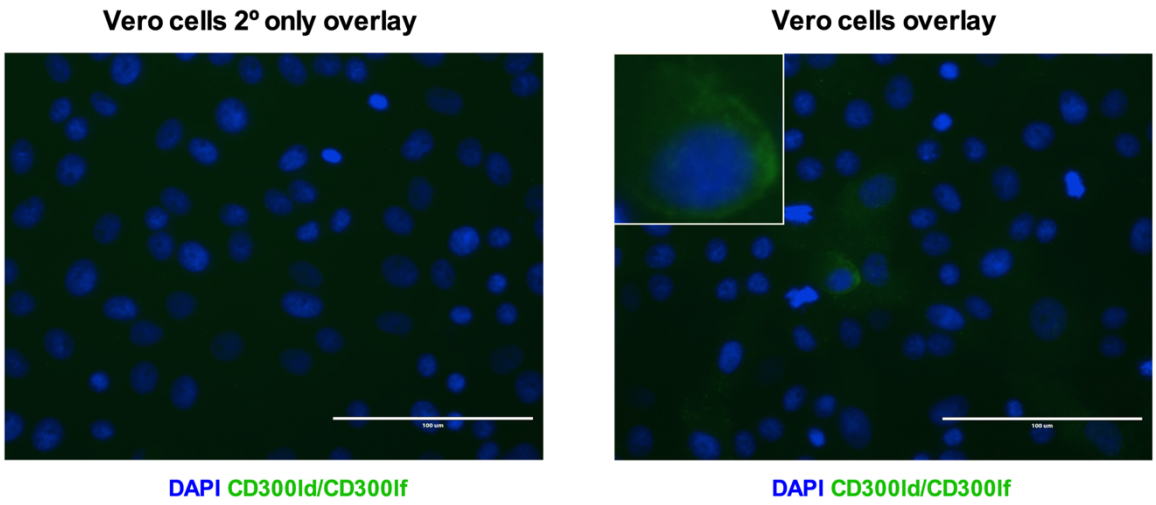

Figure 3.4: CD300ld/CD300lf expression on Vero cells by immunofluorescence assay. A representative image is shown at 40× magnification from n=3 biological replicates. The inset shows a CD300ld/CD300lf-expressing Vero cell.

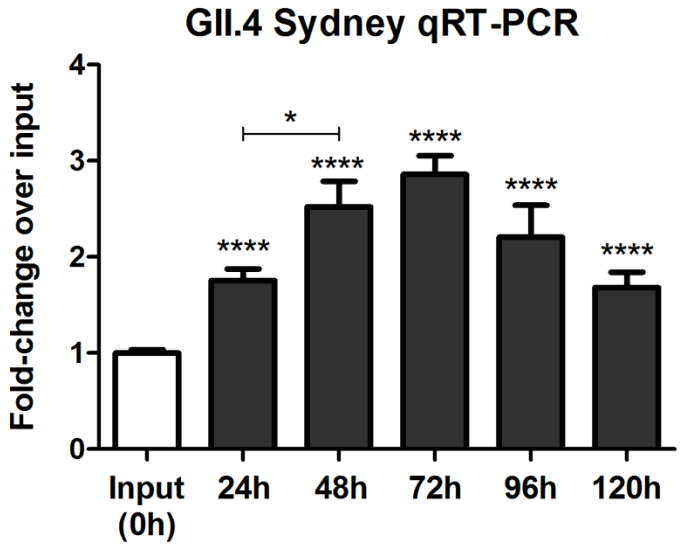

Figure 3.5: Vero cells are permissive for GII.4 Sydney HuNoV. HuNoV levels were examined over a 5-day time-course and peaked between 48-72hpi by qRT-PCR. Data represent n=3 + SEM. * $p < 0.05$ and **** $p < 0.0001$.

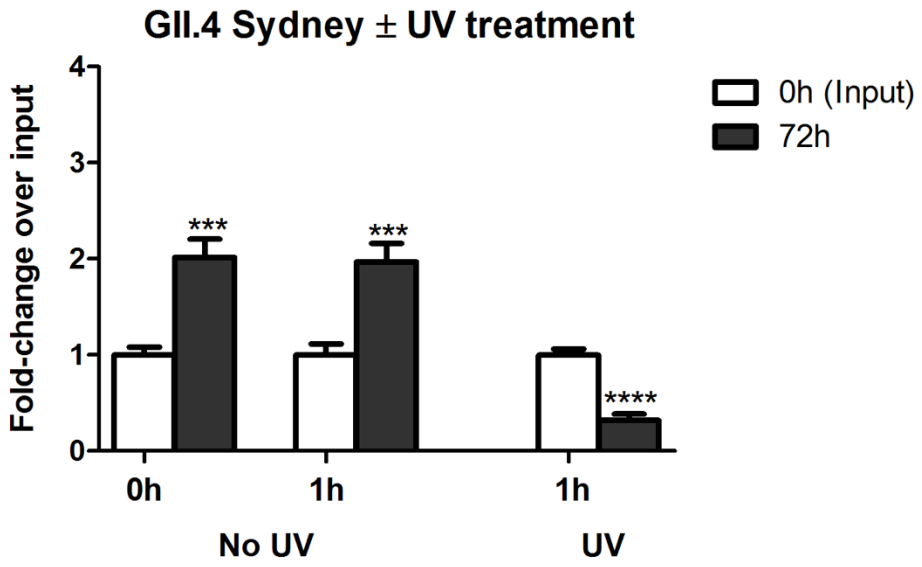

Figure 3.6: Ultraviolet (UV) light treatment inhibits HuNoV replication. 1h treatment with UV light inactivated HuNoV reducing replication at 72hpi as measured by qRT-PCR. Data represent n=3 + SEM. *** $p < 0.001$ and **** $p < 0.0001$.

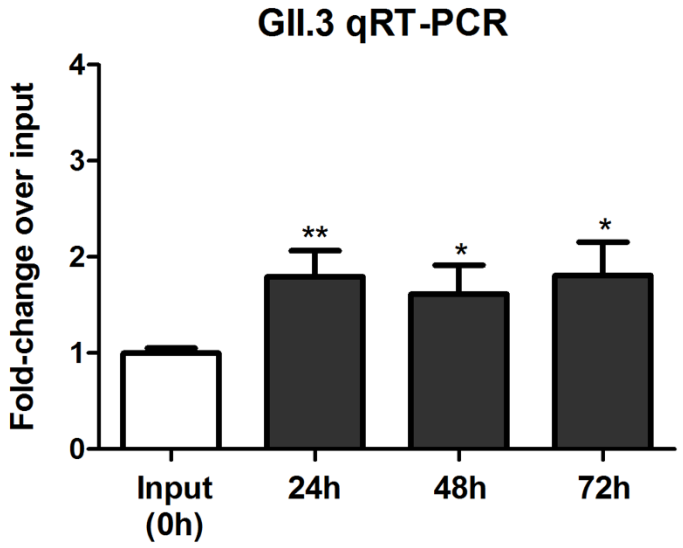

Figure 3.7: Vero cells are permissive for GII.3 HuNoVs. qRT-PCR analysis over a 3-day time-course. Data represent n=3 + SEM. * $p < 0.05$ and ** $p < 0.01$.

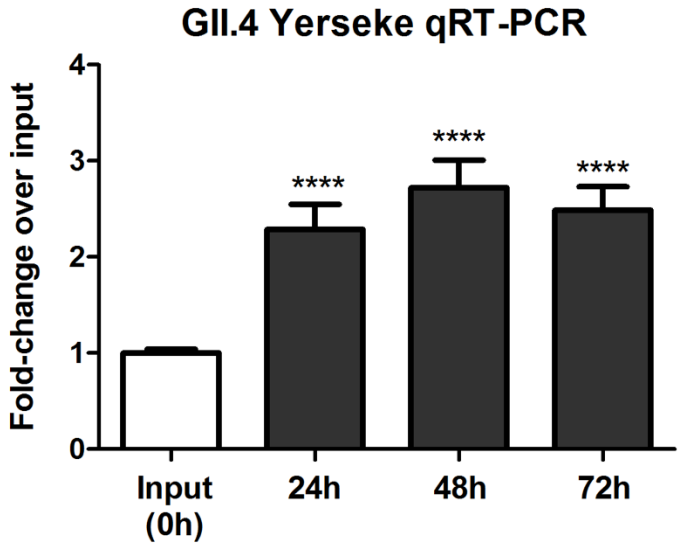

Figure 3.8: Vero cells are permissive for GII.4 Yerseke HuNoVs. qRT-PCR analysis over a 3-day time-course. Data represent n=3 + SEM. **** $p < 0.0001$.

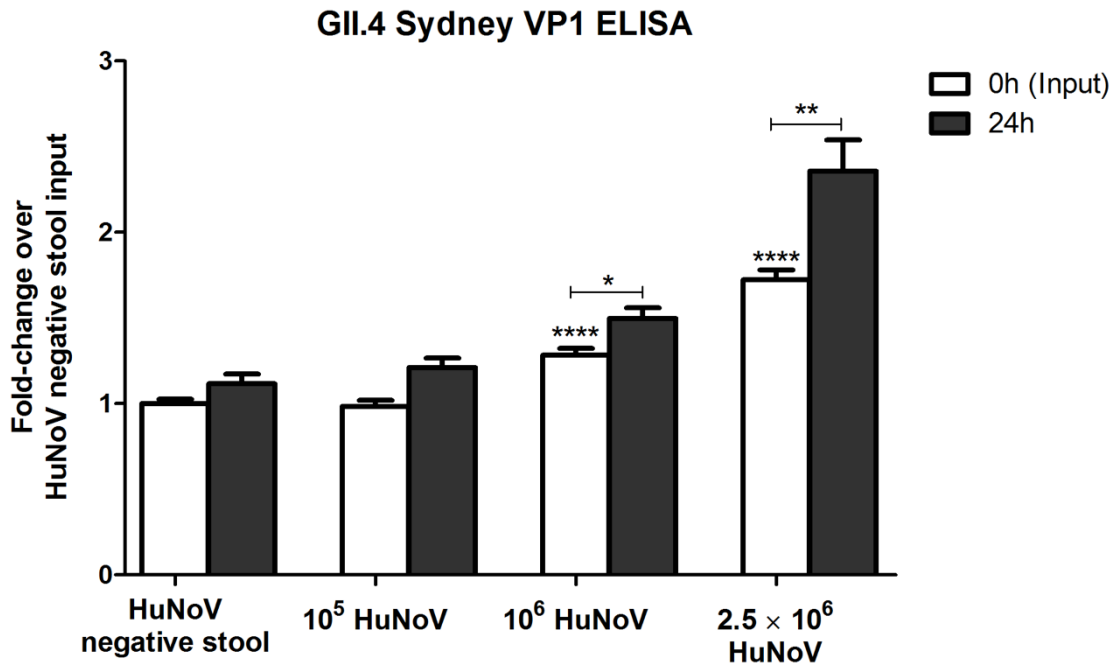

Figure 3.9: Detection of GII.4 Sydney HuNoV VP1 by ELISA. OD (450 nm) were measured and fold-changes normalized to HuNoV negative stool input values were graphed. Data represent n=3 + SEM. * $p < 0.05$, ** $p < 0.01$, and **** $p < 0.0001$.

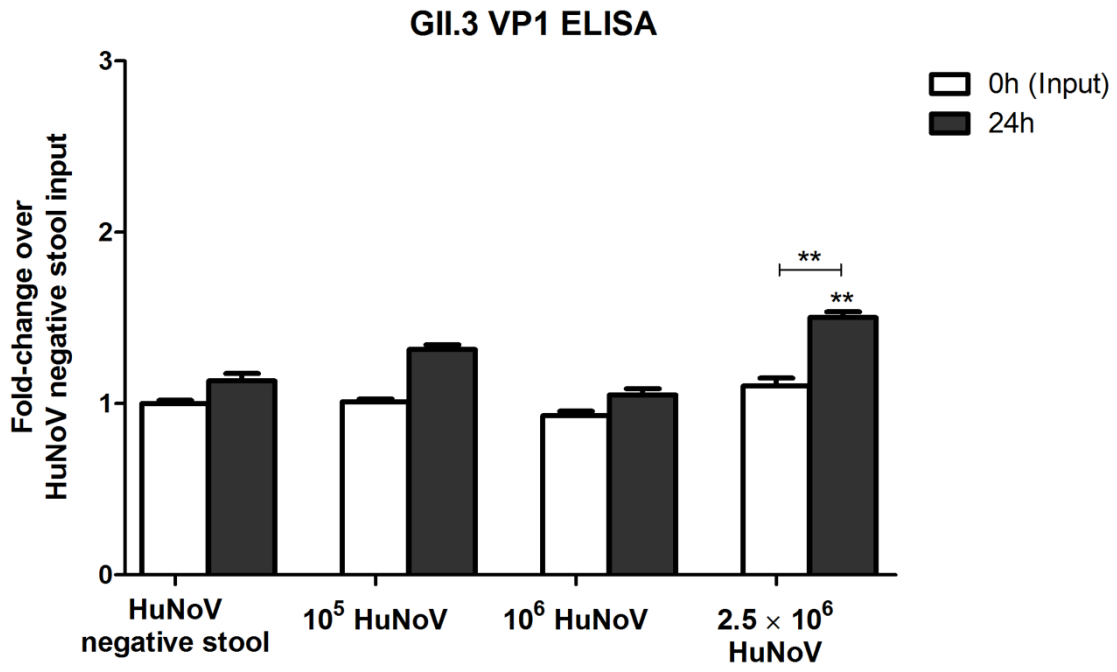

Figure 3.10: Detection of GII.3 HuNoV VP1 by ELISA. OD (450 nm) were measured and fold-changes normalized to HuNoV negative stool input values were graphed. Data represent n=1 + SEM. ** $p < 0.01$.

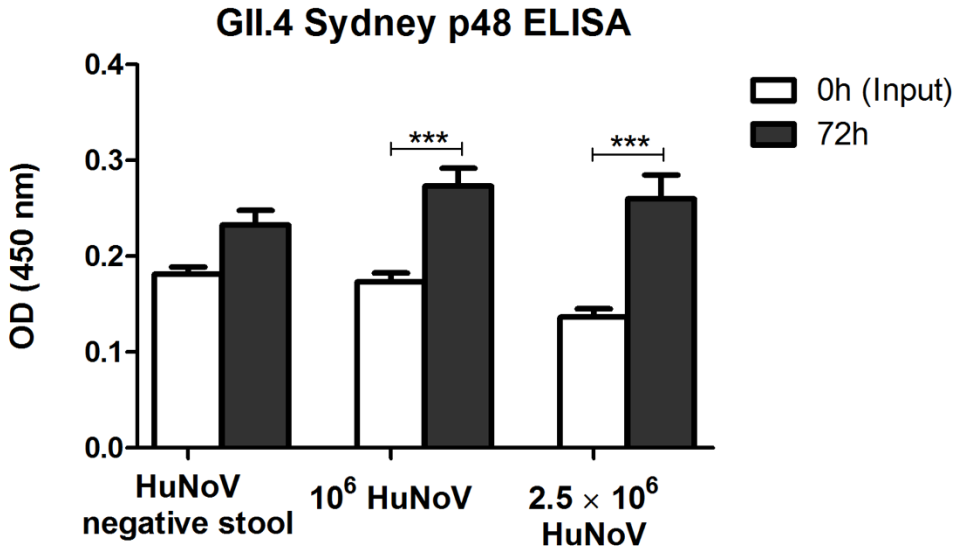

Figure 3.11: Detection of GII.4 Sydney HuNoV p48 by ELISA. Data represent n=3 + SEM. *** $p < 0.001$.

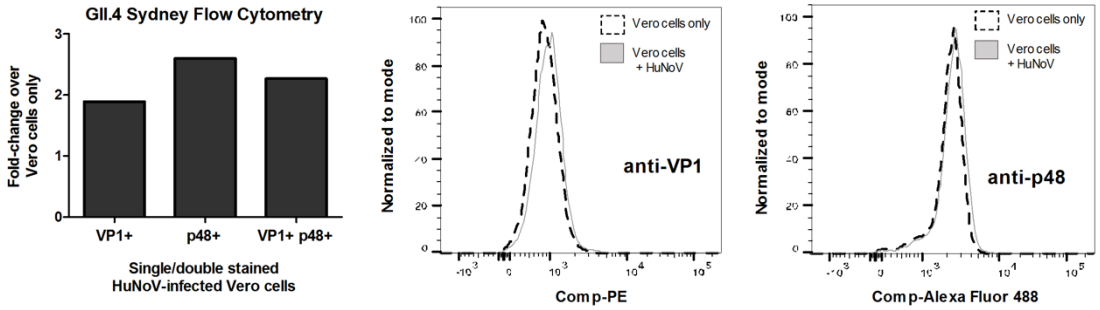

Figure 3.12: Increased VP1 and p48 staining frequency in HuNoV-infected Vero cells. Detection of single positive (VP1+ or p48+) and double positive (VP1+ p48+) Vero cell populations following HuNoV infection. Histograms generated following fluorescent bead compensation with the cell counts normalized to the mode. Data represent n=1 from 5 biological replicates.

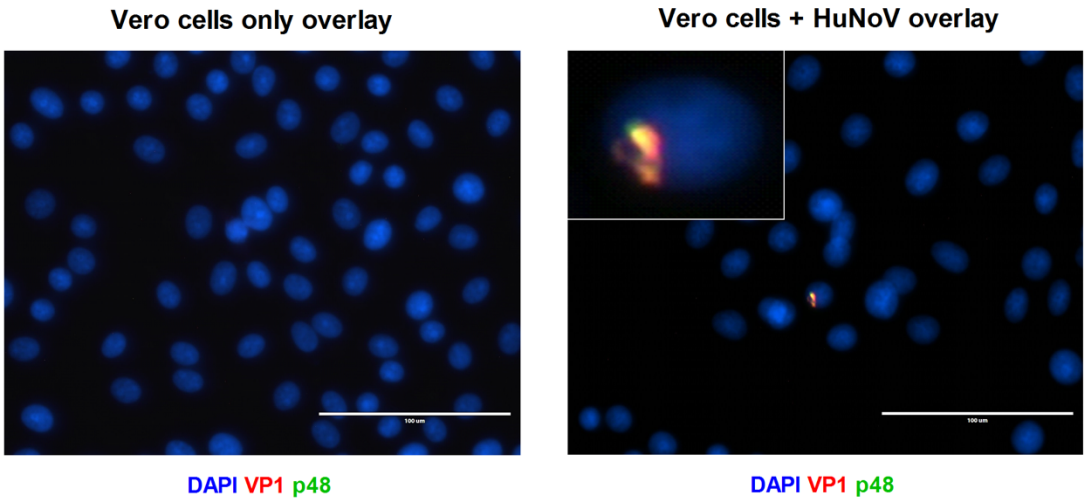

Figure 3.13: Visualization of GII.4 Sydney VP1 and p48 proteins by immunofluorescence assay. Representative image shown at 40× magnification from n=3 biological replicates. The inset shows a HuNoV-infected Vero cell.

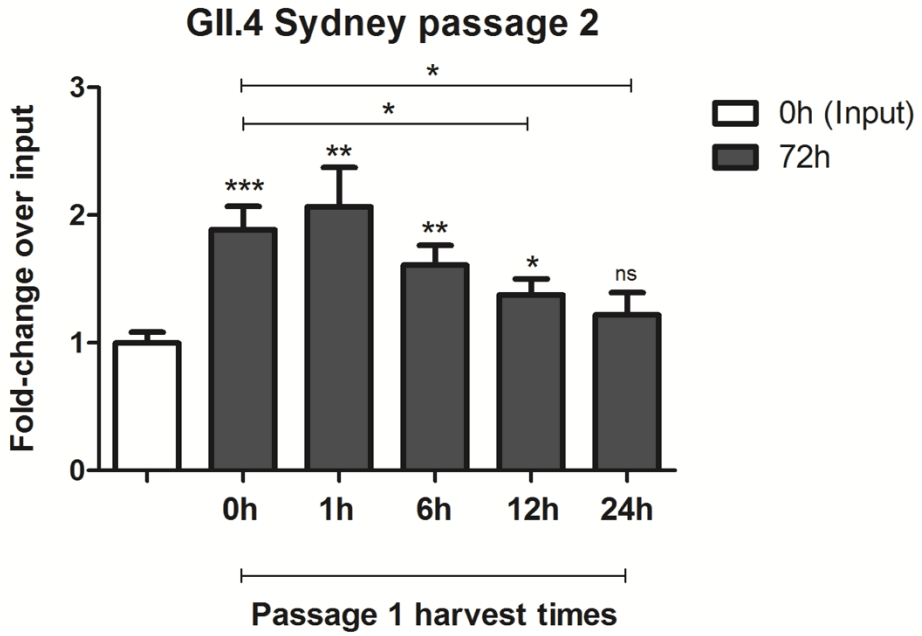

Figure 3.14: Prolonged HuNoV infection inhibits the virus' ability to be passaged. A substantial replication impediment is observed when viruses are passaged ≥12hpi. Replication fails to occur when HuNoV is passaged at 24hpi. Data represent n=3 + SEM. not significant (ns), * $p < 0.05$, ** $p < 0.01$, and *** $p < 0.001$.

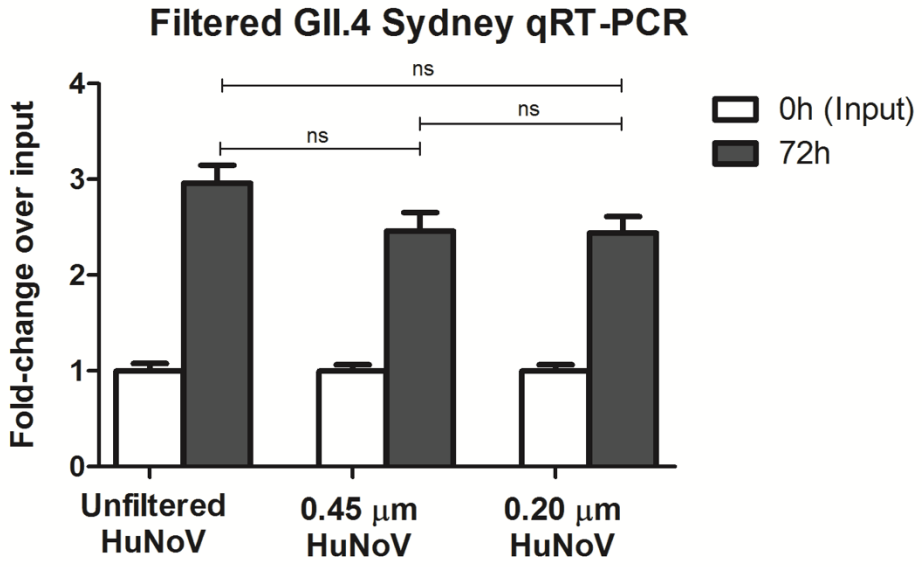

Figure 3.15: HuNoV replication is not detectably modified by filtration. 0.45 and 0.20 μm filterable agents, such as bacteria, do not affect peak HuNoV levels as measured by qRT-PCR. Data represent n=3 + SEM. not significant (ns).

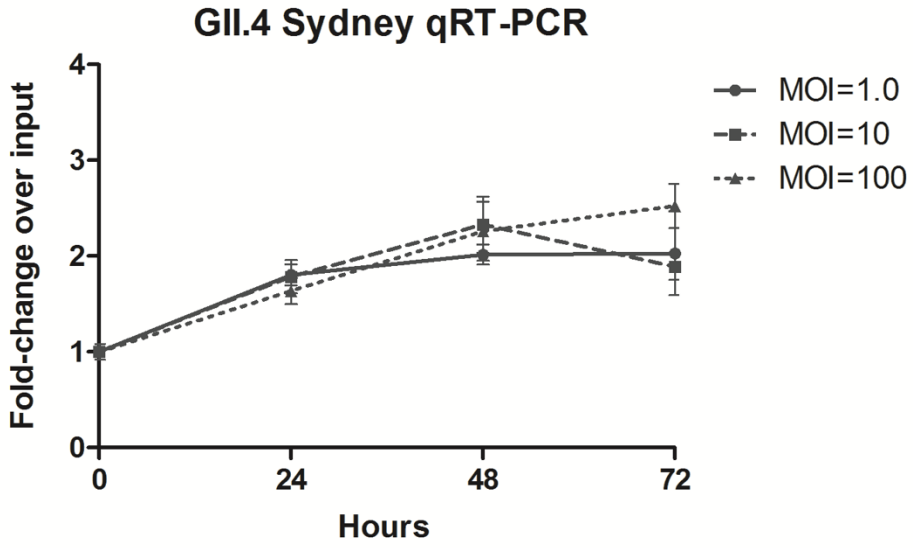

Figure 3.16: Vero cells support GII.4 Sydney HuNoV across a wide MOI range. The tempo of HuNoV replication is similar regardless of the MOI as quantified by qRT-PCR. Data represent n=3 + SEM.

CHAPTER 4

EXOSOME-MEDIATED HUMAN NOROVIRUS INFECTION OF VERO CELLS[2,3]

[2] Todd, K. V. & Tripp, R. A. Vero Cells as a Mammalian Cell Substrate for Human Norovirus. *Viruses* **12**, doi:10.3390/v12040439 (2020). Reprinted here with permission of publisher.

[3] Todd, K. V. & Tripp, R. A. Exosome-mediated human norovirus infection. Submitted to *PLOS ONE*, 5/1/2020.

Abstract

Human norovirus (HuNoV) is a leading cause of acute gastroenteritis. Outbreaks normally occur via the fecal-oral route. HuNoV infection is thought to occur by viral particle transmission, but increasing evidence suggests a function for exosomes in HuNoV infection. HuNoV is contained within stool-derived exosomes, and exosome-associated HuNoV has been shown to replicate in human intestinal enteroids. In this study, we examine exosome-associated HuNoV infection of Vero cells and show that exosomes containing HuNoV may attach, infect, and be passaged in Vero cells. These findings support earlier findings and have implications for developing HuNoV disease intervention strategies.

Introduction

Noroviruses (NoVs) are non-enveloped enteric viruses with small capsids that contain positive-sense RNA genomes [1,2]. NoVs are classified into ten genogroups (GI-GX), with GI, GII, and GIV typically causing the majority of human disease [3]. Human NoVs (HuNoVs) are globally prevalent and often cause self-limiting acute gastroenteritis. There are ~700 million infections and >200,000 deaths that occur from HuNoV infections annually [4]. GII genotype 4 (GII.4) HuNoVs are a concern because they may cause pandemics giving rise to dominant circulating strains [5-7].

There remains a need for HuNoV disease interventions including vaccines to prevent disease. Human intestinal enteroids (HIEs) [8] and human Burkitt lymphoma B cells (BJAB cells) [9] have produced encouraging results as HuNoV

cell culture models, however, these substrates are not ideal for vaccine production because HIEs are terminal mixed cell culture systems with a limited lifespan [8,10] and BJAB cells have been reported to support only a single strain of HuNoV [9,11]. A recent study from our group has shown that Vero cells support HuNoV infection and replication [12], and as Vero cells are used for the production of a variety of viral vaccines [13], the study was also encouraging for potential HuNoV vaccine production.

Infection and transmission of HuNoV are considered to occur by viral particles, however, accumulating evidence suggests that HuNoVs co-opt host cell endosome pathways for transmission [14-16]. Briefly, endocytosis of extracellular components generates endosomes in mammalian cells. These vesicles recycle and fuse leading to the formation of multivesicular bodies (MVBs). MVBs contain intraluminal vesicles that form by vesicle fusion and invagination of the endosomal membrane [17,18]. These intraluminal vesicles and their cargo are either degraded following fusion of MVBs with lysosomes, or released extracellularly as single-membraned vesicles called exosomes [19]. Exosomes are membrane-bound extracellular vesicles (EVs) ranging in size from 50–150 nm. Exosomes may carry cell-specific cargo loads of proteins, lipids, and/or nucleic acids that may be selectively taken up by neighboring or distant cells [20,21]. Exosome loading is regulated in part by post-translational protein modifications including ISGylation, phosphorylation, SUMOylation, and ubiquitination [20,22-24]. Several non-enveloped viruses, e.g. hepatitis A virus [25], hepatitis E virus [26-28], poliovirus [29], and rotavirus [14] can transmit to other cells using EVs. Transport within EVs

allows viruses to remain immunologically undetected, and to cluster enhancing the likelihood of infection. Exosomes can regulate virus infections as they may shuttle microRNAs and cytokines to neighboring cells inducing an antiviral state [30,31]. Exosomes are stable in body fluids, including stool [12,14,32]. HuNoV RNA is also contained within exosomes, and these exosomes are infectious in HIEs [12,14]. Given the importance of exosomes for HuNoV infection and transmission, we examined the potential of HuNoV stool-derived exosomes to internalize, replicate, and be passaged in Vero cells.

Materials and Methods

Cells

Vero cells (African green monkey kidney cells; CCL81.4) were obtained from the American Type Culture Collection (ATCC; Manassas, VA, USA) and maintained at low passage (passages 25–30) in Dulbecco's Modified Eagle's Media (DMEM; GIBCO, Gaithersburg, MD, USA), with 5% heat-inactivated fetal bovine serum (FBS; HyClone, Logan, UT, USA), at 37ºC and 5% CO_2. A master cell line bank was generated to ensure low passage cells were used for all experiments.

Viruses

Human stool samples containing GII.3, GII.4 Den Haag (2006b pandemic), or GII.4 Sydney (2012 pandemic) HuNoV were acquired from Murdoch Children's Research Institute (MCRI; Melbourne, Victoria, AUS) or the Viral Gastroenteritis

Branch in the Division of Viral Diseases in the Centers for Disease Control and Prevention (CDC, Atlanta, GA, USA) and stored at -80ºC. The stool samples were thawed on ice before making 10% (*w/v*) dilutions in PBS (HyClone). All samples were centrifuged 2× at 1500× *g* for 10 min at 4ºC and then at 5000× *g* for 10 min at 4ºC. The stool samples were passed through 100 µm and 40 µm cell strainers (BD, Franklin Lakes, NJ, USA) then filtered samples were filtered using 0.45 µm filters (GE Healthcare, Chicago, IL, USA) before aliquots were made and stored at –80ºC until use.

HuNoV genome equivalent (g.e.) quantification

Stool samples were treated with RNAzol (Molecular Research Center Inc., Cincinnati, OH, USA) according to the manufacturer's instructions to generate total RNA to be used for amplification and detection by qRT-PCR [12]. Briefly, $NK2P_2F$ (+) and NKP_2R (–) primers were used to amplify a segment of the HuNoV RNA-dependent RNA polymerase (RdRp) that was detected using the $RING_2$-TP probe under the following cycling conditions: 45ºC for 10 min, 95ºC for 10 min, followed by 40 cycles of 95ºC for 15s, 50ºC for 30s, and 60ºC for 30s. The resulting RdRp qRT-PCR levels are considered g.e. because the amplified site occurs once in each full-length genome. The g.e. RNA levels for the experimental time-points were divided by the mean g.e. RNA levels from the input time-point (i.e. 0h) to calculate fold-changes, normalizing the fold-change of input time-points to 1. MOI was calculated as the ratio of input g.e. to the number of cells.

Exosome isolation

The stool was processed with ExoQuick (System Biosciences, Palo Alto, CA, USA) to isolate exosomes according to the manufacturer's instructions. Briefly, stool samples were centrifuged at 3000× *g* for 15 min, then supernatants were mixed with ExoQuick (final concentration 20%) before refrigeration at 4ºC for 16h. The mixture was subsequently centrifuged at 1500× *g* for 30 min and the supernatant was removed. Exosome pellets were resuspended in PBS and stored at –80ºC until use. Stool exosome samples were tested 10× using an NS300 NanoSight (Spectris, Egham, GBR) for the determination of EV concentrations and sizes.

Phosphatidylserine (PS) exosome partitioning

Stool samples were processed using a MagCapture Exosome Isolation kit PS (FUJIFILM Wako Chemicals, Richmond, VA, USA) to enrich for PS-exosomes. Briefly, a supplied exosome capture immobilizing buffer was added to streptavidin magnetic beads, mixed, then placed on a magnetic stand before removal of the supernatant. Exosome capture immobilizing buffer and biotin-labeled exosome buffer were mixed with the streptavidin magnetic beads and rotated at 4ºC for 10 min. After centrifugation at 1000× *g* for 1 min, the beads were placed on a magnetic stand and the supernatant was removed. Subsequently, the streptavidin magnetic beads were washed 2× with exosome capture immobilizing buffer. An exosome binding enhancer buffer was diluted 1:500 in the stool before incubation with the streptavidin magnetic beads at 4ºC for 3h. Following centrifugation at 1000× *g* for

1 min, and placement on a magnetic stand, the PS-exosome-depleted stool was collected and stored at –80ºC until use. PS-exosome bound streptavidin magnetic beads were washed 2× with washing buffer containing 1:500 diluted exosome binding enhancer. The PS-exosomes were eluted 2× with the exosome elution buffer then stored at -80ºC until use.

HuNoV infection and passage in Vero cells

Stool, exosomes, PS-exosomes, or PS-exosome depleted stool was used to infect (MOIs described in figure legends) Vero cells. Briefly, 8.0×10^3 Vero cells were plated in 96-well flat-bottom plates (Corning, Corning, NY, USA), the supernatant decanted, and serum free (SF)-DMEM volume-normalized (10 µL) HuNoV infections were performed in 90 µL of SF-DMEM for the duration of the experimental time-course. All HuNoV infections were performed in SF-DMEM to avoid the presence of cofounding exosomes from FBS [33]. The cells were gently rocked then incubated at 37ºC and 5% CO_2. For 1h and 6h infections (Table 4.1), the infectious supernatants were removed from all wells except virus input controls, and the cells were washed 2× with PBS. RNAzol was used to extract RNA from the cellular fractions of experimental wells and from the cells and supernatants of virus input controls. The % total g.e. was determined by dividing the cellular fraction g.e. by the virus input controls across triplicate experimental and control wells. For exosome passage studies, 10^6 Vero cells were plated in T-25 flasks (Corning), the media decanted, and SF-DMEM volume-normalized (100 µL) HuNoV infections (MOI=0.5) were performed in SF-DMEM (4.9 mL). Exosomes

were isolated from 5 mL of infectious supernatants from each flask 72hpi using ExoQuick, then the g.e. of the exosomes was quantified by qRT-PCR. Isolated exosomes were volume-normalized in SF-DMEM (10 µL) before infection (MOI=0.2) of 8.0×10^3 fresh Vero cells in 90 µL of SF-DMEM in 96-well flat-bottom plates for 72h.

Statistical analyses

Unpaired two-tailed t-tests were performed with 95% confidence intervals using GraphPad Prism. *p*-values < 0.05 were considered significant: * $p < 0.05$, ** $p < 0.01$, *** $p < 0.001$, and **** $p < 0.0001$. Means ± standard error of the mean (SEM) are displayed.

Results

We confirmed the presence of intact stool exosomes after ExoQuick isolation and determined EV concentrations and size distributions (Figure 4.1). Stool exosomes were also found to contain a substantial portion of HuNoV g.e. (Figure 4.2). Next, we tested if exosomes from stool samples could infect Vero cells following incubation for 1h or 6h. The data showed that increased incubation times correlated with increased intracellular HuNoV as measured by qRT-PCR (Table 4.1). This observation is consistent with increased incubation times facilitating HuNoV replication in Vero cells [12]. The HuNoV g.e. levels in Vero cells were similar between stool [12] and exosome infections at both 1h and 6h time-points. Exosomes isolated from GII.4 Sydney stool and PS-exosomes enriched

from GII.4 Sydney or GII.3 stool transferred infectious virus that replicated in Vero cells as indicated by a significant increase in g.e. (Tables 4.2 and 4.3). The depletion of PS-exosomes from GII.4 Sydney or GII.3 stool by magnetic bead partitioning did not ablate HuNoV replication in Vero cells (Table 4.3). This finding suggests that non-PS-exosomes contain HuNoV, and/or virus particles not in exosomes are infectious. GII.4 Den Haag stool or PS-exosomes from GII.4 Den Haag stool did not infect Vero cells (Table 4.3), possibly indicating strain differences for infection and replication, which is consistent with a previous attempt to infect Vero cells with a GII.4 Den Haag strain [12].

In this report, we show that exosomes will transfer HuNoV infection to uninfected Vero cells (Table 4.4). This is the first account of HuNoV passage by exosomes, although additional passaging needs to be performed to confirm exosomes as a mode of transmission. We propose that infectious virus is loaded as cargo into exosomes and this occurs modestly but reproducibly.

Discussion

Exosomes from HuNoV-containing stool samples transferred infectious HuNoV to Vero cells (Table 4.1) at a level similar to that previously reported for whole stool [12]. HuNoV (<1–10%) [8,34] and exosomes from stool (6%) [14] bound and infected HIEs at similar levels. Exosomes from murine NoV-infected RAW264.7 macrophages have been tested and cannot infect RAW264.7 cells when the murine NoV receptor, CD300ld/CD300lf, is blocked indicating that passive exosome uptake of the virus is insufficient or not occurring [14,35,36]. It is

unclear if the attachment and entry mechanisms of HuNoV virions and HuNoV-loaded exosomes are identical. GII.4 Sydney replication in Vero cells was low for PS-exosomes (~1.5-fold) compared to total stool exosomes (~2.5-fold), or PS-exosome-depleted stool (~2-fold). Increased HuNoV replication from total stool exosomes over PS-exosomes indicates that non-PS-exosome subpopulations may also function to facilitate HuNoV infection. HuNoV in tetraspanin-containing (CD9, CD63, and CD81) exosomes has been reported [14]. Tetraspanins represent a diverse family of membrane-bound proteins that form tetraspanin-enriched microdomains, which coordinate diverse exosome processes including biogenesis, cargo loading, and recipient cell attachment (as reviewed in [37]). Their role in exosome development suggests tetraspanin-containing exosomes are notable subpopulations to study for exosome-mediated HuNoV infection. Additionally, differences between HuNoV stool and exosome replication in Vero cells may be due to the absence of specific stool components (host, viral, or bacterial) following exosome isolation, however this has not been further explored.

Previous attempts to mediate HuNoV infection in Vero cells using transfection reagents to load stool exosomes were unsuccessful [12]. This suggests that non-specific liposome encapsulation of HuNoV does not aid HuNoV infection or replication in Vero cells hinting at exosome loading specificity. Additionally, exosomes from uninfected Vero cells or Caco-2 cells (an intestinal epithelial cell line) co-administered with HuNoV (MOI=1.0) had no detectable effect on HuNoV replication.

It is appreciated that non-enveloped viruses are released after inducing host cell lysis. Interestingly, HuNoV replication within BJAB cells [9], HIEs [8], and Vero cells [12] does not cause cell lysis. This indicates that the replication of HuNoV in these cell culture models is likely the result of non-lytic spread. It has been reported that the majority of murine NoV is released before cell membrane lysis [14], meaning that the non-lytic spread of NoVs may occur more readily than previously thought. The upregulation of pathways associated with non-lytic spread by bile acid supplementation [15] enhances HuNoV infection in HIEs [8]. Mounting *in vitro* evidence supports the non-lytic spread of HuNoVs, however, *in vivo* experiments are needed to further validate its role in infection and transmission.

References

1 Shoemaker, G. K. *et al.* Norwalk virus assembly and stability monitored by mass spectrometry. *Molecular & cellular proteomics : MCP* **9**, 1742-1751, doi:10.1074/mcp.M900620-MCP200 (2010).

2 Pogan, R., Schneider, C., Reimer, R., Hansman, G. & Uetrecht, C. Norovirus-like VP1 particles exhibit isolate dependent stability profiles. *Journal of physics. Condensed matter : an Institute of Physics journal* **30**, 064006, doi:10.1088/1361-648X/aaa43b (2018).

3 Chhabra, P. *et al.* Updated classification of norovirus genogroups and genotypes. *The Journal of general virology*, doi:10.1099/jgv.0.001318 (2019).

4 Bartsch, S. M., Lopman, B. A., Ozawa, S., Hall, A. J. & Lee, B. Y. Global Economic Burden of Norovirus Gastroenteritis. *PloS one* **11**, e0151219, doi:10.1371/journal.pone.0151219 (2016).

5 Zhang, J. *et al.* Genotype distribution of norovirus around the emergence of Sydney_2012 and the antigenic drift of contemporary GII.4 epidemic strains. *Journal of clinical virology : the official publication of the Pan American Society for Clinical Virology* **72**, 95-101, doi:10.1016/j.jcv.2015.09.009 (2015).

6 Siebenga, J. J. *et al.* Epochal evolution of GGII.4 norovirus capsid proteins from 1995 to 2006. *Journal of virology* **81**, 9932-9941, doi:10.1128/jvi.00674-07 (2007).

7 Lindesmith, L. C. *et al.* Mechanisms of GII.4 norovirus persistence in human populations. *PLoS medicine* **5**, e31, doi:10.1371/journal.pmed.0050031 (2008).

8 Ettayebi, K. *et al.* Replication of human noroviruses in stem cell-derived human enteroids. *Science* **353**, 1387-1393, doi:10.1126/science.aaf5211 (2016).

9 Jones, M. K. *et al.* Enteric bacteria promote human and mouse norovirus infection of B cells. *Science* **346**, 755-759, doi:10.1126/science.1257147 (2014).

10 Hosmillo, M. *et al.* Norovirus Replication in Human Intestinal Epithelial Cells Is Restricted by the Interferon-Induced JAK/STAT Signaling Pathway

and RNA Polymerase II-Mediated Transcriptional Responses. *mBio* **11**, doi:10.1128/mBio.00215-20 (2020).

11 Jones, M. K. *et al.* Human norovirus culture in B cells. *Nature protocols* **10**, 1939-1947, doi:10.1038/nprot.2015.121 (2015).

12 Todd, K. V. & Tripp, R. A. Vero Cells as a Mammalian Cell Substrate for Human Norovirus. *Viruses* **12**, doi:10.3390/v12040439 (2020).

13 Barrett, P. N., Mundt, W., Kistner, O. & Howard, M. K. Vero cell platform in vaccine production: moving towards cell culture-based viral vaccines. *Expert review of vaccines* **8**, 607-618, doi:10.1586/erv.09.19 (2009).

14 Santiana, M. *et al.* Vesicle-Cloaked Virus Clusters Are Optimal Units for Inter-organismal Viral Transmission. *Cell host & microbe* **24**, 208-220.e208, doi:10.1016/j.chom.2018.07.006 (2018).

15 Murakami, K. *et al.* Bile acids and ceramide overcome the entry restriction for GII.3 human norovirus replication in human intestinal enteroids. *Proceedings of the National Academy of Sciences of the United States of America* **117**, 1700-1710, doi:10.1073/pnas.1910138117 (2020).

16 Hyde, J. L. *et al.* Mouse norovirus replication is associated with virus-induced vesicle clusters originating from membranes derived from the secretory pathway. *Journal of virology* **83**, 9709-9719, doi:10.1128/jvi.00600-09 (2009).

17 Edgar, J. R., Eden, E. R. & Futter, C. E. Hrs- and CD63-dependent competing mechanisms make different sized endosomal intraluminal vesicles. *Traffic* **15**, 197-211, doi:10.1111/tra.12139 (2014).

18 Mobius, W. *et al.* Immunoelectron microscopic localization of cholesterol using biotinylated and non-cytolytic perfringolysin O. *J Histochem Cytochem* **50**, 43-55, doi:10.1177/002215540205000105 (2002).

19 Johnstone, R. M., Adam, M., Hammond, J. R., Orr, L. & Turbide, C. Vesicle formation during reticulocyte maturation. Association of plasma membrane activities with released vesicles (exosomes). *The Journal of biological chemistry* **262**, 9412-9420 (1987).

20 Lee, H. S., Jeong, J. & Lee, K. J. Characterization of vesicles secreted from insulinoma NIT-1 cells. *J Proteome Res* **8**, 2851-2862, doi:10.1021/pr900009y (2009).

21 Skog, J. *et al.* Glioblastoma microvesicles transport RNA and proteins that promote tumour growth and provide diagnostic biomarkers. *Nat Cell Biol* **10**, 1470-1476, doi:10.1038/ncb1800 (2008).

22 Putz, U. *et al.* Nedd4 family-interacting protein 1 (Ndfip1) is required for the exosomal secretion of Nedd4 family proteins. *The Journal of biological chemistry* **283**, 32621-32627, doi:10.1074/jbc.M804120200 (2008).

23 Villarroya-Beltri, C. *et al.* ISGylation controls exosome secretion by promoting lysosomal degradation of MVB proteins. *Nature communications* **7**, 13588, doi:10.1038/ncomms13588 (2016).

24 Villarroya-Beltri, C. *et al.* Sumoylated hnRNPA2B1 controls the sorting of miRNAs into exosomes through binding to specific motifs. *Nature communications* **4**, 2980, doi:10.1038/ncomms3980 (2013).

25 Feng, Z. *et al.* A pathogenic picornavirus acquires an envelope by hijacking cellular membranes. *Nature* **496**, 367-371, doi:10.1038/nature12029 (2013).

26 Nagashima, S. *et al.* Hepatitis E virus egress depends on the exosomal pathway, with secretory exosomes derived from multivesicular bodies. *The Journal of general virology* **95**, 2166-2175, doi:10.1099/vir.0.066910-0 (2014).

27 Nagashima, S. *et al.* The membrane on the surface of hepatitis E virus particles is derived from the intracellular membrane and contains trans-Golgi network protein 2. *Archives of virology* **159**, 979-991, doi:10.1007/s00705-013-1912-3 (2014).

28 Yin, X., Ambardekar, C., Lu, Y. & Feng, Z. Distinct Entry Mechanisms for Nonenveloped and Quasi-Enveloped Hepatitis E Viruses. *Journal of virology* **90**, 4232-4242, doi:10.1128/jvi.02804-15 (2016).

29 Bird, S. W., Maynard, N. D., Covert, M. W. & Kirkegaard, K. Nonlytic viral spread enhanced by autophagy components. *Proceedings of the National Academy of Sciences of the United States of America* **111**, 13081-13086, doi:10.1073/pnas.1401437111 (2014).

30 Li, J. *et al.* Exosomes mediate the cell-to-cell transmission of IFN-alpha-induced antiviral activity. *Nature immunology* **14**, 793-803, doi:10.1038/ni.2647 (2013).

31 Pegtel, D. M. *et al.* Functional delivery of viral miRNAs via exosomes. *Proceedings of the National Academy of Sciences of the United States of America* **107**, 6328-6333, doi:10.1073/pnas.0914843107 (2010).

32 Koga, Y. *et al.* Exosome can prevent RNase from degrading microRNA in feces. *J Gastrointest Oncol* **2**, 215-222, doi:10.3978/j.issn.2078-6891.2011.015 (2011).

33 Lehrich, B. M., Liang, Y., Khosravi, P., Federoff, H. J. & Fiandaca, M. S. Fetal Bovine Serum-Derived Extracellular Vesicles Persist within Vesicle-Depleted Culture Media. *Int J Mol Sci* **19**, doi:10.3390/ijms19113538 (2018).

34 Costantini, V. *et al.* Human Norovirus Replication in Human Intestinal Enteroids as Model to Evaluate Virus Inactivation. *Emerging infectious diseases* **24**, 1453-1464, doi:10.3201/eid2408.180126 (2018).

35 Orchard, R. C. *et al.* Discovery of a proteinaceous cellular receptor for a norovirus. *Science* **353**, 933-936, doi:10.1126/science.aaf1220 (2016).

36 Haga, K. *et al.* Functional receptor molecules CD300lf and CD300ld within the CD300 family enable murine noroviruses to infect cells. *Proceedings of the National Academy of Sciences of the United States of America* **113**, E6248-e6255, doi:10.1073/pnas.1605575113 (2016).

37 Andreu, Z. & Yanez-Mo, M. Tetraspanins in extracellular vesicle formation and function. *Frontiers in immunology* **5**, 442, doi:10.3389/fimmu.2014.00442 (2014).

Figures and Tables

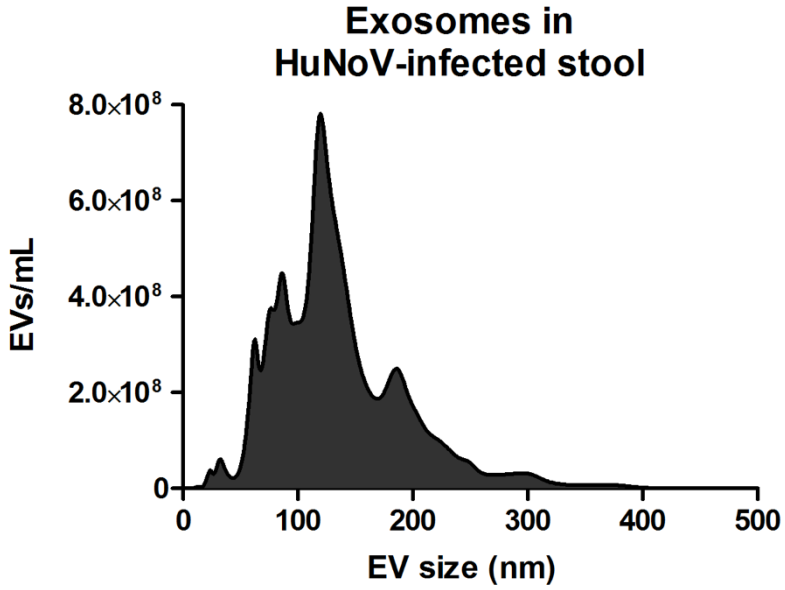

Figure 4.1: Exosomes are present in HuNoV-infected stool. NanoSight analysis indicated that high concentrations of exosomes (50–150 nm) are contained within HuNoV-infected stool. Extracellular vesicle (EV).

Figure 4.2: Approximately one-half of HuNoV g.e. in stool are associated with exosomes. Exosomal HuNoV g.e. expressed as a percentage of total expected g.e. content from the stool used for exosome extraction.

Table 4.1: GII.4 Sydney HuNoV levels by qRT-PCR. Percent total HuNoV g.e. displayed. Percent total HuNoV g.e. interaction with Vero cells after HuNoV infection (MOI=1.0) is increased at 6h post-infection (hpi) compared to 1hpi. Significant differences were observed between 1h and 6h time-points. Data represent n=3 ± SEM. ** $p < 0.01$.

Virus	Sample	Time-point	Mean ± SEM	Significance
GII.4 Sydney	exosomes	1h	2.16 ± 0.27	–
		6h	3.96 ± 0.41	**

Table 4.2: Vero cells infected with stool exosomes. qRT-PCR analysis after a 72h infection (MOI=1.0). Significant differences and mean fold-changes over 0h time-points displayed. Data represent n=3 ± SEM. ** $p < 0.01$ and *** $p < 0.001$.

Virus	Sample	Time-point	Mean ± SEM	Significance
GII.4 Sydney	exosomes	0h	1.00 ± 0.04	–
		24h	2.37 ± 0.35	**
		48h	2.76 ± 0.40	***
		72h	2.40 ± 0.39	**

Table 4.3: Vero cells infected with PS-exosomes or PS-exosome depleted stool. qRT-PCR analysis after a 72h infection (MOI=0.1). Mean fold-changes over 0h time-points displayed. Significant differences between 0h and 72h time-points were calculated. Magnetic bead partitioning was used to isolate PS-exosomes and generate PS-depleted stool samples. Data represent n=3 ± SEM. * $p < 0.05$ and **** $p < 0.0001$.

Virus	Sample	Time-point	Mean ± SEM	Significance
GII.4 Sydney	PS-exosomes	0h	1.00 ± 0.12	–
		72h	1.43 ± 0.12	*
	PS-depleted	0h	1.00 ± 0.09	–
		72h	1.94 ± 0.13	****
GII.3	PS-exosomes	0h	1.00 ± 0.08	–
		72h	1.42 ± 0.17	*
	PS-depleted	0h	1.00 ± 0.09	–
		72h	2.67 ± 0.28	****
GII.4 Den Haag	stool	0h	1.01 ± 0.13	–
		72h	1.28 ± 0.17	ns
	PS-exosomes	0h	1.00 ± 0.14	–
		72h	1.22 ± 0.18	ns
	PS-depleted	0h	0.96 ± 0.07	–
		72h	0.99 ± 0.13	ns

Table 4.4: Infected Vero cells release HuNoV-loaded exosomes. After a 72h infection (MOI=0.5) with either stool or stool exosomes, exosomes were isolated by ExoQuick and used to infect (MOI=0.2) fresh Vero cells for 72h. Exosome passage was performed at a lower MOI as there was lower virus recovery after infection and exosome isolation. Data for passage 2 are shown and represent n=3 ± SEM. ** $p < 0.01$ and **** $p < 0.0001$.

Virus	Sample	Time-point	Mean ± SEM	Significance
GII.4 Sydney	stool	0h	1.00 ± 0.06	–
		72h	1.44 ± 0.11	**
	exosomes	0h	1.00 ± 0.03	–
		72h	1.45 ± 0.06	****

CHAPTER 5

DEVELOPMENT OF A VERO CELL SUBSTRATE FOR HUMAN NOROVIRUS REPLICATION[2]

[2] Todd, K. V. & Tripp, R. A. Vero Cells as a Mammalian Cell Substrate for Human Norovirus. *Viruses* **12**, doi:10.3390/v12040439 (2020). Reprinted here with permission of publisher.

Abstract

Human noroviruses (HuNoVs) are a predominant cause of acute gastroenteritis leading to substantial disease burden. Efforts to develop a vaccine have been limited by lack of a vaccine-approved mammalian cell substrate. While Vero cells show limited replication of HuNoVs, there is a need to enhance replication levels to generate an optimal substrate for industrial vaccine production. We demonstrate that trypsin addition and host-targeted gene expression disruption are viable methods for enhancing HuNoV replication in Vero cells. These data provide a path for the development of a HuNoV vaccine.

Introduction

Globally, diarrheal diseases represent the second leading cause of non-birth related mortality in children <5 years of age [1]. Human norovirus (HuNoV) is the leading cause of acute gastroenteritis globally [2,3]. Annual HuNoV disease burden accounts for ~699 million infections, ~219,000 deaths, and ~$64.5 billion in economic loss [4]. It is believed that a vaccine with multi-year protection administered to infants ≤6 months of age has the potential to prevent 60–85% of pediatric infections [5-7]. While there is a need for HuNoV vaccines and antivirals, there are currently no licensed vaccines or therapeutics for HuNoV.

HuNoV vaccine development is complicated by a myriad of factors. The first is the genetic diversity of HuNoVs. NoVs are categorized into at least 10 genogroups (GI-GX) and over 40 genotypes, with GI, GII, GIV, GVIII, and GIX causing disease in humans [8]. Vaccine development against diverse strains is an

immunological challenge. Further, the immunological parameters of HuNoV protection are unclear as is the breadth of immunity. Existing HuNoV modeling tools are not sufficient for vaccine research (as reviewed in [9]), and HuNoV cell model systems such as BJAB cells or human intestinal enteroids (HIEs) [10,11] are not approved by the Food and Drug Administration for vaccine development.

We showed that vaccine-approved Vero cells support HuNoV [12]. As virus replication was limited in Vero cells, we explored trypsin treatment to enhance HuNoV replication as this has been successful for other enteric viruses [13-18]. We also targeted specific host genes via microRNA (miR) or small interfering RNA (siRNA) knockdown (KD) and used clustered regularly interspaced short palindromic repeat (CRISPR) gene knockout (KO) to try to elicit increased HuNoV replication. We explored canonical innate antiviral genes and leveraged gene hits from various siRNA screens [19-21] to increase our chances of success.

Enteric virus capsids that are primarily transmitted by the fecal-oral route are remarkably resilient as they have a role in protecting the viral genome when the virus is outside of the host cell. However, the capsids require proteolytic cleavage for virus activation, binding, internalization, and replication [13-18]. Proteolytic cleavage has been examined for HuNoV virions but trypsin was shown to have minor effects [22-24], likely because of the conformation of the viral capsids [25]. However, smaller conformations of HuNoV capsid proteins are trypsin-cleavable [26]. Following cleavage, the smaller capsid conformations likely have a role in viral replication, which warrants further investigation [26].

miRs are non-coding RNAs derived from genome encoded hairpin-loop structures. These structures are modified to produce mature miR duplexes 18–22 nucleotides long. These duplexes are processed into single-stranded RNAs thought to regulate >30% of protein-coding genes in the human genome [27] by base pair-specific post-transcriptional regulation [28]. siRNAs are synthetic duplexes that mimic natural miR functions but have gene-specific targets. miRs may regulate multiple genes due to their short seed sequence length which results in mismatches while siRNAs regulate only a single gene due to longer seed site length and chemical modifications resulting in increased specificity. The role of miRs in HuNoV replication has not been determined and the modulation of host genes to enhance HuNoV replication has sparsely been explored [29].

CRISPRs are used by bacteria and archaea to obstruct invading phages or evade genetic elements [30,31]. Upon infection with a phage, bacteria store viral nucleic acid sequences within protospacers of the CRISPR gene locus, to be transcribed into CRISPR RNAs to target the degradation of these viruses by a CRISPR-associated (Cas) protein. The CRISPR-Cas9 system has been adapted to perform targeted genome editing [32-34]. Briefly, a 17–20 nucleotide guide RNA, containing both a CRISPR RNA and a trans-activating RNA complementary to a protospacer DNA site, provides targeted association of the genomic DNA with the Cas9 protein. The Cas9 protein generates double-stranded DNA breaks that are repaired to create either genetic deletions (non-homologous end joining) or substitutions (homology-directed repair).

Materials and Methods

Cells

Vero cells (African green monkey kidney cells; CCL81.4) were obtained from the American Type Culture Collection (ATCC; Manassas, VA, USA) and maintained at low passage (passages 25–30) in Dulbecco's Modified Eagle's Media (DMEM; GIBCO, Gaithersburg, MD, USA), with 5% heat-inactivated fetal bovine serum (FBS; HyClone, Logan, UT, USA), at 37ºC and 5% CO_2.

Viruses

Human stool samples containing GII.3, GII.4 Yerseke (2006a pandemic), or GII.4 Sydney (2012 pandemic) HuNoV were acquired from Murdoch Children's Research Institute (MCRI; Melbourne, Victoria, AUS) or the Centers for Disease Control and Prevention (CDC, Atlanta, GA, USA) and stored at –80ºC. The stool samples were thawed on ice before making 10% (*w/v*) dilutions in PBS (HyClone). All samples were centrifuged 2× at 1500× *g* for 10 min at 4ºC and then at 5000× *g* for 10 min at 4ºC. The stool samples were passed through 100 µm and 40 µm cell strainers (BD, Franklin Lakes, NJ, USA) then filtered samples were filtered using 0.45 µm filters (GE Healthcare, Chicago, IL, USA) before aliquots were made and stored at –80ºC until use.

HuNoV genome equivalent (g.e.) quantification

Stool samples were treated with RNAzol (Molecular Research Center Inc., Cincinnati, OH, USA) according to the manufacturer's instructions to generate total

RNA to be used for amplification and detection by qRT-PCR as previously described [12]. The resulting qRT-PCR levels are considered g.e. because the amplified site occurs once in each full-length genome. MOI was calculated as the ratio of input g.e. to the number of cells.

HuNoV Infection

The media from Vero cells was decanted and HuNoV infections (MOI=1.0) were performed in SF-DMEM. The plated cells were gently rocked before incubation at 37ºC and 5% CO_2. At 72hpi, total RNA was extracted and HuNoV g.e. were evaluated. For HuNoV infections including trypsin, 0.25% trypsin (Gibco by Life Technologies; Thermo Fisher Scientific, Waltham, MA, USA) was added to the virus at a final concentration of 1% [8.8 BAEE units] for 30 min at 37ºC and 5% CO_2 before infection.

siRNA and miR gene knockdown (KD)

ON-TARGET*plus* siRNAs (Dharmacon, Lafayette, CO, USA) targeting human genes were used to KD gene expression in Vero cells. The siRNAs were previously validated to specifically target and KD the host genes in Vero cells [19,35]. Four siRNA duplexes, each targeting distinct gene-specific seed regions, were pooled and transfected simultaneously to enhance gene expression KD. siRNA KD of each host gene was confirmed by qPCR compared to non-targeting control (NTC) siRNA treatments. The siRNAs [50 nM final] were pre-plated in 96 well-plates before incubation with 0.35 µL of Dharmafect 4 (Dharmacon) diluted in

Hank's Balanced Salt Solution (HBSS; HyClone) for 30 min at room temperature (RT). Following the incubation, 8×10^3 Vero cells were reverse-transfected in SF-DMEM and incubated at 37ºC and 5% CO_2 overnight. At 16h post-transfection, the transfection media was replaced with DMEM + 5% FBS. At 48h post-transfection, the wells were infected with HuNoV for 72h. The siRNA transfection protocol was used for miR transfection with the following modification: miR mimics and inhibitors were transfected at [25 nM final].

Genes of interest during infection

8×10^3 Vero cells were plated in 96-well plates and mock-infected or infected with HuNoV (MOI=1.0) for 24, 48, or 72h. RNA samples were extracted as above and quantified on a Nanodrop 1000 Spectrophotometer (Thermo Fisher Scientific). RNA quantities were normalized across each experiment before cDNA synthesis using a Verso cDNA Synthesis Kit (Thermo Fisher Scientific). cDNA amplification was achieved using gene-specific DNA primers (Integrated DNA Technologies; Coralville, IA, USA) and the Brilliant III Ultra-Fast SYBR Green qPCR Kit (Agilent, Santa Clara, CA, USA) according to the manufacturer's instructions, on an Mx3005P qPCR system (Agilent). GAPDH-normalized host gene expression was calculated using the $2^{-(\Delta\Delta CT)}$ method.

CRISPR-Cas9 gene editing

Single-plasmid CRISPR gene editing (MilliporeSigma; Burlington, MA, USA) was performed in Vero cells. 9×10^5 Vero cells were plated in 6-well plates in

DMEM + 5% FBS at 37ºC and 5% CO_2. 12.5 µL of Lipofectamine LTX (Thermo Fisher Scientific) and 3.75 µg of CRISPR DNA were each diluted to a final volume of 100 µL in OPTI-MEM (Thermo Fisher Scientific). After mixing, the Lipofectamine and CRISPR DNA were combined and incubated at RT for 30 min. Meanwhile, the cells were washed 1× with HBSS before the addition of DMEM + 5% FBS. After adding 200 µL of the Lipofectamine and CRISPR DNA mix, the plate was incubated at 37ºC and 5% CO_2 for 6h before the addition of another 1 mL of DMEM + 5% FBS. At 24h post-transfection, the media was changed to DMEM + 10% FBS, 100 units/mL of penicillin, 100 µg/mL of streptomycin, and 250 ng/mL of amphotericin B (Thermo Fisher Scientific). Single-cell colonies were sorted using a MoFlo Astrios EQ (Beckman Coulter, Brea, CA, USA) based on GFP expression 48h post-transfection into 96-well plates. Expansion of the colonies from a 96-well plate format to a 6-well plate format was performed in duplicate to allow for genotypic (qRT-PCR followed by Sanger sequencing and next-generation sequencing) and phenotypic (HuNoV infection) validation. Gene KO was confirmed by bp deletion resulting in disruption of the open reading frame. Additionally, clones containing genes with insertions were excluded from the analysis.

Statistical Analyses

Unpaired two-tailed t-tests and one-way ANOVA with Dunnett's post hoc tests were performed with 95% confidence intervals using GraphPad Prism. *p*-

values < 0.05 were considered significant: * $p < 0.05$, ** $p < 0.01$, *** $p < 0.001$, and **** $p < 0.0001$. Error bars represent + standard error of the mean (SEM).

Results

Trypsin cleavage of enteric virus capsids is beneficial to astrovirus, poliovirus, porcine epidemic diarrhea virus, and rotavirus replication [13-18]. Therefore, we explored trypsin treatments for the enhancement of HuNoV replication. We examined a range (1.76–10,000 BAEE units) of trypsin treatments and determined that HuNoV titers slightly increased (~1.5-fold) using a higher MOI=100 when co-incubated with 8.8 BAEE units of trypsin throughout the infection time-course (Figure 5.1). This effect was consistent with the abundance of trypsin-cleavable capsid conformations. Trypsin addition also increased stool-derived exosome HuNoV replication (~1.5-fold) in an MOI-dependent manner, but at a lower MOI=1.0 (Figure 5.2). Selective loading of trypsin-cleaved capsid conformations into exosomes may not occur, explaining the inconsistency.

To elucidate some of the antiviral Vero cell genes that modify HuNoV replication, we evaluated siRNA KD of host genes previously identified to be important for influenza virus [21], poliovirus [20], and rotavirus [19] replication. KD of several genes in Vero cells, specifically empty spiracles homeobox 2 (*EMX2*), fibroblast growth factor 2 (*FGF2*), neuraminidase 2 (*NEU2*), pyrroline-5-carboxylate reductase 1 (*PYCR1*), RAD51 associated protein 1 (*RAD51AP1*), and Sec61 translocon gamma subunit (*SEC61G*) enhanced HuNoV replication in Vero cells (Figure 5.3). When several canonical innate antiviral genes were examined

following siRNA KD, specifically interferon regulatory factor 3 (*IRF3*), *IRF7*, interferon induced with helicase C domain 1 (*IFIH1*; MDA5), DExD/H-box helicase 58 (*DDX58*; RIG-I), toll-like receptor 2 (*TLR2*), *TLR3*, and *TLR7* the findings showed that these genes affect HuNoV replication (Figure 5.3). Expression of these genes during HuNoV infection was largely unaffected, following either stool or exosome infections (Figures 5.4 and 5.5).

We also attempted to corroborate the host genes needed for HuNoV replication with miR regulation using both miR mimic addition and miR depletion with miR inhibitors. Specifically, we were unable to link miR-let7 (*DDX58*; RIG-I), miR-18a (*RAD51AP1*), miR-26b (*TLR3*), miR-105 (*TLR2*), miR-223 (*TLR3*), and miR-512 (*TLR7*) to increased HuNoV replication (Figures 5.6 and 5.7). The promiscuous nature of miRs for different targets may likely have obscured any effects.

Based on earlier virus-host gene studies for influenza virus [21], poliovirus [20], and rotavirus [19] replication, we generated several CRISPR-Cas9 gene-edited Vero cell lines and tested their ability to serve as substrates for enhanced HuNoV replication (Table 5.1). Notably, the leucine-rich repeats and guanylate kinase domain-containing (*LRGUK*) gene KO enhanced GII.3 HuNoV replication (Table 5.1). The *LRGUK* gene was screened and validated as an antiviral gene that regulated rotavirus replication [19], and interestingly only the *LRGUK* KO Vero cell line, but not *LRGUK* KD improved HuNoV replication. This is likely due to the heterozygous nature of the gene KD using siRNAs or bias of the single cell-derived KO cell line population for enhanced ability to replicate GII.3 HuNoVs.

Discussion

While BJAB cells and HIEs have been used to test antivirals and antibody neutralization, these cell culture systems are unsuited for vaccine development [36,37]. BJAB cells have only been shown to support a single HuNoV strain, meaning their utility may be limited especially given the diversity of HuNoVs. HIEs are an uncharacterized mixed cell culture system with a limited lifespan, creating regulatory issues linked to batch-to-batch variation. The development of an approved vaccine cell line for HuNoV vaccine development represents a promising path forward. Vero cells are a proven and widely used substrate for viral vaccines.

While trypsin is needed for proteolytic cleavage events affecting some enteric viruses [13-18], the HuNoV capsid is understood to be resistant to trypsin-mediated cleavage as trypsin does not impact binding or internalization [22,23,38]. HuNoV capsids contain approximately 15 trypsin cleavage sites; however, each site is inaccessible to the enzyme while in its infectious form [25]. Of note, a trypsin-cleavable GII.3 norovirus virion has been described [39,40]. Smaller conformations of the HuNoV capsid form under alkaline conditions [38,41], such as those in the gastrointestinal tract, and upon exposure to trypsin can be cleaved [26]. Following cleavage, these capsid conformations may have a role in the viral replication cycle [26]. The effect of trypsin on HuNoV titers following infection with native stool may correspond to a high MOI containing increased numbers of immunomodulatory trypsin-cleaved capsid conformations. Trypsin enhancement of exosome-associated HuNoV may occur at a low MOI because of viral clustering occurring within exosomes but this remains to be explored.

The antiviral host genes that affect HuNoV replication are not well-understood, but it is known that viruses co-opt host genes to replicate, and host genes are known to be required for virus replication. We took advantage of previous findings of virus-host gene interactions from genome-wide siRNA screens [35,42,43]. The antiviral host genes identified here have diverse functions. It was shown that EMX2 functions in the Wnt/β-catenin pathway and may have a role in cell cycle regulation and apoptosis [44]. EMX2 has also been shown to bind to the translational factor eIF4E [45]. This interaction may affect HuNoV VPg recruitment of eIF4E, modulating HuNoV replication. FGF2 has been shown to stabilize basally expressed RIG-I [46], implicating its downregulation with decreased virus sensing mechanisms. NEU2 functions as a sialidase and cleaves Lewis X carbohydrates [47]. HuNoV VLPs have been shown to bind Lewis X [48-50] conceivably implicating a decrease in *NEU2* gene expression with increases in attachment factor availability. PYCR1 leads to cell cycle arrest [51,52]. A similar mechanism has been shown for the murine NoV VPg [53]. It remains unknown if VPg directs cell cycle arrest through PYCR1 downregulation. RAD51AP1 facilitates homologous recombination of host DNA [54], while SEC61G functions in membrane protein translocation and incorporation into the endoplasmic reticulum [55]. The interactions between HuNoV and these genes are speculative; however IRF3 [56,57], IRF7 [29,57], MDA5 [58-61], RIG-I [29,59,60,62], TLR3 [58], and TLR7 [60,63,64] have been previously implicated in NoV responses. Of note, TLR2 enhances cytokine production upon the detection of rotavirus [65]. No additive or synergistic effects were observed for any of the genes when two genes were KD

simultaneously. We observed limited differential gene expression of the handful of genes tested after HuNoV infection in Vero cells. Given the number of genes analyzed, this observation is in agreement with an earlier study demonstrating low levels of differentially regulated genes after HuNoV infection of HIEs [29]. Collectively, this report demonstrates that modest HuNoV replication in Vero cells may be enhanced by trypsin or by siRNA KD or CRISPR-Cas9 gene editing of antiviral host genes. Prospectively, one may seek to target multiple genes with CRISPRs and/or miRs to achieve additive or synergistic replication, and the data provided here reveals several host genes for this purpose.

References

1 Liu, L. *et al.* Global, regional, and national causes of under-5 mortality in 2000-15: an updated systematic analysis with implications for the Sustainable Development Goals. *Lancet* **388**, 3027-3035, doi:10.1016/s0140-6736(16)31593-8 (2016).

2 Payne, D. C. *et al.* Norovirus and medically attended gastroenteritis in U.S. children. *The New England journal of medicine* **368**, 1121-1130, doi:10.1056/NEJMsa1206589 (2013).

3 Halasa, N. *et al.* The Changing Landscape of Pediatric Viral Enteropathogens in the Post-Rotavirus Vaccine Era. *Clinical infectious diseases : an official publication of the Infectious Diseases Society of America*, doi:10.1093/cid/ciaa100 (2020).

4 Bartsch, S. M., Lopman, B. A., Ozawa, S., Hall, A. J. & Lee, B. Y. Global Economic Burden of Norovirus Gastroenteritis. *PloS one* **11**, e0151219, doi:10.1371/journal.pone.0151219 (2016).

5 Bartsch, S. M., Lopman, B. A., Hall, A. J., Parashar, U. D. & Lee, B. Y. The potential economic value of a human norovirus vaccine for the United States. *Vaccine* **30**, 7097-7104, doi:10.1016/j.vaccine.2012.09.040 (2012).

6 Lopman, B. A. *et al.* Norovirus Infection and Disease in an Ecuadorian Birth Cohort: Association of Certain Norovirus Genotypes With Host FUT2 Secretor Status. *The Journal of infectious diseases* **211**, 1813-1821, doi:10.1093/infdis/jiu672 (2015).

7 Shioda, K., Kambhampati, A., Hall, A. J. & Lopman, B. A. Global age distribution of pediatric norovirus cases. *Vaccine* **33**, 4065-4068, doi:10.1016/j.vaccine.2015.05.051 (2015).

8 Chhabra, P. *et al.* Updated classification of norovirus genogroups and genotypes. *The Journal of general virology*, doi:10.1099/jgv.0.001318 (2019).

9 Todd, K. V. & Tripp, R. A. Human Norovirus: Experimental Models of Infection. *Viruses* **11**, doi:10.3390/v11020151 (2019).

10 Jones, M. K. *et al.* Enteric bacteria promote human and mouse norovirus infection of B cells. *Science* **346**, 755-759, doi:10.1126/science.1257147 (2014).

11 Ettayebi, K. *et al.* Replication of human noroviruses in stem cell-derived human enteroids. *Science* **353**, 1387-1393, doi:10.1126/science.aaf5211 (2016).

12 Todd, K. V. & Tripp, R. A. Vero Cells as a Mammalian Cell Substrate for Human Norovirus. *Viruses* **12**, doi:10.3390/v12040439 (2020).

13 Fricks, C. E., Icenogle, J. P. & Hogle, J. M. Trypsin sensitivity of the Sabin strain of type 1 poliovirus: cleavage sites in virions and related particles. *Journal of virology* **54**, 856-859 (1985).

14 Wicht, O. *et al.* Proteolytic activation of the porcine epidemic diarrhea coronavirus spike fusion protein by trypsin in cell culture. *Journal of virology* **88**, 7952-7961, doi:10.1128/jvi.00297-14 (2014).

15 Saxena, K. *et al.* Human Intestinal Enteroids: a New Model To Study Human Rotavirus Infection, Host Restriction, and Pathophysiology. *Journal of virology* **90**, 43-56, doi:10.1128/jvi.01930-15 (2015).

16 Pesavento, J. B., Crawford, S. E., Roberts, E., Estes, M. K. & Prasad, B. V. pH-induced conformational change of the rotavirus VP4 spike: implications for cell entry and antibody neutralization. *Journal of virology* **79**, 8572-8580, doi:10.1128/jvi.79.13.8572-8580.2005 (2005).

17 Almeida, J. D., Hall, T., Banatvala, J. E., Totterdell, B. M. & Chrystie, I. L. The effect of trypsin on the growth of rotavirus. *The Journal of general virology* **40**, 213-218, doi:10.1099/0022-1317-40-1-213 (1978).

18 Lee, T. W. & Kurtz, J. B. Serial propagation of astrovirus in tissue culture with the aid of trypsin. *The Journal of general virology* **57**, 421-424, doi:10.1099/0022-1317-57-2-421 (1981).

19 Wu, W., Orr-Burks, N., Karpilow, J. & Tripp, R. A. Development of improved vaccine cell lines against rotavirus. *Scientific data* **4**, 170021, doi:10.1038/sdata.2017.21 (2017).

20 van der Sanden, S. M. *et al.* Engineering Enhanced Vaccine Cell Lines To Eradicate Vaccine-Preventable Diseases: the Polio End Game. *Journal of virology* **90**, 1694-1704, doi:10.1128/jvi.01464-15 (2016).

21 Bakre, A. *et al.* Identification of Host Kinase Genes Required for Influenza Virus Replication and the Regulatory Role of MicroRNAs. *PloS one* **8**, e66796, doi:10.1371/journal.pone.0066796 (2013).

22 Tamura, M., Natori, K., Kobayashi, M., Miyamura, T. & Takeda, N. Interaction of recombinant norwalk virus particles with the 105-kilodalton cellular binding protein, a candidate receptor molecule for virus attachment. *Journal of virology* **74**, 11589-11597 (2000).

23 White, L. J. *et al.* Attachment and entry of recombinant Norwalk virus capsids to cultured human and animal cell lines. *Journal of virology* **70**, 6589-6597 (1996).

24 Duizer, E. *et al.* Laboratory efforts to cultivate noroviruses. *The Journal of general virology* **85**, 79-87, doi:10.1099/vir.0.19478-0 (2004).

25 Tan, M., Meller, J. & Jiang, X. C-terminal arginine cluster is essential for receptor binding of norovirus capsid protein. *Journal of virology* **80**, 7322-7331, doi:10.1128/jvi.00233-06 (2006).

26 Hardy, M. E., White, L. J., Ball, J. M. & Estes, M. K. Specific proteolytic cleavage of recombinant Norwalk virus capsid protein. *Journal of virology* **69**, 1693-1698 (1995).

27 Rajewsky, N. microRNA target predictions in animals. *Nature genetics* **38 Suppl**, S8-13, doi:10.1038/ng1798 (2006).

28 Lee, R. C., Feinbaum, R. L. & Ambros, V. The C. elegans heterochronic gene lin-4 encodes small RNAs with antisense complementarity to lin-14. *Cell* **75**, 843-854 (1993).

29 Hosmillo, M. *et al.* Norovirus Replication in Human Intestinal Epithelial Cells Is Restricted by the Interferon-Induced JAK/STAT Signaling Pathway and RNA Polymerase II-Mediated Transcriptional Responses. *mBio* **11**, doi:10.1128/mBio.00215-20 (2020).

30 Jansen, R., Embden, J. D., Gaastra, W. & Schouls, L. M. Identification of genes that are associated with DNA repeats in prokaryotes. *Molecular microbiology* **43**, 1565-1575 (2002).

31 Mojica, F. J., Diez-Villasenor, C., Soria, E. & Juez, G. Biological significance of a family of regularly spaced repeats in the genomes of Archaea, Bacteria and mitochondria. *Molecular microbiology* **36**, 244-246 (2000).

32 Cong, L. *et al.* Multiplex genome engineering using CRISPR/Cas systems. *Science* **339**, 819-823, doi:10.1126/science.1231143 (2013).

33 Mali, P. *et al.* RNA-guided human genome engineering via Cas9. *Science* **339**, 823-826, doi:10.1126/science.1232033 (2013).

34 Jinek, M. *et al.* A programmable dual-RNA-guided DNA endonuclease in adaptive bacterial immunity. *Science* **337**, 816-821, doi:10.1126/science.1225829 (2012).

35 Murray, J. *et al.* A universal mammalian vaccine cell line substrate. *PloS one* **12**, e0188333, doi:10.1371/journal.pone.0188333 (2017).

36 Kolawole, A. O., Rocha-Pereira, J., Elftman, M. D., Neyts, J. & Wobus, C. E. Inhibition of human norovirus by a viral polymerase inhibitor in the B cell culture system and in the mouse model. *Antiviral research* **132**, 46-49, doi:10.1016/j.antiviral.2016.05.011 (2016).

37 Alvarado, G. *et al.* Human Monoclonal Antibodies That Neutralize Pandemic GII.4 Noroviruses. *Gastroenterology*, doi:10.1053/j.gastro.2018.08.039 (2018).

38 Bertolotti-Ciarlet, A., Crawford, S. E., Hutson, A. M. & Estes, M. K. The 3' end of Norwalk virus mRNA contains determinants that regulate the expression and stability of the viral capsid protein VP1: a novel function for the VP2 protein. *Journal of virology* **77**, 11603-11615 (2003).

39 Huo, Y. *et al.* Enzymatic cleavage promotes disassembly of GII.3 norovirus virus like particles and its binding to salivary histo-blood group

antigens. *Virus research* **240**, 18-24, doi:10.1016/j.virusres.2017.07.017 (2017).

40 Kumar, S., Ochoa, W., Kobayashi, S. & Reddy, V. S. Presence of a surface-exposed loop facilitates trypsinization of particles of Sinsiro virus, a genogroup II.3 norovirus. *Journal of virology* **81**, 1119-1128, doi:10.1128/jvi.01909-06 (2007).

41 Shoemaker, G. K. *et al.* Norwalk virus assembly and stability monitored by mass spectrometry. *Molecular & cellular proteomics : MCP* **9**, 1742-1751, doi:10.1074/mcp.M900620-MCP200 (2010).

42 Orr-Burks, N. *et al.* Gene-edited vero cells as rotavirus vaccine substrates. *Vaccine X* **3**, 100045, doi:10.1016/j.jvacx.2019.100045 (2019).

43 Hoeksema, F. *et al.* Enhancing viral vaccine production using engineered knockout vero cell lines - A second look. *Vaccine* **36**, 2093-2103, doi:10.1016/j.vaccine.2018.03.010 (2018).

44 Zhang, Y., Cao, G., Yuan, Q. G., Li, J. H. & Yang, W. B. Empty Spiracles Homeobox 2 (EMX2) Inhibits the Invasion and Tumorigenesis in Colorectal Cancer Cells. *Oncology research* **25**, 537-544, doi:10.3727/096504016x14756640150695 (2017).

45 Nedelec, S. *et al.* Emx2 homeodomain transcription factor interacts with eukaryotic translation initiation factor 4E (eIF4E) in the axons of olfactory sensory neurons. *Proceedings of the National Academy of Sciences of the United States of America* **101**, 10815-10820, doi:10.1073/pnas.0403824101 (2004).

46 Liu, X., Luo, D. & Yang, N. Cytosolic Low Molecular Weight FGF2 Orchestrates RIG-I-Mediated Innate Immune Response. *Journal of immunology (Baltimore, Md. : 1950)* **195**, 4943-4952, doi:10.4049/jimmunol.1501503 (2015).

47 Chavas, L. M. *et al.* Crystal structure of the human cytosolic sialidase Neu2. Evidence for the dynamic nature of substrate recognition. *The Journal of biological chemistry* **280**, 469-475, doi:10.1074/jbc.M411506200 (2005).

48 Huang, P. *et al.* Norovirus and histo-blood group antigens: demonstration of a wide spectrum of strain specificities and classification of two major binding groups among multiple binding patterns. *Journal of virology* **79**, 6714-6722, doi:10.1128/jvi.79.11.6714-6722.2005 (2005).

49 Carmona-Vicente, N., Allen, D. J., Rodriguez-Diaz, J., Iturriza-Gomara, M. & Buesa, J. Antibodies against Lewis antigens inhibit the binding of human norovirus GII.4 virus-like particles to saliva but not to intestinal Caco-2 cells. *Virology journal* **13**, 82, doi:10.1186/s12985-016-0538-y (2016).

50 Rydell, G. E. *et al.* Human noroviruses recognize sialyl Lewis x neoglycoprotein. *Glycobiology* **19**, 309-320, doi:10.1093/glycob/cwn139 (2009).

51 Cai, F. *et al.* Pyrroline-5-carboxylate reductase 1 promotes proliferation and inhibits apoptosis in non-small cell lung cancer. *Oncology letters* **15**, 731-740, doi:10.3892/ol.2017.7400 (2018).

52 Zeng, T. *et al.* Knockdown of PYCR1 inhibits cell proliferation and colony formation via cell cycle arrest and apoptosis in prostate cancer. *Medical oncology (Northwood, London, England)* **34**, 27, doi:10.1007/s12032-016-0870-5 (2017).

53 Davies, C. & Ward, V. K. Expression of the NS5 (VPg) Protein of Murine Norovirus Induces a G1/S Phase Arrest. *PloS one* **11**, e0161582, doi:10.1371/journal.pone.0161582 (2016).

54 Parplys, A. C. *et al.* RAD51AP1-deficiency in vertebrate cells impairs DNA replication. *DNA repair* **24**, 87-97, doi:10.1016/j.dnarep.2014.09.007 (2014).

55 Lu, Z. *et al.* Glioblastoma proto-oncogene SEC61gamma is required for tumor cell survival and response to endoplasmic reticulum stress. *Cancer research* **69**, 9105-9111, doi:10.1158/0008-5472.can-09-2775 (2009).

56 Thackray, L. B. *et al.* Critical role for interferon regulatory factor 3 (IRF-3) and IRF-7 in type I interferon-mediated control of murine norovirus replication. *Journal of virology* **86**, 13515-13523, doi:10.1128/jvi.01824-12 (2012).

57 Qu, L. *et al.* Replication of Human Norovirus RNA in Mammalian Cells Reveals Lack of Interferon Response. *Journal of virology* **90**, 8906-8923, doi:10.1128/jvi.01425-16 (2016).

58 McCartney, S. A. *et al.* MDA-5 recognition of a murine norovirus. *PLoS pathogens* **4**, e1000108, doi:10.1371/journal.ppat.1000108 (2008).

59 Dang, W. *et al.* IRF-1, RIG-I and MDA5 display potent antiviral activities against norovirus coordinately induced by different types of interferons. *Antiviral research* **155**, 48-59, doi:10.1016/j.antiviral.2018.05.004 (2018).

60 Enosi Tuipulotu, D., Netzler, N. E., Lun, J. H., Mackenzie, J. M. & White, P. A. RNA Sequencing of Murine Norovirus-Infected Cells Reveals Transcriptional Alteration of Genes Important to Viral Recognition and Antigen Presentation. *Frontiers in immunology* **8**, 959, doi:10.3389/fimmu.2017.00959 (2017).

61 MacDuff, D. A. *et al.* HOIL1 is essential for the induction of type I and III interferons by MDA5 and regulates persistent murine norovirus infection. *Journal of virology*, doi:10.1128/jvi.01368-18 (2018).

62 Guix, S. *et al.* Norwalk virus RNA is infectious in mammalian cells. *Journal of virology* **81**, 12238-12248, doi:10.1128/jvi.01489-07 (2007).

63 Hjelm, B. E., Kilbourne, J. & Herbst-Kralovetz, M. M. TLR7 and 9 agonists are highly effective mucosal adjuvants for norovirus virus-like particle vaccines. *Human vaccines & immunotherapeutics* **10**, 410-416, doi:10.4161/hv.27147 (2014).

64 Enosi Tuipulotu, D., Netzler, N. E., Lun, J. H., Mackenzie, J. M. & White, P. A. TLR7 agonists display potent antiviral effects against norovirus infection via innate stimulation. *Antimicrobial agents and chemotherapy*, doi:10.1128/aac.02417-17 (2018).

65 Ge, Y. *et al.* Rotavirus NSP4 Triggers Secretion of Proinflammatory Cytokines from Macrophages via Toll-Like Receptor 2. *Journal of virology* **87**, 11160-11167, doi:10.1128/jvi.03099-12 (2013).

Figures and Tables

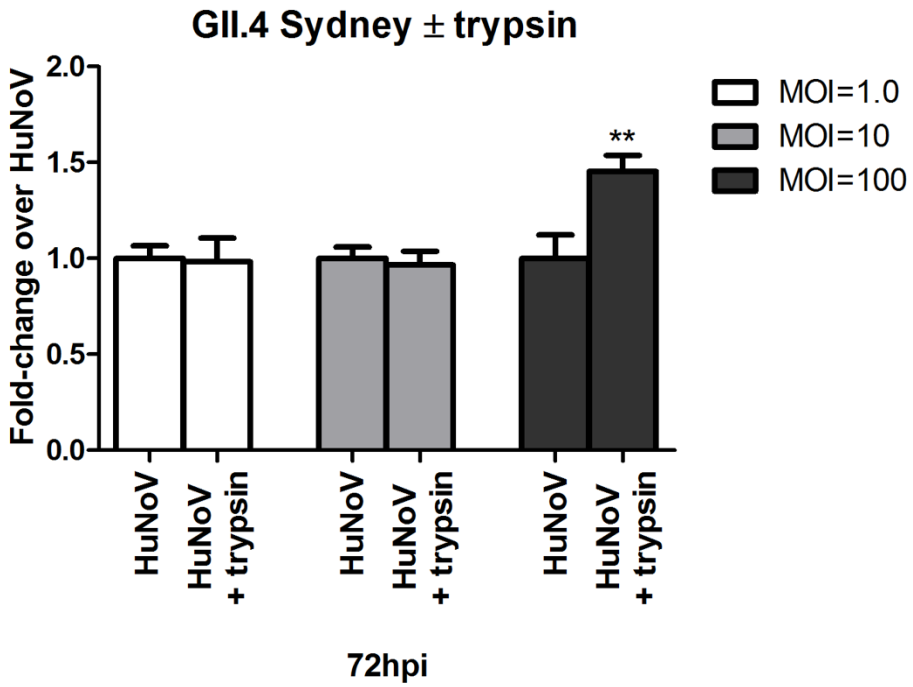

Figure 5.1: Improvement of GII.4 Sydney HuNoV replication by trypsin addition is MOI-dependent. Incubation of 8.8 BAEE units of trypsin with Vero cells increased peak HuNoV levels at a high MOI as measured by qRT-PCR. Data represent n=3 + SEM. ** $p < 0.01$.

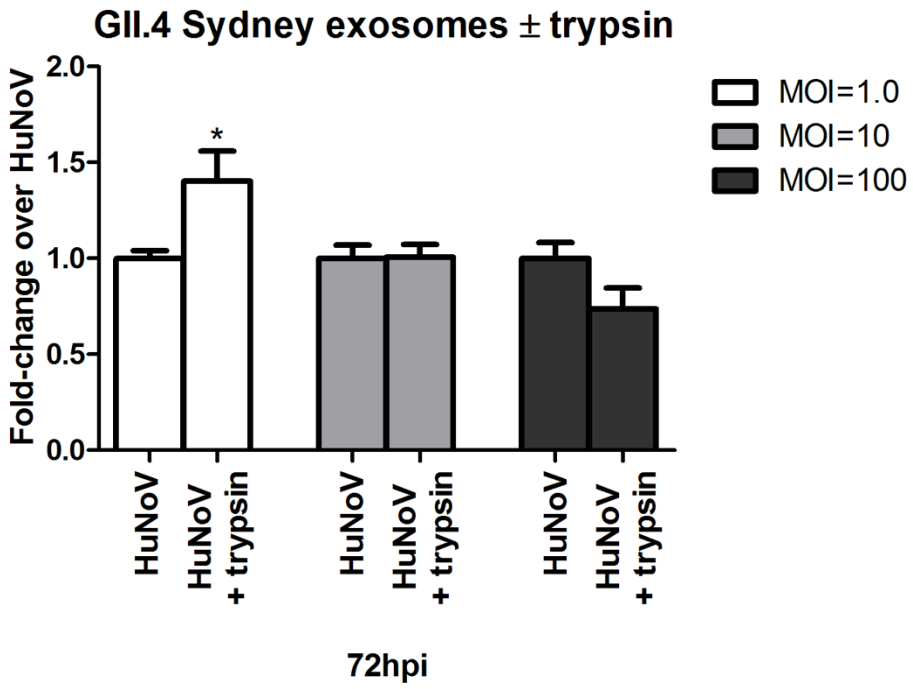

Figure 5.2: Improvement of GII.4 Sydney HuNoV exosome replication by trypsin addition is MOI-dependent. Incubation of 8.8 BAEE units of trypsin with Vero cells increased peak HuNoV levels at a low MOI as measured by qRT-PCR. Data represent n=2 + SEM. * $p < 0.05$.

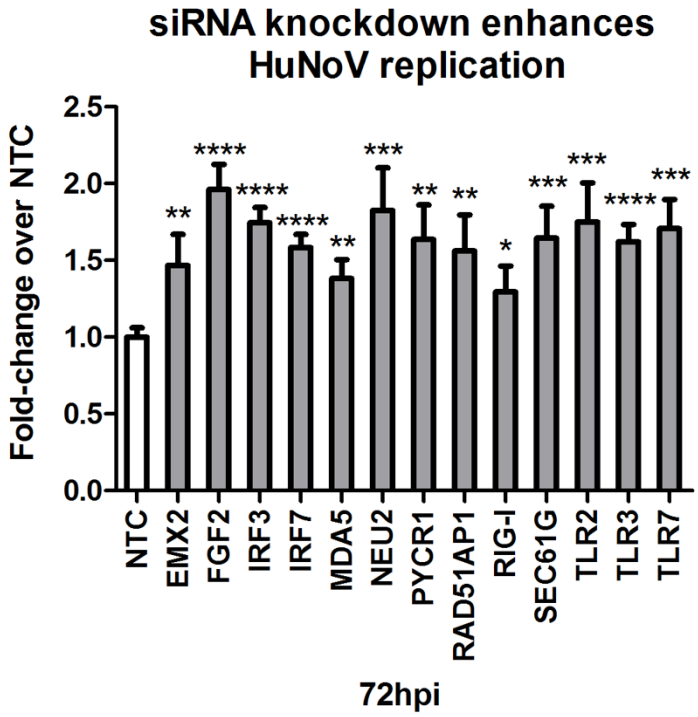

Figure 5.3: Knockdown of antiviral host gene expression increases GII.4 Sydney HuNoV replication. Treatment with pooled gene-specific siRNAs [50 nM] 48h prior to infection resulted in substantial increases in HuNoV titers 72hpi by qRT-PCR. Data represent n=3 + SEM. * $p < 0.05$, ** $p < 0.01$, *** $p < 0.001$, and **** $p < 0.0001$.

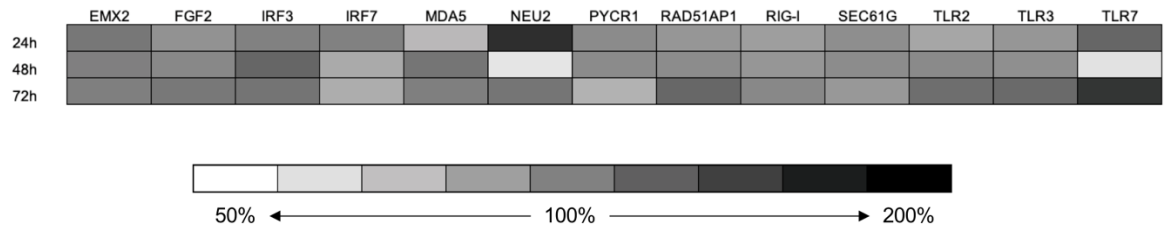

Figure 5.4: Antiviral host gene expression modulation during GII.4 Sydney HuNoV infection. GAPDH-normalized gene-specific qPCR results compared to uninfected controls at equivalent time-points. Average % gene expression relative to uninfected controls is graphed from n=3 experiments.

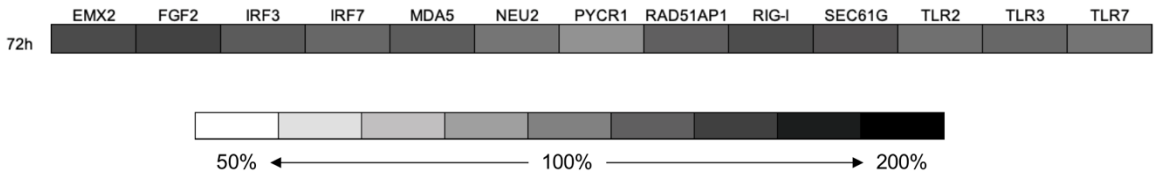

Figure 5.5: Antiviral host gene expression modulation during GII.4 Sydney HuNoV exosome infection. GAPDH-normalized gene-specific qPCR results compared to uninfected controls. Average % gene expression relative to uninfected controls is graphed from n=3 experiments.

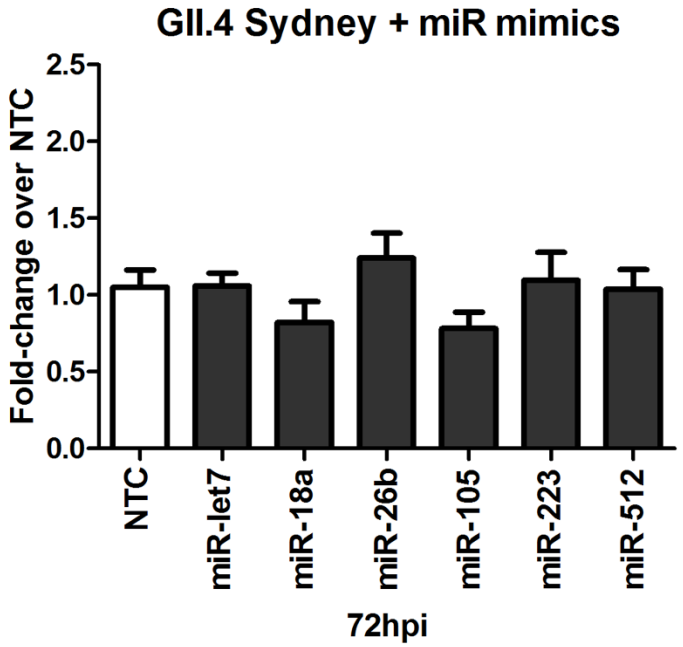

Figure 5.6: miR mimic addition does not appreciably affect peak HuNoV levels. Treatment with miR mimics [25 nM] 48h before infection did not significantly alter HuNoV titers 72hpi by qRT-PCR. Data represent n=3 + SEM.

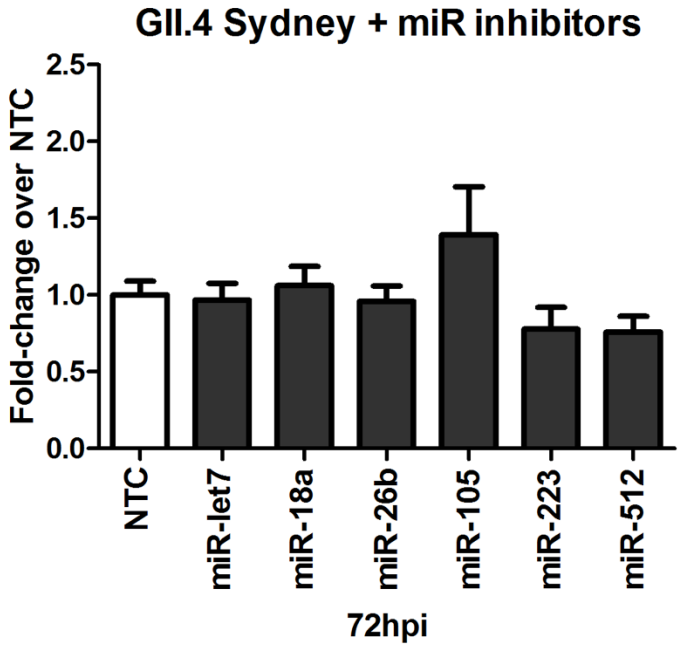

Figure 5.7: miR inhibitor addition does not appreciably affect peak HuNoV levels. Treatment with miR inhibitors [25 nM] 48h before infection did not significantly alter HuNoV titers 72hpi by qRT-PCR. Data represent n=3 + SEM.

Table 5.1: Gene knockout (KO) effects on HuNoV replication in Vero cells. qRT-PCR analysis after a 72h infection (MOI=1.0). Mean fold-changes over Vero cells displayed. Significance for enhanced replication compared to wild type Vero cells is shown. Data represent n=3 ± SEM. not significant (ns) and * $p < 0.05$. Gene KO cell lines tested include empty spiracles homeobox 2 (*EMX2*), leucine rich repeats and guanylate kinase domain containing (*LRGUK*), neuraminidase 2 (*NEU2*), and WD repeat domain 62 (*WDR62*).

Virus	Sample	Cell Line	Time-point	Mean ± SEM	Significance
GII.4 Sydney	stool	Vero	72h	1.00 ± 0.06	–
	stool	Δ*EMX2*	72h	0.74 ± 0.06	ns
	stool	Δ*LRGUK*	72h	0.85 ± 0.09	ns
	stool	Δ*WDR62*	72h	0.82 ± 0.13	ns
	stool	Vero	72h	1.00 ± 0.05	–
	stool	Δ*NEU2*	72h	0.88 ± 0.09	ns
	exosomes	Vero	72h	1.00 ± 0.05	–
	exosomes	Δ*EMX2*	72h	0.68 ± 0.04	ns
	exosomes	Δ*LRGUK*	72h	0.39 ± 0.05	ns
	exosomes	Δ*WDR62*	72h	0.56 ± 0.05	ns
GII.3	stool	Vero	72h	1.00 ± 0.10	–
	stool	Δ*EMX2*	72h	0.89 ± 0.10	ns
	stool	Δ*LRGUK*	72h	1.40 ± 0.13	*
	stool	Δ*WDR62*	72h	0.59 ± 0.15	ns
GII.4 Yerseke	stool	Vero	72h	1.00 ± 0.06	–
	stool	Δ*EMX2*	72h	1.22 ± 0.14	ns
	stool	Δ*LRGUK*	72h	1.02 ± 0.15	ns
	stool	Δ*WDR62*	72h	0.90 ± 0.07	ns

CHAPTER 6

CONCLUSIONS

Globally, HuNoVs cause substantial disease burden that remains unchecked due to the lack of a licensed vaccine or antiviral. As current vaccine methodologies are limited to recombinant protein vaccines, a vaccine-approved cell line would aid the development of all vaccines including inactivated and live-attenuated vaccines. Vero cells are well-documented and offer a faster path towards vaccine implementation. The *central hypothesis* of this undertaking was that Vero cells will support HuNoV replication and aid the development of a HuNoV vaccine. The *rationale* was that HuNoV research and translational HuNoV vaccine development would benefit from this cell culture system.

Specific Aim 1: Determine HuNoV replication in Vero cells. The *working hypothesis* is that Vero cells support HuNoV replication. In chapter 3, we demonstrate the attachment and internalization of HuNoV particles into Vero cells. Upon internalization, we observed the synthesis of new HuNoV RNA, structural proteins, and nonstructural proteins concomitant with replication. The tempo of HuNoV replication was not dependent on filterable agents, such as HBGA-expressing bacteria, or limited to a particular MOI range. Additionally, replication was observed in multiple clinically relevant HuNoV strains. While replication was

modest and limited to a single infection cycle, these data provide encouraging results for further development of the model.

Specific Aim 2: Determine exosome-driven HuNoV replication in Vero cells. The *working hypothesis* is that HuNoV infects Vero cells through exosomes. In chapter 4, we verify the presence of exosomes in HuNoV stool and that these exosomes contain substantial HuNoV RNA. HuNoV from stool exosomes associates with Vero cells at similar levels as whole stool, and HuNoV replication levels are similar between stool and exosomes. Exosomes contain infectious HuNoV, and may be responsible for a considerable portion of stool-derived HuNoV replication. Cell-derived exosomes from HuNoV-infected Vero cell supernatants contained infectious virus that was successfully passaged. The necessity of exosome isolation before passage indicates the relevance of exosomes for HuNoV infection. The importance of exosomes for HuNoV infection has been described in HIEs, but *in vivo* studies are needed to further validate HuNoV transmission by exosomes.

Specific Aim 3: Develop a Vero cell substrate for HuNoV replication. The *working hypothesis* is that the Vero cell model can be enhanced by media supplementation and host-targeted gene expression disruption. Results from chapter 5 demonstrate that trypsin addition can enhance HuNoV replication. We noted that both stool and exosome infections benefit from trypsin, at a high and low MOI respectively. We postulate that a high MOI stool infection contains larger quantities of trypsin-cleavable capsid conformations, which have an antiviral effect once cleaved. Additionally, we identified 13 antiviral genes that when KD with

siRNAs enhanced HuNoV replication. Lastly, we generated an *LRGUK* KO Vero cell line that increased peak HuNoV infection levels beyond the wild type Vero cells. Collectively, these data demonstrate the potential to develop the Vero cell substrate for enhanced HuNoV replication. These strategies for increased HuNoV propagation are needed to generate a robust Vero cell line that is ideal for HuNoV vaccine development.

In conclusion, this research showed that Vero cells can support HuNoV. Exosome-mediated infection and transmission were demonstrated in the Vero cell model. Trypsin addition and host-targeted gene expression disruption were used to enhance modest HuNoV replication in Vero cells. Collectively, these data represent the foundational research necessary to begin the development of Vero cells as a mammalian cell substrate for HuNoV vaccine development.